uOttawa

L'Université canadienne
Canada's university

FACULTÉ DES ÉTUDES SUPÉRIEURES ET POSTOCTORALES

uOttawa

L'Université canadienne
Canada's university

FACULTY OF GRADUATE AND POSDOCTORAL STUDIES

Carl Poulin

AUTEUR DE LA THÈSE / AUTHOR OF THESIS

M.Sc. (Chemistry)

GRADE / DEGREE

Department of Chemistry

FACULTÉ, ÉCOLE, DÉPARTEMENT / FACULTY, SCHOOL, DEPARTMENT

Heck-Mizoroki Reaction Using Palladium and Nickel on Yttria Stabilized Zirconia

TITRE DE LA THÈSE / TITLE OF THESIS

Dr. J. Giorgi

DIRECTEUR (DIRECTRICE) DE LA THÈSE / THESIS SUPERVISOR

Dr. Keith Fagnou

CO-DIRECTEUR (CO-DIRECTRICE) DE LA THÈSE / THESIS CO-SUPERVISOR

EXAMINATEURS (EXAMINATRICES) DE LA THÈSE / THESIS EXAMINERS

Dr. André Beauchemin

Dr. Paul Mayer

Gary W. Slater

Le Doyen de la Faculté des études supérieures et postdoctorales / Dean of the Faculty of Graduate and Postdoctoral Studies

# HECK-MIZOROKI REACTION USING PALLADIUM AND NICKEL ON YTTRIA STABILIZED ZIRCONIA

Carl Poulin

Thesis submitted to the
Faculty of Graduate and Postdoctoral studies
In partial fulfillment of the requirements
For the Masters degree in chemistry

Ottawa-Carleton Chemistry institute

Thèse soumise à
Faculté des études supérieures et postdoctorales
Université d'Ottawa
En vue de l'obtention de la maîtrise ès sciences à

L'institut de chimie d'Ottawa-Carleton

Department of Chemistry
Faculty of Science
University of Ottawa

*Your file Votre référence*
*ISBN: 978-0-494-50918-0*
*Our file Notre référence*
*ISBN: 978-0-494-50918-0*

## TABLE OF CONTENT

## LIST OF SCHEMES

## LIST OF FIGURES

## LIST OF TABLES

## LIST OF ABBREVIATIONS AND SYMBOLS

| | |
|---|---|
| 5%Pd-YSZ | 5mol% palladium on yttria stabilized zirconium |
| as-syn | As-synthesised |
| 600 | Calcinated at 600°C |
| 950 | Calcinated at 950°C |
| used | Catalyst used once in HR |
| R | Reduced |
| Acs | Molecular cross-sectional area of the adsorbate molecule |
| $A_m$ | Cross-sectional area of surface atom |
| ASA | Metal active surface area |
| Bu-cin | Butyl-cinnamate |
| CTAB | Cetyl-trimethylammoniumbromide |
| $\Delta d/d$ | XRD strain |
| C | Energy of adsorption in the first adsorbed layer |
| d | Average crystallite size |
| DBU | 1,8-Diazabicyclo[5.4.0]undec-7-ene |
| DCC | Dicyclohexylcarbodiimide |
| DCM | Dichloromethane |
| DIPEA | *N, N*-Diisopropylethylamine |
| DMA | N, N-Dimethylacetamide |
| DMAP | 4-Dimethylaminopyridine |
| DMF | N,N-Dimethylformamide |
| DMSO | Dimethylsulfoxide |
| Et-gly | Ethylene glycol |
| F | Response factor |
| FTIR | Fourier transformed infrared spectroscopy |
| GC | Gas chromatography |
| GC-MS | Gas chromatography - mass spectrometry |
| HR | Heck reaction |
| Ibz | Iodobenzene |
| $K_2CO_3$ | Potassium carbonate |
| $K_3PO_4$ | Tribasic potassium phosphate |
| L | Metal percent loading |
| M | Molecular weight |
| *M* | Molar mass of the adsorbate |
| m/z | Mass to charge ratio |
| N | Avogadro's number |
| $N_m$ | Monolayer uptake |
| NMP | *N*-methyl-2-pyrrolidone |
| NMR | Nuclear magnetic resonance |
| P/Po | Relative pressure |
| p-XRD | Powder X-ray diffraction |
| Pd, $Pd^0$ | Palladium |
| PdO, $Pd^{2+}$ | Palladium oxide |
| $Pd(OAc)_2$ | Palladium acetate |
| $Pd_{sol}$ | Soluble palladium |

| | |
|---|---|
| $r_k$ | Inner capillary radius |
| S | Adsorption stoichiometry |
| S/C | Substrate to catalyst ratio |
| SA | Surface area |
| t | Crystallite size |
| $t_l$ | Physisorbed layer thickness |
| TFA | Trifluoroacetic acid |
| THF | Tetrahydrofuran |
| TLC | Thin layer chromatography |
| TOF | Turn-over frequency |
| TON | Turn-over number |
| UV | Ultra-violet |
| V | Volume desorbed |
| $V_m$ | total amount of gas chemisorbed |
| W | Weight of adsorbed gas |
| Wm | Weight of adsorbate which forms a monolayer |
| YSZ | Yttria stabilized zirconia |
| Z | Metal density |

## PUBLICATIONS

During the past years, some of this thesis work was published.

Poulin, Carl, Matthew A. Brown, Yamile A. Wasslen, Catherine M. Grgicak, Keith Fagnou and Javier B. Giorgi, *Reactivity of mesoporous palladium yttria-stabilized zirconia for solution phase reactions*, Canadian Journal of Chemistry, **2006**, 84, 1520

This article describes the structural characterisation and reactivity of mesoporous Pd-YSZ for the Heck reaction. It relates most of sections 3.1, 3.3 and 3.4.

All other work presented in the present thesis is original and was produced by me unless otherwise mentioned.

## SUMMARY

This work was composed of studies analysing the capacity of Pd-YSZ and Ni-YSZ as a heterogeneous catalyst for the Heck-Mizoroki reaction. Following an optimization, mechanistic studies were undertaken with Pd-YSZ. P-XRD measurements showed a decrease in the amount of metal present in the catalyst after a cycle of Heck reaction. Also, two triple phase test were done. Using a resin supported reactant, it was showed that palladium leaches into solution and reacts through a homogeneous cycle. Also, the contribution of true heterogeneous surface catalysis was examined by means of a thiol-based palladium scavenger that neutralised homogeneous catalysis. While it is impossible to completely dismiss true surface catalysis, the negative result showed that surface catalysis did not contribute significantly to the overall reactivity.

Reactions showed reactivity up to 770'000 TON with mesoporous 5% Pd-YSZ calcinated to 600°C.

Using the self-assembly and the co-precipitation method, Ni-YSZ catalysts of 1%, 5% and 10% were synthesized and calcinated to 400°C, 600°C and 950°C. Catalyst characterization through p-XRD, physisorption and chemisorption allowed knowledge of the crystallite size surface area and metallic surface area. A structure-reactivity relationship study showed a limited effect in the ability of high surface area and low particle sizes to accelerate catalysis.

## ACKNOWLEDGEMENTS

The first person I have to thank is, without a doubt, Dr. Giorgi. Thank you for taking me into your lab, your generosity and patience is without limit. I know that the knowledge and experience I acquired will follow me all my life. It was an honour to be your student.

I would also like to thank Dr. Fagnou for all the advices you provided over the year. You always took the time to answer my numerous questions. Your, always constructive, criticism allowed me to fully understand the complexity of mechanistic studies. Thanks to Mathieu Parisien and Louis-Charles Campeau.

A special thanks goes to Catherine Grgicak, Richard Green, Shiliang wang, Nguon Lim and Luke Barre. You guys are a wonderful team. You all bring such a great energy to science and I'm grateful to be part of it.

Finally, I would like to my parents, Marcel and Lisette for all they've done. To my brother and sister, Jonathan and Valerie, I love you both very much. To my in-laws, Jacques and Helene, for you understanding during the past year and last, but certainly not least, to my lovely girlfriend Elizabeth, to who I dedicate this thesis.

# Chapter 1- INTRODUCTION

## 1.1 Heck-Mizoroki Reaction

The Heck-Mizoroki reaction was independently discovered by R.F. Heck[1-3] and T. Mizoroki[4,5] at the end of the 1960's and was further developed throughout the 1970's by Heck.[6-9i] It is a C-C coupling between an aryl/alkenyl halide or triflate and an olefin containing at least one hydrogen. This reaction has grown, particularly in the past 10-15 years,[10] to become an essential reaction in organic synthetic chemistry due to its versatility and flexibility.[11,12] The Heck reaction has the ability to accommodate a large number of functional groups, which makes it almost indispensable for the synthesis of complex organic molecules.[13]

The HR is part of the growing family of palladium and nickel catalyzed C-C coupling reactions which include the Heck-Mizoroki, the Suzuki-Miyaura,[14,15] the Kumada-Corriu,[16,17] the Negishi,[18] the Stille,[19,20] the Sonogashira[21] and the Hiyama[22] coupling.

Palladium is the metal that has been the most widely used and that has shown the best reactivity for the HR. However, due to its high cost, many recent publications propose the use of various other promising and cheaper metals like nickel,[23-29] cobalt,[30,31] copper[32] and manganese.[33,34] In most instances, almost any source of these metals can be used as catalyst and they are classified in two main groups: homogeneous and heterogeneous catalysts. Homogeneous catalysts are composed of a variety of metal-ligand complexes as well as ligand-free catalysts (also known as naked catalyst). There are many types of ligands: phosphines and other donor ligands,[35-37] palladacycles[38-44] and carbenes[45,46] that have been

---

[i] To simplify the text, the Heck-Mizoroki reaction will simply be referred to as the Heck reaction (HR) and the ''aryl/alkenyl halide or triflate'' reactant will be referred as the aryl halide unless otherwise mentioned.

commonly used. The heterogeneous catalysts consist of carbon[47-57] or oxide (Silica,[58-62] $Al_2O_3$,[63,64] MgO,[65-68] $ZrO_2$[69] other[70-72]) supported nanoparticules, zeolites[73,74] and other exchange support,[75-77] supported metal-ligand complex,[78-80] polymer and oxide encapsulated catalysts,[81,82] as well as soluble nanoparticules, and colloids.[83-89] The classification of soluble nanoparticules and colloids is in a grey area but we shall group them, for the purpose of this thesis, with heterogeneous catalyst.[90]

## 1.2 Heck Mechanisms

Based on the large body of literature investigating the Heck mechanism in the last decade, the mechanism is now believed to be guided by the type of catalyst used and the experimental conditions.[90] As such, there are four main mechanisms which are proposed: a neutral, a cationic and an anionic $Pd^0/Pd^{II}$ cycle, as well as a $Pd^{II}/Pd^{IV}$ cycle. Every $Pd^0/Pd^{II}$ cycle goes through the same steps (Scheme 1.1) and the variations of each will be explained in the following sections.

The vast majority of the mechanistic studies examined palladium catalysts while other metals like nickel have only been scarcely studied by a few groups.[23,91] We will first introduce the palladium mechanisms and then discuss the variations that apply to nickel throughout the text.

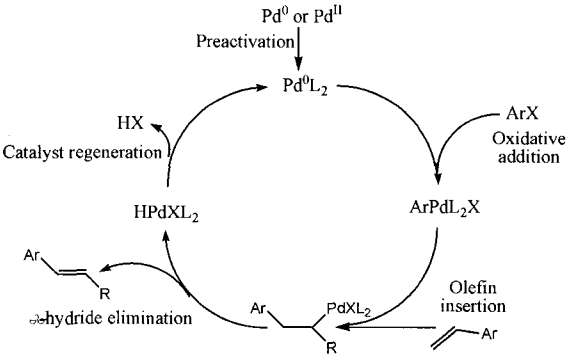


Scheme 1.1: Simplified textbook Heck mechanism

### 1.2.1 Neutral and Cationic (polar) Cycle

Both the neutral and cationic $Pd^0/Pd^{II}$ catalytic cycles[11] are widely accepted as being the mechanism for low-temperature metal-ligand catalyzed reactions.[90] We will use these mechanisms to analyze every step of the catalytic cycle and only evoke the determining factors in the other two mechanisms.

The pre-activation allows the catalyst to enter the catalytic cycle. It refers to ligand exchanges and *in situ* reduction of a $Pd^{II}$ species, or various ligand exchange of a $Pd^0$ complex with the end result being a catalytically active $Pd^0$ complex. While ligand-exchanges are not necessarily synonymous of a pre-activation, they can be a mean to obtain an active catalyst. The *in situ* reduction can be caused by phosphines, amines, quaternary ammonium or phosphonium salt, as well as the potential reductive elimination of a phosphonium species.[11] Other more direct methods such as *N*-butyl-lithium or sodium borohydride are also widely used,[92] especially for heterogeneous catalysts.[91] The kinetic repercussion of the pre-activation is an induction period.

The oxidative addition marks the true beginning of the catalytic cycle. It is during that step that the metal catalyst binds itself to the aryl halide. The oxidative addition for both nickel[93] and palladium[94] is facilitated by electron-rich phosphines[95] and electron-withdrawing groups on the aryl halide. This is most likely due to a 3-center transition state that causes a negative build-up on the ring and a positive charge near the metal. For both metals, studies regarding the oxidative addition to aromatic iodide showed a positive Hammett plot ($\rho$=2) which indicated an increase in the aromatic ring's electron density.[92]

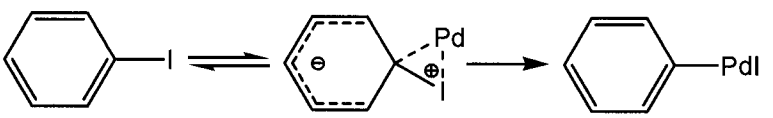


Scheme 1.2: 3-center transition state for the oxidative addition

The typical result from such a transition state would be the cis-isomer. The concerted approach explains why this step is very sensitive to the C-X bond strength of the aryl halide as their reactivity is: I > OTf > Br > Cl.[13] However, the vast majority of isolated intermediates are the trans-isomers,[11,96,97] the cis-isomer having been isolated only once,[98] but this can be explained by the more thermodynamically stable nature of trans-isomers. The oxidative addition is believed to be the rate limiting step for aryl bromides and chlorides when using a palladium catalyst.[23]

The olefin insertion marks the variation between the neutral and the cationic mechanism. While there are various proposed mechanisms for the olefin insertion such as a nucleophilic or electrophilic attack, it is generally accepted as being a concerted process.[11] This step is believed to vary depending on the ligand(s) used as one ligand has to dissociate to allow the olefin to approach.[99] The need of a free coordination site was demonstrated by a lower rate when excess phosphines were present.[100] Catalysts using σ-donor ligands usually go through a neutral pathway with the loss of a neutral ligand while strongly bound or ligand-free reactions are believed to go through a cationic (polar) pathway through the loss of an anionic ligand[101,102] (Scheme 1.3).

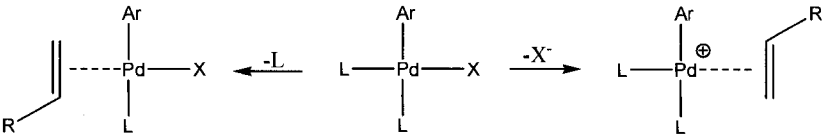


Scheme 1.3: Olefin insertion pathway

As the olefin approaches the palladium complex, it has to rotate to be in the plane of reaction for a concerted process to occur. It is this rotation, as well as its orientation, that will decide whether the product is the α- (E or Z) or the β(1,1)- derivative.[103] Because this process can adjust to the electronic properties of the intermediate formed,[11] this makes steric hindrance

the main driving force in the reaction's selectivity[104] and is true for catalysts that go through the neutral pathway.

In the case of the polar pathway, we must first mention that this does not mean that the palladium will react as a standard cation. The formal charge is relatively small[101] such that electronic effects of the reactant, that could guide the regioselectivity, are often overshadowed by steric considerations.[104] However, in the polar pathway, the α-substitution will experience a build-up of positive charge near the α-carbon (Scheme 1.4) that can be stabilized by electron rich groups on the olefin. On the other hand, no such stabilisation can occur for the β-substitution since the build-up occurs at the β-carbon.[92,105]

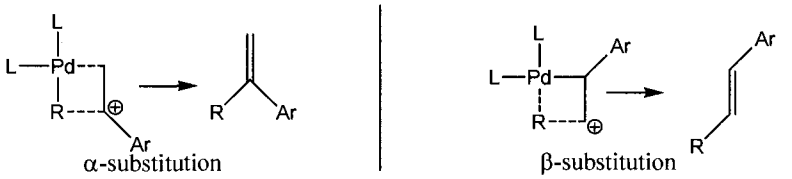


Scheme 1.4: Regioisomer selective step[105]

Therefore, while steric effects dominate the neutral pathway and push the reaction toward β-substitution, it is possible to attain a certain degree of selectivity in the polar pathway since α-substitution will be favoured by electron rich olefins while β-substitution will be favoured by electron poor olefins, such as acrylates, who, since they cannot stabilise the intermediate, are guided by steric hindrance.[99] This is part of the fundamentals of asymmetric HR.[92,106,107] The polar route is supported by the fact that strongly bounded or ligand-free reactions are often facilitated by polar solvents and additives such as quaternary ammonium salts (Jeffery conditions[108]).[11]

The β-hydride elimination is the product forming step. It is believed to be the rate determining step for nickel catalysts[23] and the palladium catalyzed HR of aryl iodides.[109] It begins with the rotation of the olefin's terminal carbon atoms to form a β-agnostic complex

between the β-carbon, a β-hydrogen and palladium (Scheme 1.5). What follows is the formation of a metal-hydride bond and the product moiety whose dissociation will liberate the reaction's product.[23] In the case of β-substitution, the E/Z ratio will be decided by mainly by steric consideration depending on which hydrogen is transferred to the metal. The reaction usually favours the E isomer.[11]

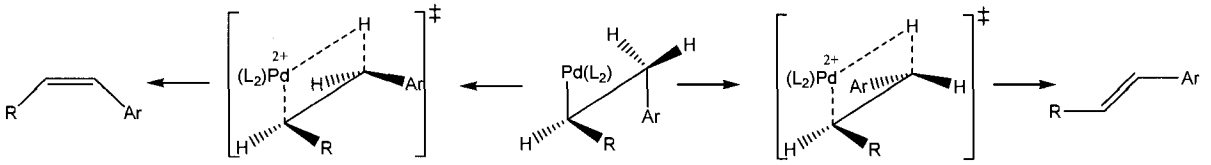


Scheme 1.5: E and Z isomers[11]

The liberation of the product leaves an empty coordination space on the palladium ($L_2PdH$ or LPdHX). Because of this, the entity can be stabilized by a ligand or an anionic species from the solution to form $L_2PdHX$, which can then go through a reductive elimination to give HX and $PdL_2$.[23] The acid formed is then neutralised by the base in solution. It is also possible that in the case of $L_2PdH$ (neutral pathway), the hydrogen can be scavenged by a base to form $PdL_2$, thus, also regenerating the catalyst. The contribution of the base is still being debated in the literature.[11]

While the amount of data concerning the differences between the Palladium and Nickel Heck mechanism is limited, we can say that since the β-hydride elimination is the rate determining step for Nickel, this may explain its poor reactivity compared to palladium but due to an easier oxidative addition, we can expect an easier reaction with aryl chlorides. As such, nickel should more easily use aryl bromides and chlorides. In addition, the HX elimination is considerably harder with nickel than palladium so nickel requires a stronger base.[23]

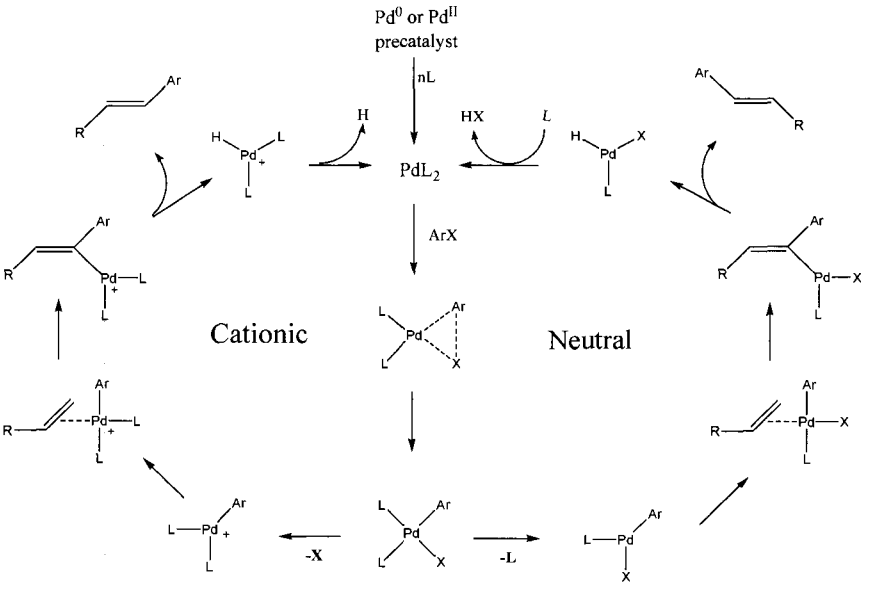


Scheme 1.6: Neutral and cationic mechanism

### 1.2.1.1 Donor Ligand

Palladium-stabilizing ligands are the most common form of Heck catalysts. Of those, phosphine ligands are by far the most used and studied but others, such as nitrogen, arsine, sulphur and carbenes based ligands have also been tested.[90] In most cases, the catalyst is produced *in situ* by the mixture of a palladium source, mostly $Pd(OAc)_2$ (but almost every type of palladium source has shown some reactivity), with the chosen ligand(s).[8] It was found quite early by Heck that phosphine ligands increase the half-life of the catalyst and therefore prevent to a certain extent the formation of relatively inactive palladium black.[9] The reaction is usually done at low temperature to help prevent the decomposition of the palladium-phosphine ligand complex which ultimately leads to palladium aggregation and/or palladium black, and thus, inactivation.

The electron donating nature of the ligand has shown to be an important feature of phosphine ligands. Electron-rich phosphines are thought to help the oxidative addition by counteracting

the positive charge which is formed on palladium during that step[92] (Scheme 1.3) and enables the use of non-reactive aryl-chloride as reactants.[95] In the late 90's, bulky phosphine ligands were used to accelerate the reductive elimination via steric effect.[110]

Many publications demonstrated that the P:Pd ratio influenced directly the reaction kinetics. In most cases, the reactivity was best when the P:Pd ration was of 1.5-2.0 or lower. Since the palladium is known to be in equilibrium with various amounts of ligands, one of those equilibrium states must be the active form. It was shown via NMR that the reaction speed was slower with two ligand compared to one[111] but that was only one study.

However, phosphine ligands are toxic, which makes their removal an expensive part of any commercial process. Some of the more complex phosphines can be quite expensive, even more valuable than the palladium metal used. At the same time, most phosphines are also air sensitive, which complicates the synthetic procedure.

There has been a recent interest in non-phosphorous based ligands, especially N, O and S based ligands. Despite the fact that they are much less studied than their P counterpart, interesting mechanistic data has emerged. In a trial with an iminophosphine ligand, it was shown that a polar solvent increases the rate of reaction and they also noticed an induction period. The reaction's temperature was 140°C indicating that the palladium-ligand complex probably degraded into colloids and may have gone through a ligand-free mechanism (section 1.2.4).[39]

### 1.2.2 $Pd^{II}/Pd^{IV}$ Cycle and Palladacycles

The $Pd^{II}/Pd^{IV}$ mechanism was first theorised by Herrmann[112] whose studies showed that their palladacycle did not add to an aryl bromide, only reacted in the presence of the olefin and showed no sign of reduction.[113] Following this, a full mechanistic proposal was made by Shaw.[114] The mechanism (Scheme 1.7) involves the coordination of the olefin to the palladacycle. This complex is susceptible to a reversible nucleophilic attack that could come from various sources, such as acetate ion or amines, already present in most reactions as the base. The palladium is now bound to two σ-donating carbons and a phosphine ligand which makes it electron rich and facilitates its oxidative addition. Following the reversible loss of the acetate ion, the rest of the cycle is fairly similar to the traditional mechanism with subsequent β-hydride and HX elimination to regenerate the catalyst.

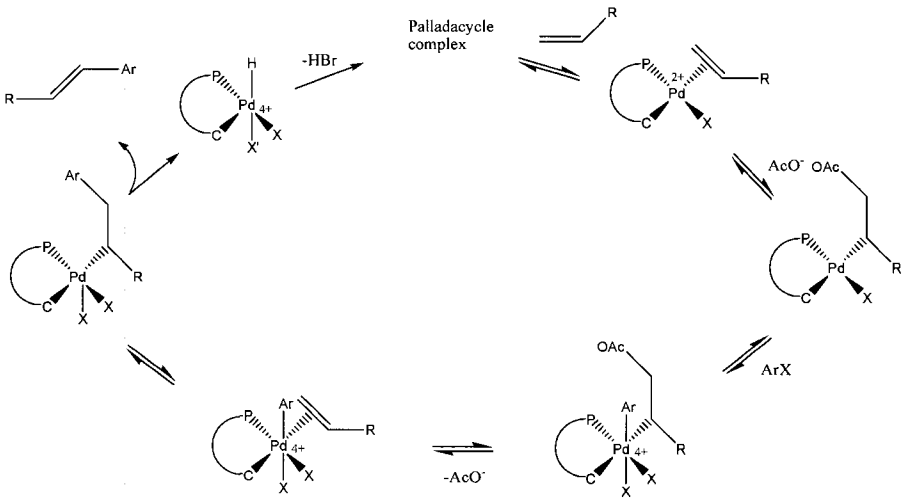


Scheme 1.7: Shaw's $Pd^{II}$-$Pd^{IV}$ mechanism for the HR[114]

$Pd^{IV}$ species are usually unstable but since a few have been isolated and characterized, it gave some credibility to the proposed mechanism.[115,116] Recent publications still acknowledge this mechanism as a valid option,[38,41,112,117] but there is a mounting evidence (nanoparticules in solution, induction period) that palladacycles only act as a reservoir for catalytically active

ligand-free species reacting through the traditional or anionic $Pd^0/Pd^{II}$ mechanism (section 1.2.4).[11,43,44,78]

Palladacycles showed early activity toward aryl chlorides. Palladacycles tend to be more air-stable and resistant to degradation than conventional phosphine ligands.[44] Some showed stability up to 250°C which is more than 100°C over most phosphines ligands[112] and may explain their longer half-life.[118] Despite the high stability of palladacycles, it was shown by many groups that some palladium broke free and formed colloids and nanoparticules.[43,44] Also, chiral non-racemic SC palladacycles gave racemic product, in conjunction with an induction period.[42,43] These observations indicate that the palladacycles are most likely reservoirs for a catalytically active, ligand-free, $Pd^0$ species.

In recent years, there has been an increase in the use of heteroatoms for palladacycles; the most common being P, N and S.[44]

### 1.2.3 Anionic Cycle: Ligand-mediated anionic mechanism

The anionic mechanism has two variations; the ligand-mediated and the ligand-less cycle. The ligand-mediated anionic mechanism for the HR was first proposed by Amatore and Jutand.[119] Throughout the 1990's, they have accumulated a large body of evidence that show chlorine or acetate ions intimately participating in the reaction by forming anionic intermediates.[100,120-125] They attribute their discovery to the use of electrochemical techniques that allowed the study of *in situ* short-lived intermediate ($10^{-1}$-$10^{-8}$s) and enabled investigations on real catalytic cycle rather than with stable complexes or selected segments of the catalytic cycle.[126]

When acetate ions are present in solution, either from the precursor ($Pd(OAc_2)$) or the base (KOAc), they observed a rapid formation of $L_2Pd(OAc)_2$ followed by a slow formation of $L_2Pd\ (OAc)^-$.[120] Studies where chlorine ions were present showed similar results where $PdL_2$ formed the anionic complex $L_2PdCl^-$.[126]

The anionic mechanism explains ion effects that the previously viewed mechanisms cannot account for. The speed of the oxidative addition is affected by the anions or cations in solution (Halide salt, Pd precursor and reducer). The oxidative addition is accelerated by cations in solution due to an ion-pairing effect that weakens the acetate or halide bond (scheme 1.8) forming a more naked complex closer to $PdL_2$. The use of organic bases like $Et_3N$ can inhibit this ion-pairing effect and reduce the rate of oxidative addition.

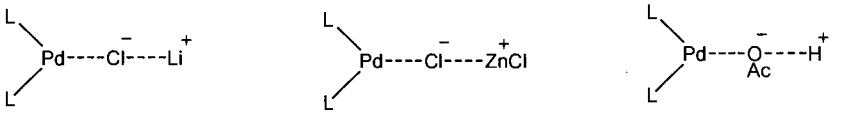


Scheme 1.8: Ion pairing effect

The result of the oxidative addition is an unstable[127-129] penta-coordinated species $PhPdL_2IX$ or $PhPdIL_2(OAc)$ that quickly degrades to a neutral tetracoordinated species through the loss

of the best leaving group between the halide(s) or acetate ($PhPdL_2X$ or $PhPdL_2(OAc)$).[130,131] $PhPdL_2(OAc)$ showed higher activity than $PhPdIL_2$, which can be explained by its ability to protect the olefin insertion site (Scheme 1.9).

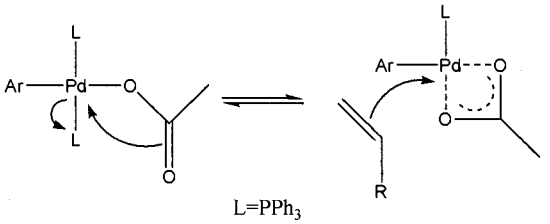


$L=PPh_3$

Scheme 1.9: Protection of the olefin insertion site

Before ligation to the olefin, the $PhPdL_2(OAc)$ species can lose the acetate to form a cationic intermediate in the same fashion as the cationic mechanism. The activity of this intermediate was assessed and the slower reactivity was attributed to the formation of an unreactive trans adduct. This unfavourable reaction was used Amatore and Jutand to explain the reactivity of this particular intermediate. The equilibrium between those two olefin insertion intermediate (neutral and cationic) is strongly affected by acido-basic reaction between the acetate and cations in solution in a similar fashion to the oxidative addition as cations reduces the strength of the Pd-OAc bond. Therefore, the base has the effect of interacting with free cations from solution which strengthens the Pd-OAc or Pd-X bond and thus, pushes the equilibrium toward the more reactive neutral species. To resume, the base slows the oxidative addition and accelerates the β-hydride elimination[126].

It is important to understand the fluidity of this mechanism. As the reaction progresses, the amount of ions in solution will increase and this is due to the acid formed during the reaction (HX). It is therefore very likely that the neutral or cationic mechanism may be more efficient at the beginning of the reaction but as it evolves, the anionic pathway may be more and more significant. In conclusion, Amatore and Jutand exposed an anionic mechanism that works in

parallel with the traditional neutral and cationic mechanism. Which mechanism the reaction proceeds through is determined by the types of ion and ligand present as well as their respective concentration.

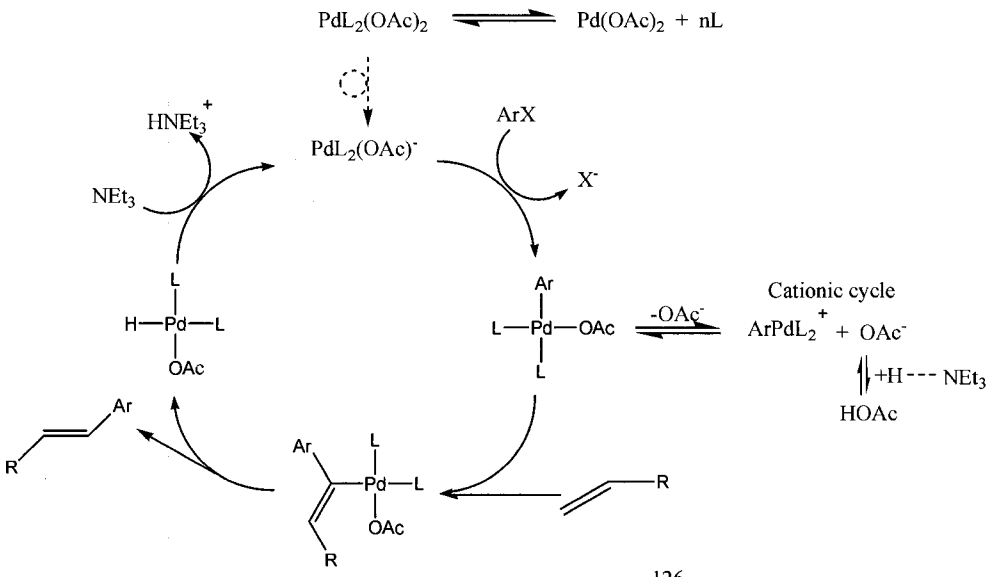


Scheme 1.10: Ligand-mediated anionic mechanism[126]

### 1.2.4 Anionic Cycle: Ligand-less anionic mechanism

The ligand-less anionic mechanism is the other variation of the anionic mechanism. Ligand-free, or ligand-less HR refers, as its name suggests, to a reaction done without traditional ligands such as donor ligands and palladacycles.[90]

The first HR were done without any ligands[4,6] and ligand-less catalysts have since been studied by many groups but it is only recently that there were direct investigations into their mechanism.[132] Independent studies by Evans[132] and deVries[10,111,133-135] showed many intermediates that were later incorporated by deVries in an anionic mechanism (Scheme 1.12).[134] In 2002, Evans was able to grow crystals of $(Pd_2I_6)(NEt_3H)_2$, when all the reagents of a HR were together. He proposed from this that the resting state of Palladium in solution was as a dimmer ($Pd_2I_6^{2-}$). Also, EDE and QEXAFS measurements during the first forty minutes showed a co-ordination sphere of 3 iodines that was interpreted as being a dimer of the oxidative addition that, when broken, exposed a free co-ordination site for the olefin (Scheme 1.11).

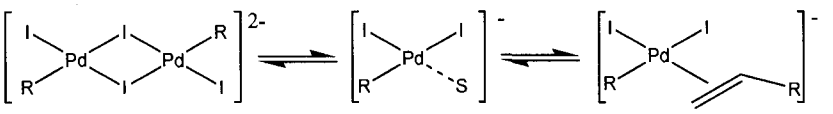


Scheme 1.11: Oxidative addition product equilibrium

In the same year, deVries published a study in which they followed the reaction between iodobenzene and butyl-acrylate using $Pd(OAc)_2$ through ES-MS. Throughout the reaction they were able to detect many intermediates ($(H_2O)PdOAc^-$, $PhPdI_2^-$ and $PdI_3^-$) and monitored their evolution. They observed that the amount of $(H_2O)PdOAc^-$ diminished when the amount of $PhPdI_2^-$ and $PdI_3^-$ increased.[10]

At the onset of the reaction, they observed a quick formation of $(H_2O)PdOAc^-$ that went through the oxidative addition to form $PhPdI_2^-$. They propose, as did Evans[132], that these

species can be bound to the solvent and/or exist as a dimmer (Scheme 1.12). No intermediates for the olefin insertion or β-hydride elimination was observed but, from Amatore and Jutand's anionic mechanism, we may suggest that the solvent or ions in solution (base, salt) can act as ligands to stabilise the various palladium species. The next intermediate to be observed is $PdI_3^-$ which is believed to be, as Evans suggested, a reservoir of soluble palladium species. At the end of the proposed cycle, the $PdI^-$ can either return in the cycle or react with $I_2$ (whose presence is presumed to be due to trace oxygen in solution) to form $PdI_3$, or its dimmer $Pd_2I_6^{2-}$.

While ligand-free catalysts can work at relatively low temperature[28], the ligand-free anionic cycle is also believed to apply in all high temperature and heterogeneous reactions where the catalysts are now believed to leach into solution and degrade into colloids.[112,126] DeVries[10] recently exposed the growing evidence that at high temperature, low S/C ratio, despite what type of catalyst is used, almost always leads to higher TON. This is best explained through equilibrium between the active monomeric palladium species ($PdI^-$) and colloids. Based on LeChatellier principle, low S/C can push the equilibrium toward monomeric palladium and slow or stop the formation of colloids and palladium black.

It was observed that those systems could be stabilized by the use of quaternary ammonium compounds or phosphonium salt[36] (Jeffery conditions[108]). These additives improve the TON by stabilising colloids which partially suppresses the formation of palladium black.

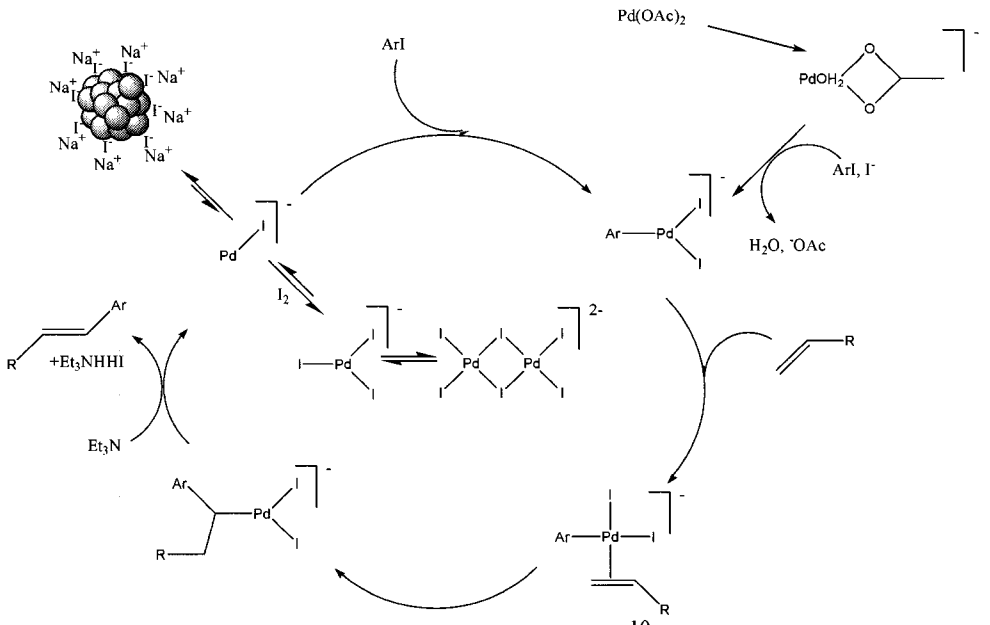


Scheme 1.12: deVries anionic ligand-less mechanism[10]

### 1.2.4.1 Colloids and Soluble Nanoparticles

The first example off palladium colloids and soluble nanoparticules for the HR were reported respectively by Beller[88] and Reetz[86] in the mid-1990's. Colloids can be stabilized in solution by surfactants, salts, polymer or ligands.[86] Nickel colloids have been scarcely studied by Reetz whose Ni/Pd bi-metallic clusters were more reactive than Palladium alone.[89] Their reactivity was first believed to occur on the surface[90] but early investigation gave mixed results as some catalysts showed bleeding[84] and others did not.[89]

In recent years, using a PVP(poly(vinylpyrrolidone))-stabilized nanoparticules with the Suzuki-Miyaura reaction, El-Sayed has gathered strong mechanistic evidence indicating that the boronic acid binds to the surface of the nanoparticle and reacts afterward with aryl halides in solution.[136-138] He proposes that the morphological changes on the surface are due to the harsh experimental conditions and suggests that the leached palladium species are

scavenged by PVP thus negating the homogeneous catalysis mechanism.[139] While we found no similar studies for the HR, alkene oxidation is known occur heterogeneously.[140,141]

Using colloids of various sizes, Antonietti demonstrated that the smaller the colloids, the faster the reaction.[85] Afterward, Blackmond was able to correlate the initial reaction rate with the particle size by calculating the amount of kink sites available[87] estimating that surface catalysis would needs to occur at kink (defect) sites to allow the palladium atom enough coordination space to go through the whole cycle.[142]

Dupont[143] recently demonstrated that the amount of leached species in solution followed the reaction. They used the Pd dissolution and re-precipitation cycle proposed by Kohler[144] to explain the reactivity and the increase in colloid size during the reaction.

While the proportion of the catalysis that occurs on the surface of the colloids and nanoparticules is difficult to assess, it is becoming increasingly accepted that most of the catalysis occurs via leached palladium species.[90] Since most of these reactions are done without ligands and at high temperature, leached species are likely to go through the ligand-less anionic mechanism proposed by deVries and Reetz.[10,84,145] Despite this, no convincing evidence indicates that the reaction cannot, to a certain degree, occur on the surface of the colloids.

#### 1.2.4.2 Supported Nanoparticules

Mizoroki was the first to use a heterogeneous source, palladium black, for the HR.[4,5] Subsequently, this area of heterogeneous catalysis was only studied by a few groups[90] until Augustine[63,64,140,141] resuscitated it in the early 1990's. Using various supports such as carbon, silica, alumina and magnesia, he reported that acidic supports, such as silica, removed electron density from the palladium and lead to β-substitution while basic supports

lead to α-substitution. This is in line with the $Pd^0/Pd^2$ mechanism (scheme 1.4). Basic supports were also shown to be active against leaching presumably due to their ability to recapture Pd from solution.[146] A similar study by Kohler gave the following order of reactivity for the supports; $C>TiO_2>ZrO_2>MgO>ZnO>SiO_2$.[69]

Augustine[63,64] also drew a parallel between the catalysts activity and the availability of coordinatively unsaturated corner atoms as only these sites possess enough available orbitals to interact with both reactants. They also found no activity after filtration. These results suggested true heterogeneous catalysis. However, recent studies have shown that the kink sites are prone to leach via oxidative addition of the aryl halide thus liberating the palladium to react in a homogeneous fashion.[147-149]

More recently, a vast amount of mechanistic studies were made independently by Kohler[69,144,146,149-152] and Arai[153-159] using Pd/C and $Pd/MO_x$ respectively. By monitoring the amount of Pd in solution, Arai found that organic base and coordinating solvents (DMF, NMP) facilitate leaching.[158] Organic bases are able to coordinate leached species and stabilize them to a certain degree, something most inorganic bases cannot do. By using organic and inorganic bases together, they proposed that they play a complementary role with the organic base responsible to the activation and stabilisation of leached palladium while the inorganic base regenerates the catalyst via HX elimination. This was found for palladium[158] and nickel[155] alike.

Arai also observed a rapid redeposition of palladium on the support occurs toward the end of the reaction and the amount depends on the temperature and the support,[158] two subject that were investigated in detail by Kohler.

Kohler studied in particular the leaching and found that low temperature and high concentration increased leaching and the amounts leached in solution followed very well

with the product formation; growing rapidly at the onset of the reaction with a quick decrease as the conversion neared 100%.[144,149] He discovered that high temperature favoured redeposition as weak binding ligands such as organic bases and coordinating solvents are unable to completely stabilize palladium in solution leading to aggregates that precipitate on the available support. Other factors such as the exclusion of air/oxygen and reducing agents also help with the redeposition.[149,152]

The above detailed studies were performed with palladium catalysts. The only mechanistic investigation into the nickel heterogeneous cycle we found was performed by Lipshultz using mesoporous Ni/C.[91,160-164] By monitoring nickel bleeding (leaching), they found that its concentration did not vary as the reaction proceeded, unlike Arai observed for Pd. Nickel showed a rapid dissolution during the first minute of reaction followed by an eventual redeposition, only when the reaction ended. In an earlier study, Lipshultz proposed that the amount leached was not enough to account for the entire catalysis and this was based on a side reaction that, with the same amount of a homogeneous catalyst, showed less reactivity.[164] Because they used a mesoporous support, they recently referred to leaching inside the pores as a possible explanation to explain this difference. The amount inside the pores is not seen in solution and augments the amount of reactive catalyst. However, they also noticed that the redeposition of leached species seemed to block the pores thus cancelling the added advantage of a porous catalyst. Pore blocking seemed to increase with the catalyst loading.[91]

In their experiments, Lipshultz et al. used ligands in their reaction mixture following standard reaction conditions, although it is unclear if a true heterogeneous catalysis would needs ligands to work. When debating the possibility of true heterogeneous catalysis, they wonder how the nanoparticles surface can accommodate the reactants and ligands[164] but they

most likely only stabilise leached nickel species. Their conclusion was that the nickel heterogeneous Heck mechanism was similar to the palladium mechanism where the aryl halide oxidatively adds to Ni(0) and transports it in solution where the catalysis occurs, with subsequent redeposition on the support.[91]

## 1.3 Scope of this Thesis Work

The palladium heterogeneous Heck mechanism has been widely studied and it is becoming accepted that the majority of the activity is promoted by leached species. However, the contribution of true surface chemistry is still being debated and since metal catalysts such as palladium have been shown to be in their most active state when speciated as nanoparticles[165] we would like to further analyse the implication of the surfaces in the heterogeneous HR by using various analysis such as the triple phase test.[166]

Various supports have been tried throughout the years and reducible transition metal oxide appeared to promote a high reactivity.[69] We believe it would be interesting to examine the aptitude of YSZ as a support for organic C-C coupling reactions such as the HR. As Kohler demonstrated, $ZrO_2$ and other acidic supports showed an increase in reactivity. YSZ is also acidic and has the additional ability of allowing ionic mobility[167]. We hope that its electronic properties will facilitate reactivity. Using various simple synthetic procedures such as the self-assembly[168] and the co-precipitation method[167], coupled with various calcination temperatures, we will be able to control, to a certain degree, the surface area, metal loading and particle size of the catalytic material.

Finally, Kohler studied the structure activity relationship between palladium and various supports[152] but similar work have yet to be done with other metals. It is in this optic that we decided to do a structure-activity relationship study using a nickel heterogeneous catalyst for the HR. Especially due to its potential for the use of accessible and affordable aryl chlorides,[23] nickel could replace palladium as the choice metal in Heck catalysis.

It is our goal to find a simple and practical method for an efficient Heck reaction using Pd-YSZ and Ni-YSZ.

# Chapter 2 - EXPERIMENTAL

## 2.1 Characterization

During the course of our experiments, various techniques and instruments were used in order to obtain, analyse and/or characterize the data. This section goes through their specific utility in our research.

### 2.1.1 Gas Chromatography (GC) and Gas Chromatography-Mass Spectrometry (GC-MS)

The reactions were monitored through a GC or a GC-MS. The GC separates the various compounds from a solution mixture by their polarity and molecular weight. In the GC-MS, as soon as each separated compound leaves the GC, they enter the MS. This instrument ionizes species enables us to identify them by their mass to charge ratio (m/z). Components elution time and characteristic m/z ratios were used to identify the distinct chemical species. The peaks were well separated and no overlap occurred. In both GC's, the components eluted at similar times. The reactants, butyl-acrylate and iodobenzene, had elution time of 3.5 and 5.3 minutes and m/z ratio of 127 and 204 respectively. The standards, decane and tetradecane, eluted at 4.8 and 8.0 minutes and had m/z ratios of 142 and 190 respectively. The product, butyl-cinnamate, eluted between 11 to 12 minutes and had a m/z ratio of 204. In our experiments, we focussed on fragments with a single charge which makes the ratio equal to their molecular mass.

The GC was an Agilent 6890N. The column was an Agilent 19091J-413 with Helium as the mobile phase and hydrogen for the flame detector. The GC program used a 2 minute solvent

delay at 60°C and then went from 60°C to 180°C at 15 °C/min and from 180 °C to 300°C at 30 °C/min.

The GC-MS was an Agilent 6890N coupled with a 5973 Network Mass Selective Detector. The column was an Agilent 190915 HP5MS and the mobile phase was high purity helium. The GC program used a 2 minute solvent delay at 60°C and then went from 60°C to 255°C in 13 minutes (15°C/min).

### 2.1.2 Powder X-Ray Diffraction (p-XRD)

A crystal structure is composed of a repetitive structure called a unit cell [169,170]. X-ray diffraction for a crystalline material obeys Bragg's law where n is an integer, λ is the wavelength of the X-ray and d the distance between the atomic plane:

$$n\lambda = 2\mathrm{d}\sin\theta \qquad (1)$$

From the width of the peaks, we can calculate the crystallite size using the Williamson-Hall plot. The width is influenced by the crystallite size (t), the strain (Δd/d) and the instrument. After correcting for the instrument, we assume a Lorentzian shape for the peaks:

$$B = 0.92/t\cos\theta + 2(\Delta d/d)\tan\theta \qquad (2)$$

The Williamson-Hall plot is B cosθ versus sinθ and it enables us to find the crystallite size (t) and the strain (Δd/d) using many peaks from the spectrum, minimizing the error.

In the case of partially crystallized material, the area of the peaks represents only the crystallized portion.

The instrument was a Philips PW130 using Cu K α radiation at wavelength of 1.54Å with a Kevex Psi Peltier cooled solid state detector. The diffraction patterns were analysed with MDI JADE 6.1.

Two sample preparations were used for powder XRD (p-XRD) measurements; the disk and slurry methods. In the disk method, the sample was finely crushed and packed in a sample disk until it was flush with the height of the disk. In the slurry method, the powder was crushed in acetone and deposited on a quartz slide forming a thin film. The slurry method has an intrinsic error since the sample is slightly elevated above the axis of rotation of the instrument.

### 2.1.3 X-Ray Fluorescence (XRF)

When an X-ray of a certain energy hits an atom, it can eject a core electron, following this event, an electron from an outer shell will go down to replace it and in doing so, will emit X-ray with an energy characteristic for each element[171]. XRF was used to analyse the precise composition of our nickel catalysts.

Our catalyst (0.1g, very finely crushed) was mixed with a paraffin binder (1.9g). The whole was stirred thoroughly to obtain homogeneity and was pressed into a disk shape. The disk was exposed to X-ray on both sides and the average was compared with a calibration curve. The calibration curve had been previously done using 4 standards containing the following mass ratios of products;

1- 0.0 Ni, 11.7 $Y_2O_3$, 91.3 $ZrO_2$

2- 23.70 Ni, 8.20 $Y_2O_3$, 44.12 $ZrO_2$

3- 39.29 Ni, 31.25 $Y_2O_3$, 5.86 $ZrO_2$

4- 55.0 Ni, 18.91 $Y_2O_3$, 3.51 $ZrO_2$

The instrument was a Philips 2400 and the analysis was done using the Super Q quantitative software.

### 2.1.4 Surface area

The surface area of a powder can be defined as: the extent of available surface as determined by a given method under stated conditions. It is generally found by exposing a powder to a gas that binds, or is adsorbed, in representative way to the powder. There are 2 types of adsorption process; physisorption and chemisorption. Physisorption is an adsorption process without chemical bonding and usually has low specificity while chemisorption is an adsorption process where chemical bonds are formed and is strongly affected by the reactivity of the adsorbent and adsorptive[172].

The measurements were done using a Quantachrome Autosorb I-C. Our measurements were only done once, however the intrinsic error of the measurement is typically small. An overestimation of the error in these measurements is 10%, and therefore we assume this value as the error of our measurements.

#### 2.1.4.1 Physisorbtion

The method that is used the most to asses the surface area of solids was published in 1938 by Brunauer, Emmet and Teller (BET)[172,173]. The BET equation uses a linear plot in the adsorption isotherm (equation 3), normally found between P/Po of 0.05 and 0.35. In the equation, W is the weight of the gas adsorbed, P/Po is the relative pressure and Wm is the weight of adsorbate which forms a monolayer. The term C refers to the BET C constant that correlates to the energy of adsorption in the first adsorbed layer. This term is affected by the adsorbent-adsorbate interactions and is usually known prior to the experiment.

The surface area is found by plotting 1/ W((Po/P)-1) v.s. ($P/P_o$). Using the slope and the intercept, we find Wm (equation 4) which we use to find the surface area (SA) (equation 5) where N is Avogadro's number, Acs is the molecular cross-sectional area of the adsorbate molecule and $M$ is the molar mass of the adsorbate.

$$\frac{1}{W[(P_0/P)-1]} = \frac{1}{W_m C} + \frac{C-1}{W_m C}(P/P_0) \qquad (3)$$

$$W_m = \frac{1}{s+1} \qquad (4)$$

$$SA = \frac{W_m \times N \times Acs}{M} \qquad (5)$$

The calculation of the mesopore size distribution was done using the Barrett, Joyner and Halenda (BJH) methodology developed in 1951.

At high P/Po (close to one), all pores are filled with a physisorbed layer (thickness $t_l$) as well as an inner capillary (radius $r_K$). As $P/P_o$ is lowered (n=1), there will be a thinning of the inner capillary of the largest pores (radius $r_p$). When $P/P_o$ is lowered anew (n=2), the volume desorbed (V) refers to physisorbed layer of the largest pore but also to the thinning of the inner capillary the next largest pore. The volume desorbed can be expressed as:

$$V_{pn} = \left[\frac{r_{pn}}{r_{Kn} + \Delta t_n/2}\right]^2 \left[\Delta V_n - \Delta t_n \sum_{j=1}^{n-1} Ac_j\right] \qquad (6)$$

The mesopore area, assuming the geometry is cylindrical, is:

$$A_p = \frac{2V_p}{r_p} \qquad (7)$$

The methodology was as follow. The sample was put inside the physisorption cell and degassed for at least 3hr to remove any volatile molecule (mostly water). Following this, the sample was precisely weighted and a nitrogen isotherm, at -196 °C, was taken.

### 2.1.4.2 Chemisorbtion

Chemisorption was used to measure the metallic surface area, their average crystallite size and the percent metal dispersion of our Ni-YSZ and Pd-YSZ powders. Since physisorption is usually easier to achieve than chemisorption, the isotherm obtained is combination of physisorption and chemisorption. Minimisation of the physisorption is made by doing the isotherm at a high (above 0°C) temperature where the chemisorption process becomes more important than the physisorption. A correction is needed to isolate the chemisorption.

The correction method used to isolate the chemisorption was the extrapolation to p=0. At high enough pressure, the isotherm usually forms a plateau where all the chemisorption sites have already been filled and any further increase in adsorption is only physisorption. By drawing a strait line from points at high temperature and extrapolating it to p=0, the y intercept will give us the total amount of gas chemisorbed (Vm) from where we can calculate the monolayer uptake ($N_m$) (equation 6) and the metal's active surface area (ASA) (equation 7). The example below is for hydrogen and S is the adsorption stoichiometry and $A_m$ is the cross-sectional area of each surface atom.

$$N_m = 44.61 V_m \qquad \textit{(8)}$$

$$ASA = \frac{N_m \times S \times A_m}{166} \qquad \textit{(9)}$$

The percent metal dispersion (D) (equation 10) gives us the fraction of metal atom that are exposed on the surface and therefore, reactive toward catalysis. M represents the molecular weight and L represents the percent loading of the metal.

$$D = \frac{N_m \times S \times M}{100 L} \qquad \textit{(10)}$$

Lastly, the calculations for the average crystallite size (d), assuming a spherical particle shape, can be found using equation (11) where Z is the density of the metal.

$$d = \frac{600L}{ASA \times Z} \qquad (11)$$

To analyse our samples, our catalyst was put inside a chemisorption cell and reduced for 2 hours at 600°C under flowing $H_2$ (99.999% Praxair). An isotherm at 40°C was taken (Hydrogen for nickel and carbon monoxide for palladium).

### 2.1.5 Fourier Transformed Infrared Spectroscopy (FTIR)

Functional groups such as OH, NH and C=O present in many organic molecules absorb light in the IR range of 4000-1500cm$^{-1}$ through a vibrational excitation.[174] Because of this specificity, the infrared spectrum is often used to identify organic compounds.

The instrument used was a Bruker equinox 55 that scanned from 4000cm$^{-1}$ to 600cm$^{-1}$ and the spectra was analysed by the associated OPUS software.

### 2.1.6 Nuclear Magnetic Resonance (NMR)

NMR is widely used to determine the structure of molecules. It can give information on the type and number of atoms with their respective connectivity along with the ability to differentiate molecules in a known solution mixture.[174]

The instrument used was a Bruker Advance 300MHz. The runs were made in Chloroform-d and the program used to analyse the spectrums was MestReC.

## 2.2 Catalysts Synthesis

This section goes through the various synthesis procedures used for this work. The first method we explain will be the self-assembly method and it was used to make Nickel as well as Palladium catalysts. The subsequent co-precipitation methods were only used to make Nickel catalysts. The reactants and solvents of this section were all bought from Aldrich chemical and were used without further purification, unless otherwise specified.

### 2.2.1 Self-assembly Method (SA)

The self-assembly method is a three step process. The first step is the synthesis of the zirconium glycolate and the second is the synthesis of the yttrium glycolate. The last step involves the mixture of both glycolates with the desired amount of metal to obtain the metal-yttria stabilized zirconia.

The zirconium glycolate was prepared in a 100mL round bottom flask fitted with a vertical condenser (air cooled) on top of which is a distillation setup (horizontal condenser with running water). One equivalent of zirconium ethoxide was introduced (18.45mmol, 5.0g, Strem chemical, 99.9+%) along with 2.4 equivalent of sodium hydroxide (44.87mmol, 1.7g) and a large excess of ethylene glycol (50mL, spectroscopic grade). The solution was refluxed (~195°C) for 24 hours under flowing nitrogen. Subsequently, the ethylene glycol was evaporated by augmenting the temperature and isolating the vertical condenser with glass wool.[ii]

A zirconium glycolate was also prepared using zirconium chloride (18.45mmol, 4.30g) instead of zirconium ethoxide (see section 2.2.5 for nomenclature). This was done using the same methodology as above

[ii] Without isolation, the vertical condenser remained cool enough to retain the ethylene-glycol.

The yttria glycolate was prepared in a 100mL round bottom flask with yttrium acetate tetra hydrate (3.54mmol, 1.2g, Alfa Aesar, 99.9%) and a large excess of ethylene glycol (31mL). The solution was stirred at room temperature for 30 minutes.

The final solution was prepared while the zirconium glycolate was still warm (150°C). The yttrium glycolate was added drop wise and under heavy mixing to the zirconium glycolate solution. Separately, in a one litter plastic bottle was mixed the distilled water (120mL), Cetyltrimethylammoniumbromide (CTAB) (4.0g), NaOH (1.71g) and a metal source. For the palladium catalyst, Palladium nitrate (2.0mL of a 10wt%$Pd(NO_3)_2$ in 10%Nitric acid solution) was used while for the nickel catalyst we used Nickel chloride hexahydrate (1.06mmol, 240.30g). The example above is for the 5mol% ratio. The amount of metal added was varied to obtain the desired molar ratio (1, 5 or 10 mol%).

When both these solutions were prepared, the zirconium-yttrium glycolate solution was added to the plastic bottle. The solution was shaken and stirred for 30 min to ensure homogeneity. The solution was heated in at 80°C for five days. Afterward, the precipitated obtained was filtered, rinsed three times with deionised water (DI) and dried at 120°C for six hours to obtain 5mol% metal-Yttria Stabilized Zirconia as-synthesized (nomenclature in section 2.2.5).

The CTAB will form micelles in solution that will force the oxide to form around it. Following the calcination (section 2.2.3) the CTAB will burn leaving mesopores throughout the oxide (scheme 2.1). The stability of the mesostructure is affected by the calcination temperature.[175]

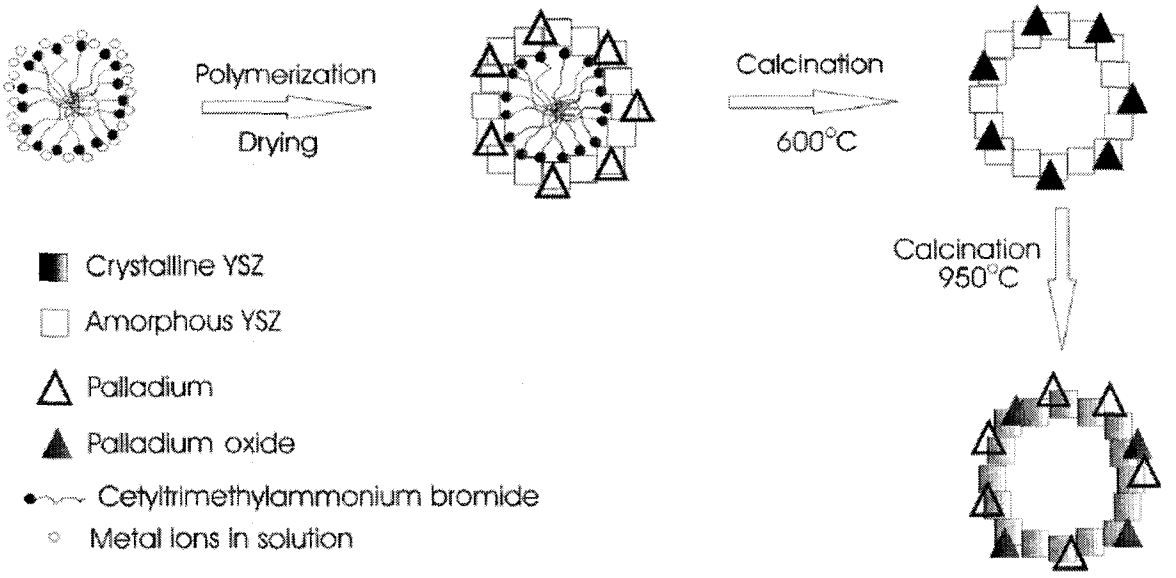


Scheme 2.1: Mechanism of formation of mesoporous Pd-YSZ

### 2.2.2 Co-precipitation Method

The co-precipitation method was only used for nickel catalysts. Yttrium oxide (8.55mmol, 2.032g) was dissolved overnight in 20mL of 50%HCl solution under heavy stirring. Zirconium chloride (86.45mmol, 20.145g), the dissolved yttrium oxide and nickel chloride hexahydrate (5.00mmol, 1.129g) were mixed in a 1 litre beaker containing 300mL of DI water.

When using sodium hydroxide (NaOH) as precipitating agent, we added, drop wise, a 2M solution of NaOH while stirring, up to a pH of 9.5. The precipitate obtained was filtered and rinsed three times with DI water.

When using ammonia ($NH_3$) as the precipitating agent, gaseous ammonia was bubbled through the solution up to a pH of 9.5, while stirring. The nickel forms a soluble nickel-chloride-ammonia complex that is in equilibrium with the precipitated nickel and as such, a greater amount of nickel was necessary. Since approximately 80% of the metal remains in

solution, we added 5X more nickel chloride (25.00mmol, 5.70g). The precipitate obtained was filtered and rinsed three times with DI water.

### 2.2.3 Calcination Parameter

Three calcination temperatures were used; 950°C, 600°C and 400°C. The calcinations to 950°C and 600°C were done in a Barnstead international F46110CM high temperature muffle furnace while the calcinations to 400°C were done in a tubular furnace. All calcinations were done in air.

For the calcinations at 950°C, the furnace was ramped from room temperature to 950°C at 25°C/min, the temperature was maintained there for 2 hours then cooled back to room temperature at 50°C/min.

For the calcination at 600°C, the rate from room temperature to 600°C was 5°C/min. The sample was kept at that temperature for 2 hours then cooled back to room temperature at 50°C/min.

For the calcination at 400°C, no specific rate could be programmed. The temperature increased from 25°C to 400°C in ~15min. When the temperature was reached, it was kept there for 2 hours then the furnace was turned off and left to cool back to room temperature (~4hr).

### 2.2.4 Reduction Parameter

The palladium catalysts previously calcinated to 950°C was reduced under flowing nitrogen at 800°C. Nitrogen was flowed for 20 minutes to remove all the oxygen in the heating chamber. The catalyst was then heated at 800°C for 30 minutes under flowing nitrogen.

Over 800°C, the palladium is reduced and since no oxygen is present during the cooling step, it remains reduced[176].

The palladium catalysts previously calcinated to 600°C was reduced under flowing hydrogen at 600°C for two hours

Every nickel catalyst was reduced under flowing hydrogen at 400°C for three hours.

### 2.2.5 Catalysts Nomenclature

In order to simplify the comparisons between catalysts, each was given a specific name detailing its composition as well as its synthesis. The general formula was;

1 2 3 4 5
(metal mol%) (metal-YSZ) (synthesis) (calcination temperature) (reduction status)

1- metal mol%– 3 different metal loading were prepared: 1, 5 and 10%

2- metal-YSZ – Two metals were studied; nickel (Ni-YSZ) and palladium (Pd-YSZ). The support was always 9%YSZ.

3- synthesis – The 4 different synthesis methods are:

(SA) self-assembly using $Zr(EtO)_4$

(ZrCl4) self-assembly using $ZrCl_4$

(OH) coprecipitation with NaOH

(NH3) coprecipitation with $NH_3$

4- calcination temperature – The 3 calcination temperatures were 400°C (400), 600°C (600) and 950°C (950). As well, prior to calcination, the sample was labelled ''as-syn''

5- reduction status - An oxidised palladium catalyst will be ''PdO'' and the reduced ''Pd''. Similarelly, we will refer to ''Ni'' and NiO'' to indicate the oxidation state of nickel catalysts

Finally, a catalyst which has already been utilized in a reaction will be labelled ''used''

Here are two examples to clarify.

A 1 mol% nickel sample synthesised by coprecipitation with $NH_3$, prior to calcination, will be labelled as follow:

1%Ni-YSZ NH3 as-syn

A 5 mol% palladium sample which was synthesised using the self-assembly method, calcinated to 950°C will be labelled as follow;

5%PdO-YSZ SA 950

Following its reduction at 800°C under air:

5%Pd-YSZ 950*

*note: since every palladium catalyst was synthesized using the self assembly method, the method name (SA) will not always be shown to avoid redundancy.

## 2.3 Reaction Procedure

The reactants and solvents of this section were all bought from Aldrich chemical and used without further purification unless otherwise specified. The error on the data points have been estimated to 4% based on the sampling method.

### 2.3.1 Heck reaction using Pd-YSZ

The reaction was run in 10mL round bottom flask with condenser and septum. The reactants were iodobenzene (4.0mmol, 445μL) and butyl-acrylate (4.8mmol, 685μL). The internal standard was decane (0.4mmol, 78μL) at a ratio of 0.1 to iodobenzene. The catalyst was 5% Pd-YSZ (0.004mmol, 0.0097g) at a ratio of 0.001 (or 1000/1) to iodobenzene. The base was *N,N*-diisopropylethylamine (DIPEA) (8mmol, 1.4mL) at a ratio of 2 to iodobenzene. The solvent was *N,N*-dimethylformamide (DMF) (1.4ml) to have the concentration of iodobenzene at 1.0M[iii].

The flask was inserted in an oil bath at 140°C and stirred with a magnetic bar. Reactions using Pd showed no noticeable difference when doing the experiment under argon or under air. To simplify the procedure, the experiments were done under air.

A sample of 50μL was taken from the reaction solution every 30 minutes and put in a 1 dram vial. The vial was filled with a 1:1 ratio of water:ether and shaken. The ether phase was extracted using a glass pipette and put in a GC vial.

[iii] Due to the high concentration of reactant, the concentration of reactants was always calculated as the moles of iodobenzene over the total volume.

#### 2.3.1.1 Procedure modifications for other Heck reactions using Pd-YSZ

This section shows the different products and their quantities used when doing the various other experiments. The general procedure of section 2.3.1 applies to all of section 2.3.3.1.

To check the catalyst under different oxidation state, we tested palladium (5% Pd-YSZ 950) versus palladium oxide (5% PdO-YSZ 950). The catalyst calcinated to 950°C was used as the oxidized catalyst and a portion of the same catalyst was reduced at 600°C, and used as the reduced catalyst. The reactants were the following: iodobenzene (2.0mmol, 223μL), butyl-acrylate (2.0mmol, 285μL), 5mol%Pd-YSZ (0.002mmol, 4.9mg), DIPEA (4mmol, 695μL) and DMF (10mL). The temperature was set at 120°C.

The reactivity of two bases were studied; DIPEA (0.8mmol, 1.39mL) and $K_2CO_3$ (0.8mmol, 110.5mg). The solution contained: Ibz (0.4mmol), Bu-cin (0.48mmol), 5%Pd-YSZ 950 (0.004mmol, S/C 100), Decane (0.4mmol) and DMF (1.8mL) at 120°C.

To test the reactivity at different temperatures, the reaction was monitored at 120°C, 130°C and 140°C. The solution contained: Ibz (0.4mmol), Bu-cin (0.48mmol), DIPEA (0.8mmol), 5%Pd-YSZ 950 (0.004mmol, S/C 100:1), Decane (0.4mmol) and DMF (1.8mL).

Four concentrations of reactants were tested; 0.2M, 0.5M, 1.0M and 1.2M. The solution contained Ibz (4.0mmol), Bu-cin (4.8mmol), DIPEA (8.0mmol), 5%Pd-YSZ 950 (0.004mmol, S/C 1000), Decane (0.4mmol), DMF (respectively 17.40, 5.40, 1.40 and 0.73mL) at 140°C. The concentration was varied by changing the amount of solvent.

The pre-incubation experiment was done by making a solution with every reagent except one (one without iodobenzene and another without butyl-acrylate). Both solutions were mixed and heated at 140°C for 4hr. Following this, the missing reactant was added and the reaction was monitored. The solutions contained: Ibz (4.0mmol), Bu-cin (4.8mmol), DIPEA (8.0mmol), 5%Pd-YSZ 950 (0.004mmol, S/C 1000), Decane (0.4mmol) and DMF (5.4mL) at 140°C.

Solutions of 0.2M and 0.4M were studied at room temperature for 6hr. The amounts were as follow; iodobenzene (0.8mmol, 89μL), butyl-acrylate (1.2eq.), DIPEA (2eq.), Pd-YSZ (0.01eq.), decane (0.1eq.) and DMF (3.48mL-0.2M and 1.48mL-0.4M). Since no reaction occurred at that temperature, the solution was heated at 140°C for an hour, removed from the oil bath, left to cool to room temperature and monitored for 2hr

In order to verify the reusability of our catalyst, we compared the activity of 5% Pd-YSZ 950 versus 5% Pd-YSZ 950 used R. The solutions contained: Ibz (4.0mmol), Bu-cin (4.8mmol), DIPEA (8.0mmol), catalyst (0.004mmol, S/C 1000), Decane (0.4mmol) and DMF (5.4mL) at 140°C.

We tried the reaction with a higher substrate to catalyst ratio (s/c) of 100'000 / 1. In a 500mL round bottom flask, we added the following reactant; iodobenzene (0.20mol, 22.30mL), butyl-acrylate (0.24mol, 34.30mL), 5mol%Pd-YSZ 950 (0.002mmol, 4.9mg), DIPEA (0.40mol, 68.96mL) and DMF (78.49mL). The final volume was 200mL making a concentration of 1.0M. The temperature was 140°C.

The reaction was also tried with a s/c ratio of 1'000'000 / 1. This was done twice, the first time it was done in the following way. In a 2L round bottom flask, we mixed; iodobenzene (1.0mol, 111.48mL), butyl-acrylate (1.0mol, 142.73mL), 5%Pd-YSZ 950 (0.001mmol, 2.5mg), DIPEA (2.0mol, 348.38mL) and DMF (397.41mL). The final volume was 1000mL. The concentration was 1.0M and the temperature was 140°C.

The second trial was done exactly the same way except that only 230mL of DMF were added for a concentration of 1.2M and the catalyst was 5%Pd-YSZ 600 (0.001mmol, 2.5mg).

To check the catalyst under different calcination temperatures, we compared the activity of 5% Pd-YSZ 950 versus 5% Pd-YSZ 600. The solutions contained: Ibz (4.0mmol), Bu-cin (4.8mmol), DIPEA (8.0mmol), 5%Pd-YSZ 950 (0.004mmol, S/C 1000), Decane (0.04mmol) and DMF (5.4mL) at 140°C.

The Heck reaction was tried with chlorobenzene (2.0mmol) and bromobenzene (2.4mmol) instead of iodobenzene. The solutions also contained: DIPEA (4.0mmol), 5%Pd-YSZ 950 (0.004mmol, S/C 1000), Decane (0.02mmol) and DMF (0.75mL) at 130°C.

### 2.3.2 Heck reaction using Ni-YSZ

Some modifications were introduced when we tested our nickel catalysts. Most of the tests were performed at 130°C and the reactants were used in a 1:1 ratio. A different internal standard was used, tetradecane, at a concentration of 0.5 equivalents instead of 0.1.

The reaction was run in a 2mL vial with a septum in the cap. The reactants were iodobenzene (1.0mmol, 111μL) and butyl-acrylate (1.0mmol, 143μL). The internal standard was tetradecane (0.5mmol, 130μL) at a ratio of 0.5 to iodobenzene. The catalyst was 5% Ni-YSZ OH 600 (0.01mmol, 0.042g) at a ratio of 0.01 or 100/1 to iodobenzene. The base was potassium acetate (KOAc) (2.0mmol, 196mg) at a ratio of 2 to iodobenzene. The solvent was *N, N*-dimethylacetamide (DMA) (282μL) which gave a concentration 1.5M,

The vial was closed and argon was bubbled through the solution to remove oxygen[149]. The vial was then inserted in an aluminum plate at 130°C and stirred with a magnetic bar.

A sample of 5-10μL from the solution was put in a 1 dram vial every 30 minutes for the first hour and then every hour for up to six hours. The vial was filled with a ratio of 1:1 with water and ether and shaken. The ether phase was taken with a glass pipette, put in a GC vial and run on the GC.

#### 2.3.2.1 Procedure modifications for other Heck reactions using Ni-YSZ

This section shows the different products and their quantities used when doing the various other experiments. The general procedure of section 2.3.3 applies to all of section 2.3.3.1, only the changes are mentioned.

The reaction was tried at 120°C, 130°C and 140°C. The solutions contained: Ibz (1.0mmol), Bu-cin (1.0mmol), KOAc (2.0mmol), 5%NiO-YSZ 600 (0.01mmol, S/C 100), Tetradecane (0.5mmol) and DMA (270μL).

To examine the effect of the solvent, we tested *N, N*-dimethylacetamide (DMA), *N, N*-dimethylformamide (DMF), ethylene glycol and *N*-methyl-2-pyrrolidone (NMP). The solutions contained Ibz (1.0mmol), Bu-cin (1.0mmol), DIPEA (2.0mmol), 5%Ni-YSZ OH 600 (0.01mmol, S/C 100), Tetradecane (0.5mmol), solvent (270μL) at 130°C.

Another solvent test was done, this one with the following amounts of reactant; iodobenzene (0.2mmol, 22μL) and butyl-acrylate (0.2mmol, 29μL). DIPEA (0.4mmol, 70μL) was the base and the catalyst was 5%Ni-YSZ OH 600 (0.004mmol, 10mg). Four solvents (1mL each) were tested; dioxane (90°C), toluene (90°C), acetonitrile (60°C) and THF (60°C). All components were mixed in a 5mL round bottom flask, fitted with a condenser and argon balloon, which was set in an oil bath preheated at the indicated temperature. The samples were analyzed by GC-MS.

Three bases were tested; potassium acetate (KOAc) (2.0mmol, 196mg), *N, N*-diisopropylethylamine (DIPEA) (2.0mmol, 348μL) and sodium carbonate ($Na_2CO_3$) (2.0mmol, 212mg). The solutions also contained Ibz (1.0mmol), Bu-cin (1.0mmol), 5%Ni-YSZ 600 (0.01mmol, S/C 100), Tetradecane (0.5mmol), DMA (270μL) at 130°C.

Another experiment compared DIPEA and KOAc while taking into consideration the solid nature of KOAc. The amount of solvent was changed to obtain the same total volume for both solutions. The solutions contained Ibz (1.0mmol), Bu-cin (1.0mmol), base (2.0mmol),

5%NiO-YSZ 600 (0.01mmol, S/C 100), Tetradecane (0.5mmol), DMA (620μL and 270μL respectively) at 130°C.

We explored the effect of concentration of reactant. The concentration was varied by changing the amount of solvent. The solutions contained Ibz (4.0mmol), Bu-cin (4.0mmol), KOAc (8.0mmol), 5%NiO-YSZ 600 (0.004mmol, S/C 100), Tetradecane (0.4mmol), DMA (respectively 1616μL, 616μL, 282μL and 116μL) at 130°C.

To test the catalyst under different oxidation state, we compared 5%NiO-YSZ OH 600 to 5%Ni-YSZ OH 600 under two set of conditions. The first experiment used DIPEA/DMF as base/solvent and contained Ibz (1.0mmol), Bu-cin (1.0mmol), DIPEA (2.0mmol), nickel catalyst (0.01mmol, S/C 100), Tetradecane (0.5mmol), DMF (270μL) at 140°C. The second experiment used KOAc/DMA as base/solvent and contained Ibz (1.0mmol), Bu-cin (1.0mmol), DIPEA (2.0mmol), nickel catalyst (0.01mmol, S/C 100), Tetradecane (0.5mmol), DMF (270μL) at 140°C.

We also tried other aryl halides such as bromobenzene (0.2mmol, 21μL), butyl-actylate and DIPEA at a 1:1:2 ratio under reflux. The catalyst was 5%Ni-YSZ SA 600 (0.01mmol, 25mg) (s/c ratio of 20/1) and the solvent, DMA (1mL). The mixture was put in a 5mL round bottom flask fitted with condenser and argon balloon, under reflux (~160°C) overnight.

The reactants for the reaction using microwaves as the energy source were bromobenzene (2mmol, 468μL) and butyl-acrylate (2mmol, 285μL). The base was DIPEA (4mmol,

697μL), the catalyst was 5%Ni-YSZ SA 600 (0.2mmol, 58mg) and everything was diluted in 2mL of DMF. The mixture was put inside the microwave cell and the microwave was set to hold at 200°C (600W, 100%) for an hour under maximum stirring.

We also tested the effect of the calcination temperature on reactivity. Every synthetic method (SA, ZrCl4, OH, NH3) was calcinated to 600°C and 950°C. Also, just for the SA method, samples were calcinated to 400°C. Using every synthetic method (SA, OH, NH3), catalysts were made with nickel loadings of 1, 5 and 10mol%. These were analyzed by XRF to know the precise nickel content and each catalyst was compared based on identical s/c ratio. The solutions contained Ibz (1.0mmol), Bu-cin (1.0mmol), base (2.0mmol), 5%NiO-YSZ 600 (0.01mmol, S/C 100), Tetradecane (0.5mmol), DMA (270μL) at 130°C.

## 2.4 Product Isolation

The isolation of products was done by flash chromatography. The column was filled with silica (20cm) and topped with sand (2cm). The column was wet with the elution solvent, in our case 2.5% ethyl acetate in hexane. The solvent line was lowered to the sand level. The sample was added on top and absorbed into the sand. Following this, the column was filled with the solvent and put under pressure. The elution was collected in test tubes which were each tested by thin layer chromatography (TLC) for the product. Our product was visible under UV and reacted when put in a permanganate solution. When the product was all eluted (confirmed by TLC), the test tubes containing the products were emptied in a round bottom flask and the elution solvent was evaporated.

## 2.5 Catalyst Isolation

When the reaction was over, the solution was filtered through nylon membrane filter with pore size of 0.45um (Life sciences, Nylaflo). The inside of the vial was rinsed with acetone and water to remove all the catalyst. The filter was also rinsed with acetone and water to remove any impurities on the catalyst. The filter was inserted in a 1 drum vial and left to air-dry for a few days. Following this, the filter was scratched with a spatula over wax paper and stored.

## 2.6 Triple Phase Test (TPT)

The triple phase test allows the determination of the heterogeneous nature of a catalyst[166]. During our experiments, two TPT were tried; one where a reactant was bound to a resin and the other where a solid metal scavenger is used. A detailed explanation of the tests and their ramifications will be discussed in section 3.3.3.

### 2.6.1 Reactant on resin test

A Wang resin was loaded with 4-iodobenzoic acid. We mixed the Wang resin (1.7033g, 1.36mmol, Nova Biochem, 100-200 mesh), 4-iodobenzoic acid (1.011g, 4.08mmol), DCC (841.82mg, 4.08mmol) and DMF (15mL) in a 25mL round bottom flask. A few grains of DMAP were added as catalyst. All components were mixed at 60°C for 4 days. The resin was filtered and washed sequentially with; water, methanol, DCM and ether. No special precautions were taken for its storage.

We compared two catalysts; palladium acetate and 5%Pd-YSZ 950. The theory is based on the concept that two solids, our catalyst and the reactant loaded resin, will be unable to bind solidly enough or in the correct orientation to promote catalysis. Palladium acetate, a known

homogenous catalyst, should work under those conditions and will validate the experimental protocol.

We assumed 100% loading to ensure that the resin is not the limiting reactant. The tests were done using the loaded resin (100mg, 0.08mmol), butyl-acrylate (34μL, 0.24mmol), DIPEA (41μL, 0.24mmol), DMF (250μL). For the validation test, we used $Pd(OAc)_2$ (0.89mg, 4umol). The catalyst tested was 5%Pd-YSZ 950 (9.7mg, 4umol). The reactions were mixed at 130°C for 2 days. The resin was filtered and washed sequentially with water, methanol, DCM and ether.

The product was cleaved off the resin using trifluoro acetic acid (TFA). Equal amounts of TFA and DCM (~2mL each) were added to the filtered resin and left to react at room temperature for 2 hours. Afterward, the resin was filtered and washed sequentially with methanol, DCM and ether. The solution was dried with magnesium sulphate and filtered anew. The solvents were evaporated under vacuum at 70°C to remove the TFA (boiling point 72°C). The analyses were done by NMR using Chloroform-D.

### 2.6.2 Thiol resin test

Thiol resins have a good affinity for palladium and will tend to trap any palladium in solution. Therefore, if palladium leaches, there should be little or no reaction.

The reactants were iodobenzene (0.4mmol, 45μL) and butyl-acrylate (0.48mmol, 69μL). The base was DIPEA (0.8mmol, 140μL), the catalyst was 5%Pd-YSZ cal 950 (0.004mmol, 9.7mg) and the solvent was DMF (150μL). As poison, we used a thiol resin (1.21mmol/g, 0.2mmol, 165mg) at a 500/1, thiol/palladium ratio. Using the same reaction condition, without the thiol resin, a second reaction was used as standard. Both reactions were monitored by GC-MS.

## 2.7 Calculations

During our reactions, quantification of reactants and products by GC-MS required the use of internal standards. Two internal standards were used (decane or tetradecane) to follow the product formation (butyl-cinnamate) as well as the disappearance of the reactant (iodobenzene). As such, we needed to find the response factor for each standard versus the reactant and the product.

To do so, a solution was made containing 1 equivalent of decane (0.20mmol, 39μL), tetradecane (0.20mmol, 52μL), butyl-cinnamate (0.20mmol, 41μL) and iodobenzene (0.20mmol, 22μL) in 20mL of ether. The final concentration in the mixture was calculated to be as close as possible to the concentrations from the kinetic trials.

The response factor illustrates the relation between the development of the reaction and the ratio of product over standard monitored. The formula used to find the response factor (F) is equation 12.

$$\frac{Area\ product}{Area\ standard} \times F = \frac{n_{(t_f)} product}{n_{(t_i)} reactant} \qquad (12)$$

Where n(t) is the number of moles of each species in solution.

The turn-over number (TON) is usually described as the number of catalytic cycles per metal atom. We used the following formula to obtain the TON from the peak area ratio where s/c is the substrate to catalyst ratio of the experiment.

$$TON = (s/c) \times F \qquad (13)$$

For nanoparticle catalyst, a better definition of the TON would be the number of cycles per active site. However, since the number of active sites is not well defined in these materials,

we normalized by the total amount of metal, thereby obtaining a conservative value for the turnover of the catalyst.

It is important to mention that the graphs relating to all palladium experiments, unless where mentioned, are based on the conversion % of iodobenzene, rather than the TON of butyl-cinnamate. In all those cases, the GC-MS always showed minimal side-product and the reaction is known to go to completion[60,62,66,117]. We were forced to reconsider the data presentation because the amount of reactant lost and the amount of product created did not always match. The standard for the palladium experiments, decane, was subject to evaporation and due to the small amount of internal standard in those reactions (ratio of standard to reactant was 0.1 for all palladium reactions), it affected the results. Seeing as the effect of the evaporation is cumulative, the induced error is more pronounced in the later stages of the reaction and caused an overestimation on the amount of product present[iv]. Because of this, the emphasis for those results will always be by comparison with reactions done at the same time, using the same methodology, rather than the empirical value given. The experimental error is estimated at 4%[v] which is in line with similar studies.[158] To conclude, using the amount of reactant to monitor the reaction's development is frequent in the literature for the Heck reaction[52,85,143,158].

The conversion% of iodobenzene (Ibz) often used to asses the palladium reactions development.

$$Ibz\ conversion\ \% = \left(1 - \left(\frac{r_{Ibz(t_i)}}{r_{Ibz(t_{initial})}}\right)\right) \times 100\% \qquad \textbf{(14)}$$

[iv] The standard being at the denominator position (eq 12), a diminution in its amount will result in a larger number

[v] Three samples were extracted from the same solution. Following a ether-water extraction (section 2.3.1), the samples were run through the GC-MS and the standard error was calculated

Where $r_{Ibz(t)}$ is:

$$r_{Ibz(t)} = \frac{Area\ Ibz_{(t)}}{Area\ Standard_{(t)}} \qquad \textbf{(15)}$$

To counter this problem for the nickel experiments, the standard was changed to tetradecane (higher boiling point, 253°C rather than 174°C), and the ratio of standard to substrate was augmented from 0.1 to 0.5.

## Chapter 3- EXPERIMENTAL RESULTS AND DISCUSSION

### 3.1 Palladium Optimization

The HR is often used, due to its experimental simplicity and wide array of easily accessible reactants, as a ''sharpening tool'' to examine new catalysts.[11] Of those reactants, iodobenzene and butyl-acrylate are the most common in the literature.[75,155,177] By using these reactants, we will be able to compare our catalyst with others within the field of heterogeneous Heck catalysis.

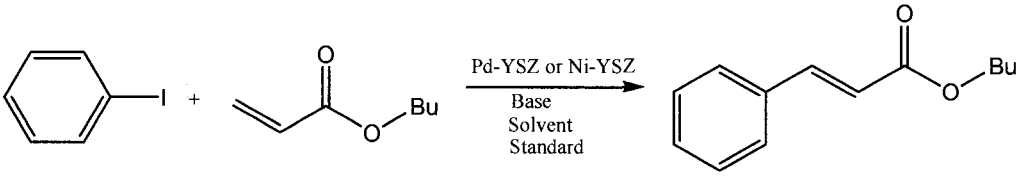


Scheme 3.1: Heck reaction between iodobenzene and butyl-acrylate

In order to find the optimal experimental conditions, various bases, solvents, temperatures, concentrations of reactants and metal oxidation states were tested. In all the trials, 5mol%Metal-YSZ was used as the catalyst. A detailed explanation of the experimental protocol was presented in the experimental section (section 2.3.1) and, to simplify the text, only the variable being studied will be restated. Throughout the discussion, we will propose mechanistic implications only when pertinent and a complete mechanistic analysis will be presented in section 3.3. This section covers the palladium-YSZ optimisation and the nickel-YSZ optimisation will be covered in section 3.2.

### 3.1.1 Palladium Oxidation State

Due to our catalyst's heterogeneous nature, which can be described as dispersed nanoparticules, the reactivity of metallic ($Pd^0$) versus oxidized (PdO)[vi] Pd nanoparticules was tested. In the accepted catalytic cycle for the homogeneous HR, the Pd atom undergoes a redox process where the active species is $Pd^0$.

Since we usually reduce our catalyst under flowing nitrogen at 800°C (section 2.2.4), even if both catalysts were previously calcinated to 950°C (5%PdO-YSZ 950), to ensure that no additional sintering occurred, we decided to use a lower reduction temperature (600°C) for the reduced catalyst (5%Pd-YSZ 950). Because the calcination temperature is much higher than the reduction temperature, there should be no additional sintering and both catalysts (Pd and PdO) are expected to have comparable morphology.

We observed a shorter induction period for the reduced catalyst (5%Pd-YSZ 950) (4hr vs. 20hr). The longer induction period and slower overall rate of the oxidized catalyst can be explained by a necessary pre-activation, through an *in situ* reduction, that is required before the metal can enter a $Pd^0/Pd^{2+}$ catalytic cycle.

The reduced catalyst also had a higher reactivity with a conversion of 80% versus only 22% for the oxidized catalyst (5%PdO-YSZ 950). This test was done at the beginning of the optimization process which explains its relatively slow rate when compared to later trials.

In association with Arai's leaching and redeposition cycle,[156] various studies have concluded that it is through the oxidative addition that palladium leaches into the solution.[109,147-149] The oxidation state influenced leaching as reduced catalysts displayed higher amounts of Pd in solution.[158] However, a higher reactivity for $Pd^0$ does not necessarily involve leaching.

---

[vi] At 950°C, PdO reduces to Pd. When exposed to air during cooling, the surface will re-oxidise and some core Pd atoms could remain reduced making the nanoparticules partially oxidized. Only surface atoms are believed to be active in the HR and XRD showed no PdO but due to the low loading, it was not discounted.

### 3.1.2 Base

The HR has been shown to work best in a neutral to basic environment as a base is required at the end of the cycle to either regenerate the catalyst or neutralise the acid formed during the reductive elimination step.[12] Previous work that tested DIPEA, $K_2CO_3$, $K_3PO_4$, DBU and KOAc established $K_2CO_3$ and DIPEA as the two most efficient bases for the HR using mesoporous supported Pd catalysts.[178] Since the results for these two were similar, we re-tested them and DIPEA was the most effective (figure 3.1.1).

The induction period is very similar for both bases, indicating that the base does not play a significant role in the pre-activation. Co-ordinating organic bases, such as DIPEA, are believed to lead to a more active catalyst by stabilising palladium species in solution ($Pds_{ol}$).[158]

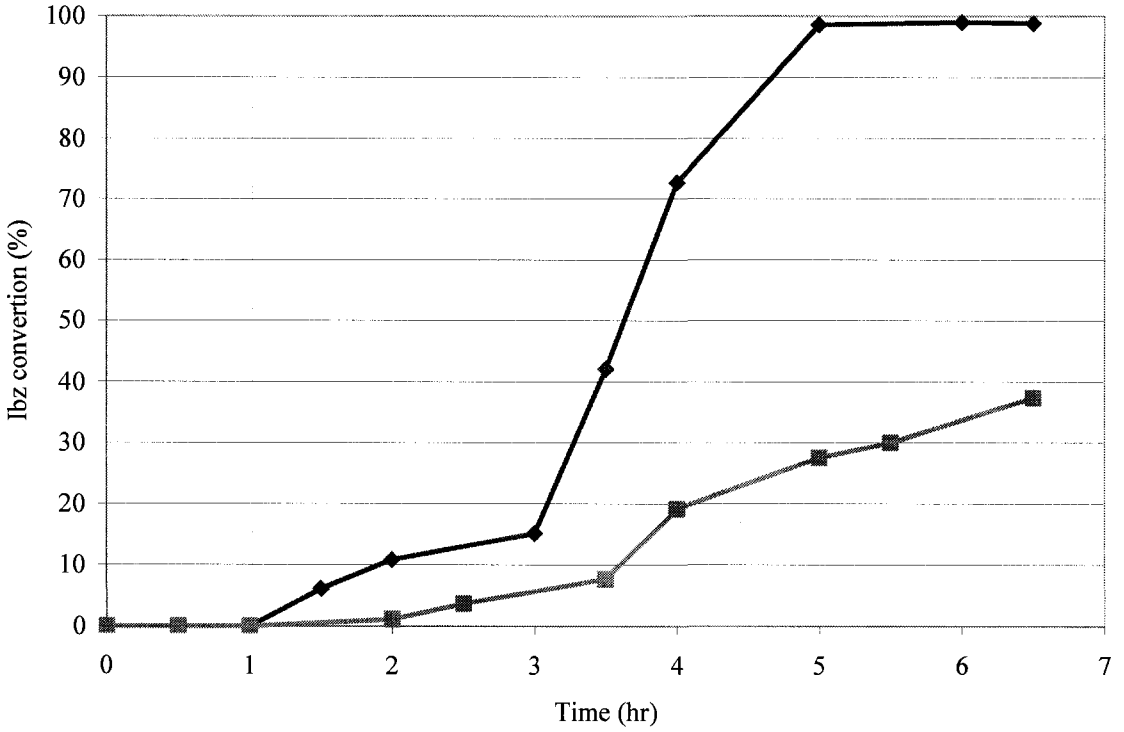


Figure 3.1.1: Reaction profile comparing (♦) DIPEA and (■) $K_2CO_3$. The solutions contained: Ibz (0.4mmol), Bu-cin (0.48mmol), base (0.8mmol), 5%Pd-YSZ 950 (0.004mmol, S/C 100), Decane (0.4mmol) and DMF (1.8mL) at 120°C.

### 3.1.3 Temperature

The heterogeneous HR using nanoparticules is usually done at high temperatures in order to have good reactivity.[179] A higher temperature generally means a higher rate[155] as more energy is placed into the system but this can also translate into more side-reactions.

To optimise reactivity, we tested the reaction at 120°C, 130°C and 140°C. Figure 3.1.2 shows that the reaction was most rapid at 140°C and all the reactions went to completion in less than four hours. No increase in by-products was detected on the GC-MS.

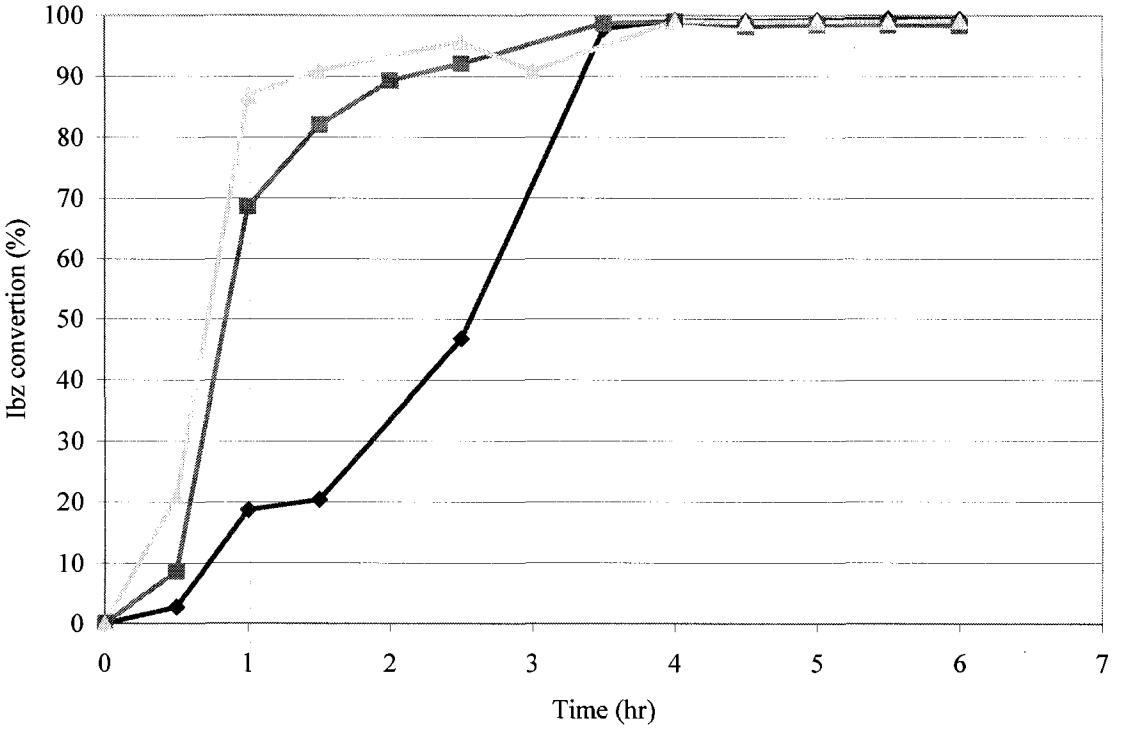


Figure 3.1.2: Reaction profile at various temperatures: (♦)120°C, (■)130°C and (▲) 140°C. The solutions contained: Ibz (0.4mmol), Bu-cin (0.48mmol), DIPEA (0.8mmol), 5%Pd-YSZ 950 (0.004mmol, S/C 100:1), Decane (0.4mmol) and DMF (1.8mL).

The curves have sigmoidal shapes that has been attributed to the pre-activation step (Scheme 1.1).[149] Given that we used a reduced catalyst (5%Pd-YSZ 950), the *in-situ* reduction proposed in section 3.1.1 as the observed pre-activation seems unlikely, or at least only a

partial explanation. Therefore, we must consider that the induction period is either caused by metal leaching[10] or surface cleaning.[91] This will be further discussed in section 3.3.

Reactions are usually faster at high temperatures but sensitive side-groups may prevent the use of such harsh conditions. Because of this, and to minimise energy waste, it is preferable to have a catalyst that reacts at low temperature. However, a trial at room temperature showed no reactivity.

### 3.1.4 Concentration of Reactants

The rate of a reaction is often directly related to the number of collisions between the reactants. Seeing as the number of collisions is proportional to the concentration of the reactants, it was varied from 0.2M to 1.2M. We observed that it had a strong influence on the reactivity as higher concentrations lead to an increase in product formation (Figure 3.1.3). No visible increase in by-products was detected (GC-MS).

The induction period was practically non-existent at 1.0M and 1.2M indicating that either the concentration has a pronounced effect on the pre-activation step or that the activity of every active catalyst is increased proportionally. Since the activity of the solution at 0.5M is, after one hour, ten times lower than the solution at 1.0M (9.7% vs. 98%, figure 3.1.2), it is highly probable that both these possibilities occurred and work concomitantly as either explanation cannot account completely for the increase in activity.

Higher concentrations were tested, as well as a solvent free reaction, but they all showed lower reactivity.

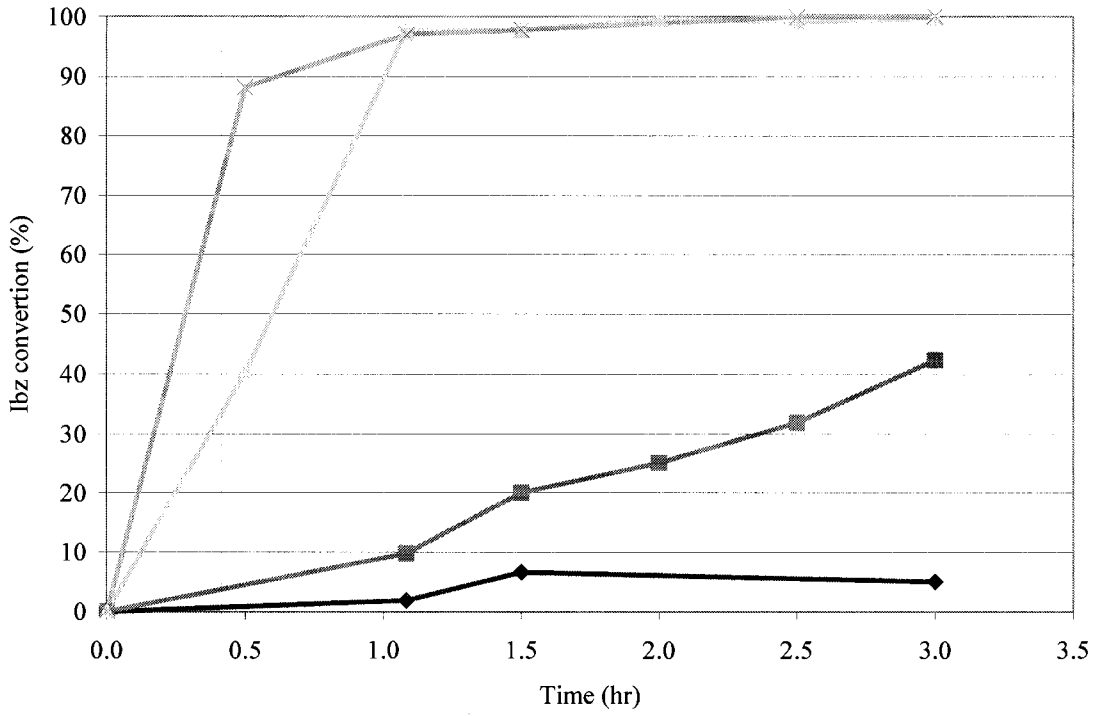


Figure 3.1.3: Reaction profile analysing the effect of the reactants concentration. (♦)0.2M, (■)0.5M, (▲)1.0M and (**x**) 1.2M. The solutions contained Ibz (4.0mmol), Bu-cin (4.8mmol), DIPEA (8.0mmol), 5%Pd-YSZ 950 (0.004mmol, S/C 1000), Decane (0.4mmol), DMF (respectively 17.40mL, 5.40mL, 1.40mL and 0.73mL) at 140°C.

### 3.1.5 Summary of the Optimal Conditions

These experiments allowed us to find the optimal conditions for our palladium-YSZ catalyst. Prior work tested DMA and DMF as solvents, and determined that DMF promoted a faster reaction (TOR)[178]. These two solvents are often used due to their high boiling point[92] and ability to stabilise $Pd_{sol}$.[149]

The optimization phase gave us the following conditions: concentration of 1.2M, temperature of 140°C, reduced catalyst, DIPEA as the base. Using those conditions, 1000 TON could be easily accomplished in 1hr (Figure 3.1.2).

## 3.2 Nickel Heck Optimization

This section presents the optimization for our Ni-YSZ catalyst. The experimental protocol for this section was presented in the experimental section (section 2.3.2). The data gathered will be compared to the data obtained for Pd-YSZ shown in section 3.1.

### 3.2.1 Temperature

We subjected our nickel catalyst to the same three temperatures as our palladium catalyst; 120°C, 130°C and 140°C. The results demonstrate that the highest temperature showed the highest reactivity, with no visible increase in side-products (figure 3.2.1).

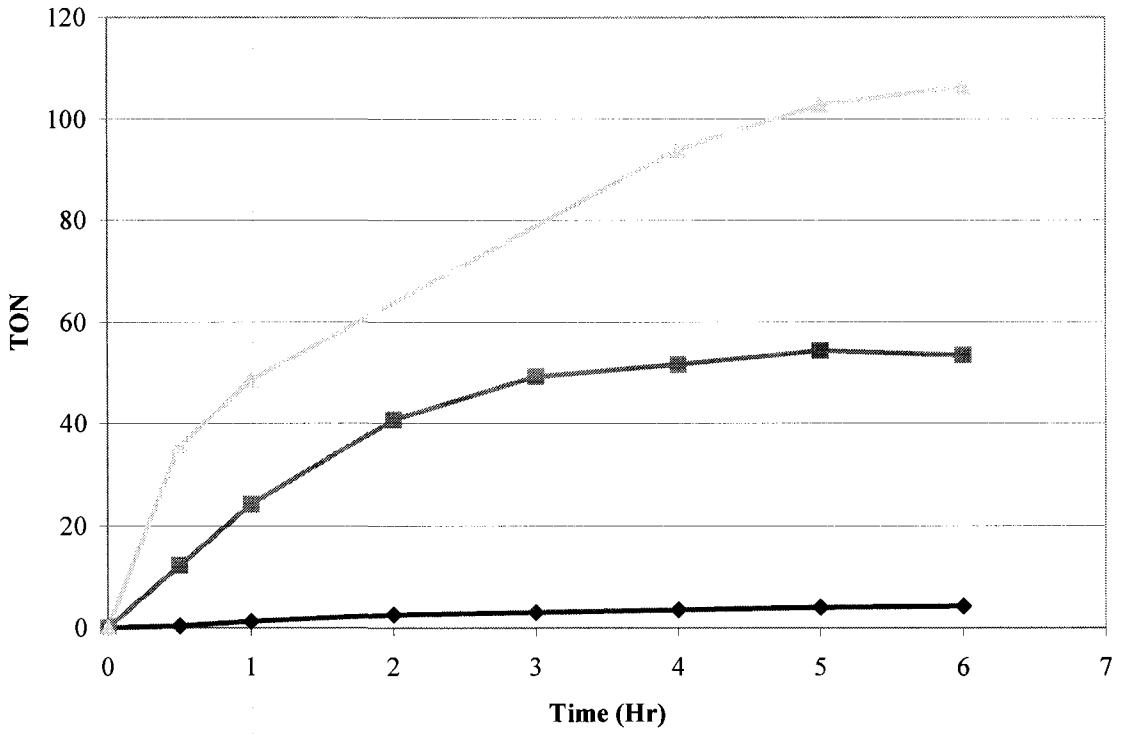


Figure 3.2.1: Reaction profile at various temperatures: (♦)120°C, (■)130°C and (▲) 140°C. The solutions contained Ibz (1.0mmol), Bu-cin (1.0mmol), KOAc (2.0mmol), 5%NiO-YSZ 600 (0.01mmol, S/C 100), Tetradecane (0.5mmol) and DMA (280µL).

The curve at 140°C displays a TON of 106 which is impossible since the s/c ration was of 100. There are two possibilities for this observation; it is either an experimental error (estimated at 4% for all data set) or it shows evaporation of the standard. For that reason, even if a higher reactivity is observed at 140°C, it was decided to use lower temperature (130°C) for all future experiments. This also slowed the reaction which allows for a greater visible difference in reactivity.

### 3.2.2 Solvent

Various solvents were tested to establish if the reaction could work at a lower temperature and how it behaves under varying polarity. Four common solvents were tried at, or close to, their reflux point; acetonitrile and tetrahydrofuran at 60°C as well as dioxane and toluene at 90°C. Neither of these reactions gave any product. The most probable answer for the lack of reactivity is the low reaction temperature. The sigmoidal shape of the kinetic curve indicates that the catalyst requires an activation that does not occur at low temperatures.[34,54,149,179-181] The same was believed to be true for our palladium catalyst.

Since temperature appeared to be a significant factor, four solvents that can operate at high temperature were examined; *N,N*-dimethylformamide (DMF), *N,N*-dimethylacetamide (DMA), ethylene glycol (Et-gly) and *N*-methyl-2-pyrrolidone (NMP). Of those, DMA provided the best environment for a fast reaction (Figure 3.2.2).

After six hours, the reaction in NMP joins the one in DMA (Fig 3.2.2). However, despite the fact that the solutions with NMP and DMA show a similar reactivity after six hours, the large difference between them in the first hours makes DMA the preferred solvent.

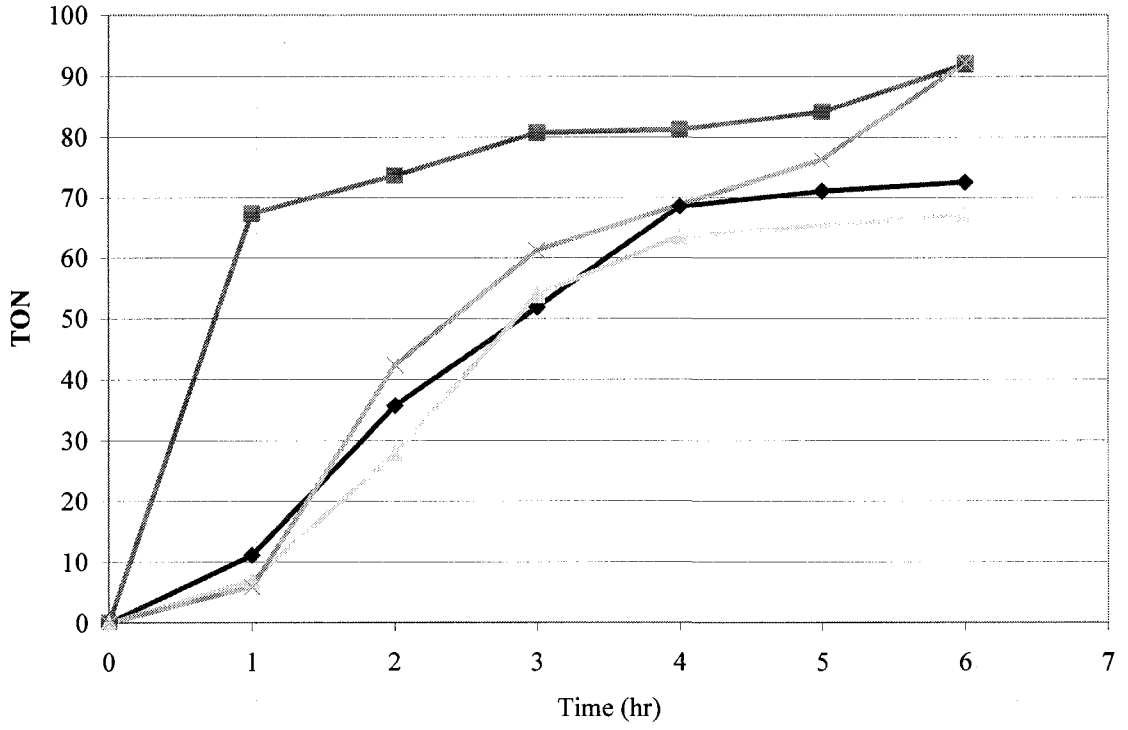


Figure 3.2.2: Reaction profile under various solvents. (♦)DMF, (■)DMA, (▲)Ethylene glycol, (x)NMP. The solutions contained Ibz (1.0mmol), Bu-cin (1.0mmol), DIPEA (2.0mmol), 5%Ni-YSZ OH 600 (0.01mmol, S/C 100), Tetradecane (0.5mmol), solvent (270μL) at 130°C.

### 3.2.3 Base

Three bases were tested: DIPEA, KOAc and $Na_2CO_3$. Of those, KOAc promoted the highest reactivity (Figure 3.2.3). However, all three solutions had the same amount of solvents and since DIPEA is a liquid, while KOAc is a solid, the solution containing DIPEA was more diluted which may have slowed the reaction. The effective concentration for the solution containing KOAc was 1.53M while it was 1.0M for the one with DIPEA.

A reaction where the total volume (done by varying the amount of solvent) in each vial was the same was carried and despite this correction, the same results were obtained; namely that the reaction performed with KOAc as the base was faster than the one with DIPEA as the

base (Figure 3.2.4). The kinetics are closer between both curves indicating that there may have been a slight concentration effect.

A significant difference between nickel and palladium can be observed regarding the effect of the base on the induction period. In Figure 3.2.3, an induction period can be seen for DIPEA but not for KOAc. Coordinating bases are believed to affect leaching[158] but since we observed no variations in the induction period for our palladium catalyst, it is possible that they only stabilize the metal already in solution, increasing its activity but not its amount. However, we are not able to explain the lack of induction period for KOAc as inorganic bases are not believed promote leaching.[155] Based on the literature, we expected DIPEA to have the shorter induction period.

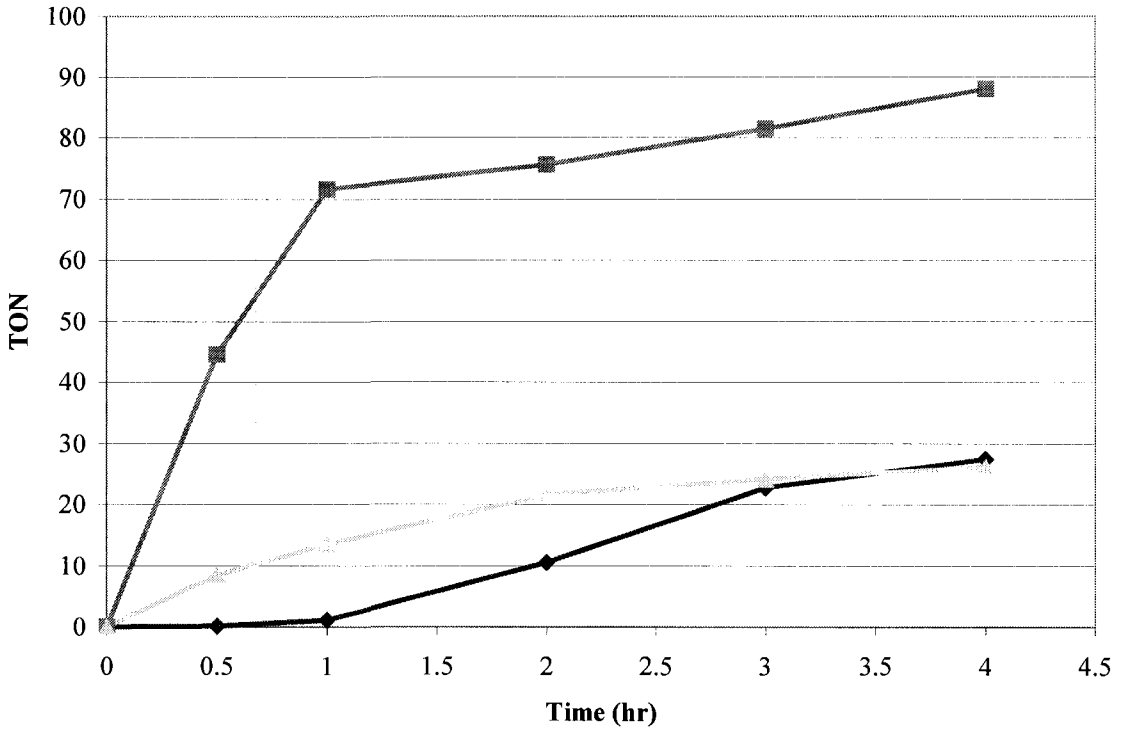


Figure 3.2.3: Reaction profile comparing (♦)DIPEA, (■)KOAc, (▲)$Na_2CO_3$. The solutions contained Ibz (1.0mmol), Bu-cin (1.0mmol), base (2.0mmol), 5%Ni-YSZ 600 (0.01mmol, S/C 100), Tetradecane (0.5mmol), DMA (270μL) at 130°C.

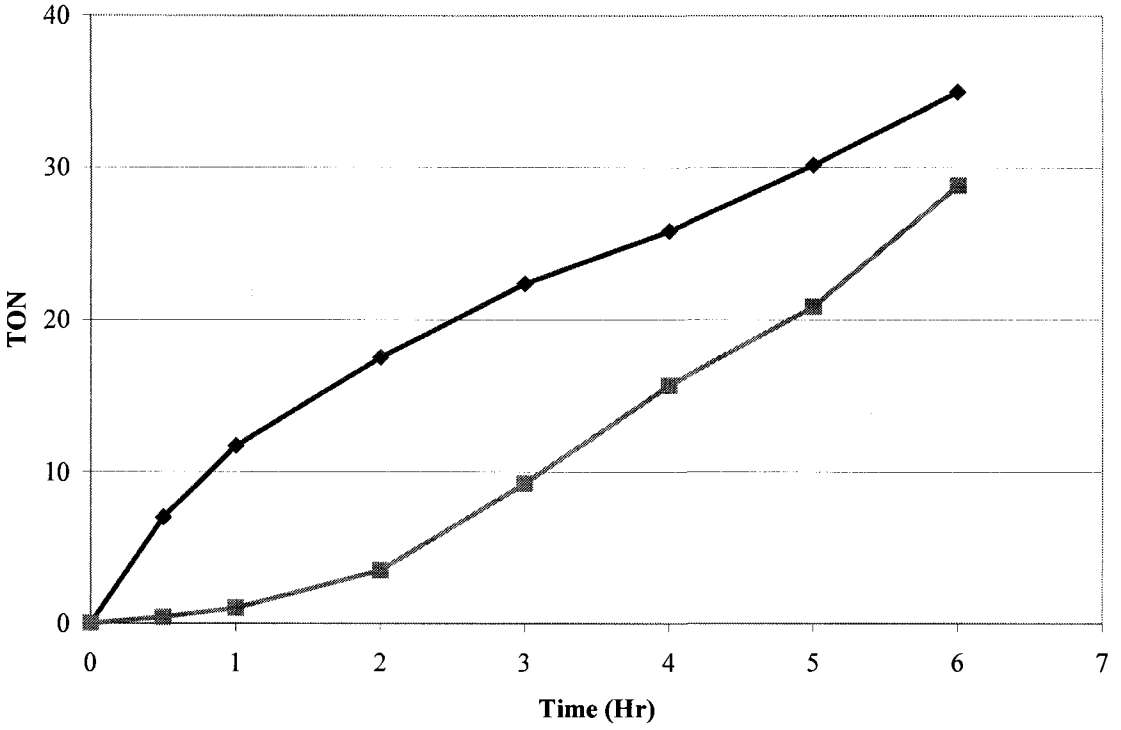


Figure 3.2.4: Reaction profile comparing (♦)KOAc, (■)DIPEA. The solutions contained Ibz (1.0mmol), Bu-cin (1.0mmol), base (2.0mmol), 5%NiO-YSZ 600 (0.01mmol, S/C 100), Tetradecane (0.5mmol), DMA (620μL and 270μL respectivelly) at 130°C.

One of the fundamental differences between nickel and palladium in the HR is the rate limiting step. Based on theoretical studies, the rate limiting step for nickel is the reductive elimination while it is the oxidative addition for palladium.[23] Based on this, with nickel, the base affects the rate limiting step. Arai[154] proposed that organic bases are better apt at stabilizing $Ni_{sol}$ while inorganic bases regenerate the catalyst. The poor activity of organic bases was observed by other groups.[182]

### 3.2.4 Concentration of Reactants

The reactant's concentration had a great effect on the reaction's speed with our palladium catalyst and this was also true with our nickel catalyst (figure 3.2.5). Of the four concentrations tested (0.5M-2.0M), the fastest was 1.5M.

The differences between each concentration are not as significant with nickel as they were with palladium. With nickel, the differences, after two hour, between the fastest (1.5M) and slowest (0.5M) reaction varies only by a three fold (TON of 14 v.s. 41) increase while in the palladium experiment (figure 3.1.3), after two hours, the higher concentrations (1.0M and 1.2M) were already complete while the one at 0.5M was only starting.

Also, with nickel, every concentration shows some degree of reactivity. This can be rationalized by the lower energetic barrier for oxidative addition calculated by Lin.[23] Assuming Arai's leaching and re-deposition cycle, an easier oxidative addition will raise the amount of leached species, increasing the proportion of active catalyst. At the same time, deVries' high temperature colloids-mediated cycle proposed that high s/c ratios will slow the formation of colloids and ultimately Ni black. While the s/c ratio is the same for all concentrations, based on this principle, high concentrations of reactants will accelerate the formation of aryl-Ni complexes lowering the amount of time $Ni_{sol}$ stays in solution and will limit its ability to aggregate.

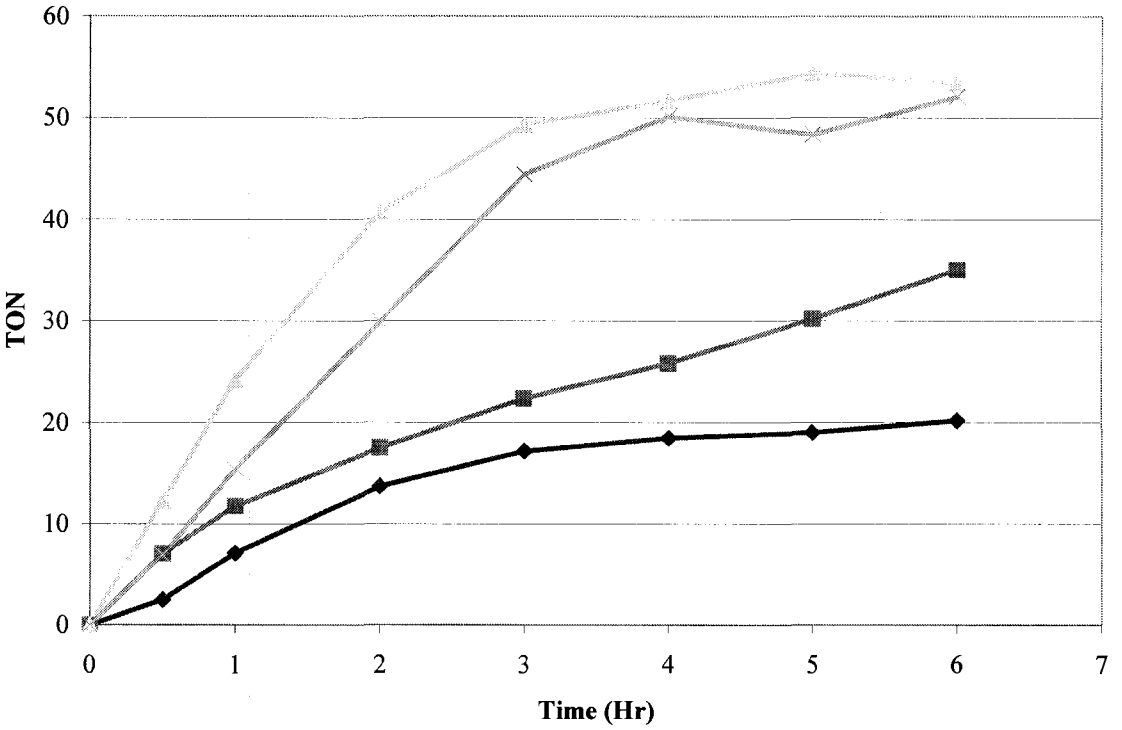


Figure 3.2.5: Reaction profile analysing the effect of the reactants concentration. (♦)0.5M, (■)1.0M, (▲)1.5M and (x) 2.0M. The solutions contained Ibz (1.0mmol), Bu-cin (1.0mmol), KOAc (2.0mmol), 5%NiO-YSZ 600 (0.01mmol, S/C 100), Tetradecane (0.5mmol), DMA (respectively 1616µL, 616µL, 282µL and 116µL) at 130°C.

### 3.2.5 Nickel Oxidation State

Nickel is in the same family as palladium and has the same two main oxidation state; 0 and +2, that corresponds to metallic nickel ($Ni^0$) and nickel oxide (NiO).

Figure 3.2.6 and 3.2.7 are the result of two experiments which compare Ni to NiO under different conditions (see figures for details). Despite the varying environment, NiO always showed more reactivity.

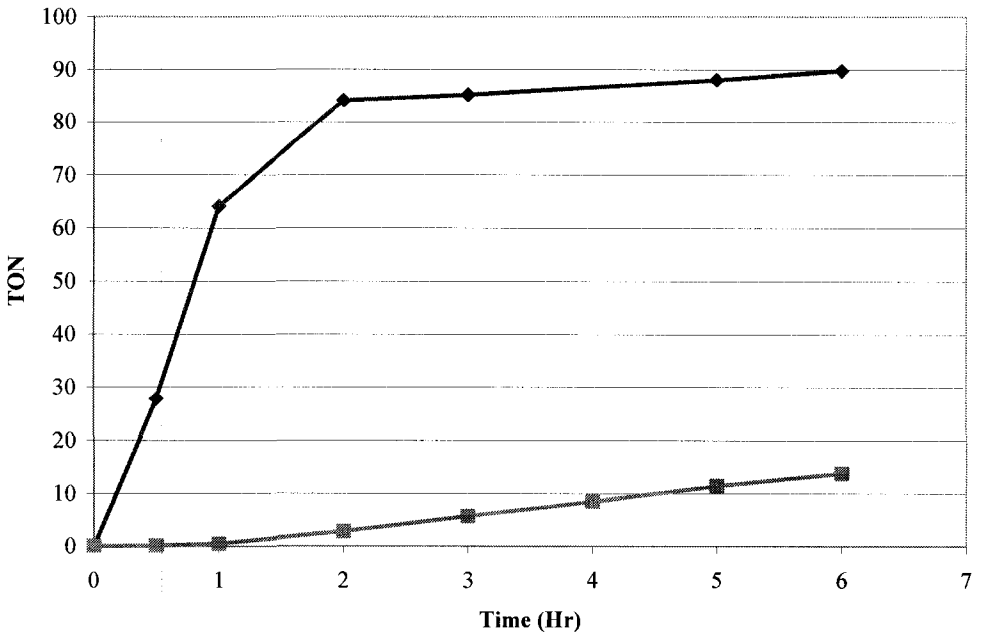


Figure 3.2.6: Reaction profile examining the nickel oxidation state effect. (♦)5%NiO-YSZ OH 600, (■)5%Ni-YSZ OH 600. The experiment used DIPEA/DMF as base/solvent. The solutions contained Ibz (1.0mmol), Bu-cin (1.0mmol), DIPEA (2.0mmol), nickel catalyst (0.01mmol, S/C 100), Tetradecane (0.5mmol), DMF (270μL) at 140°C.

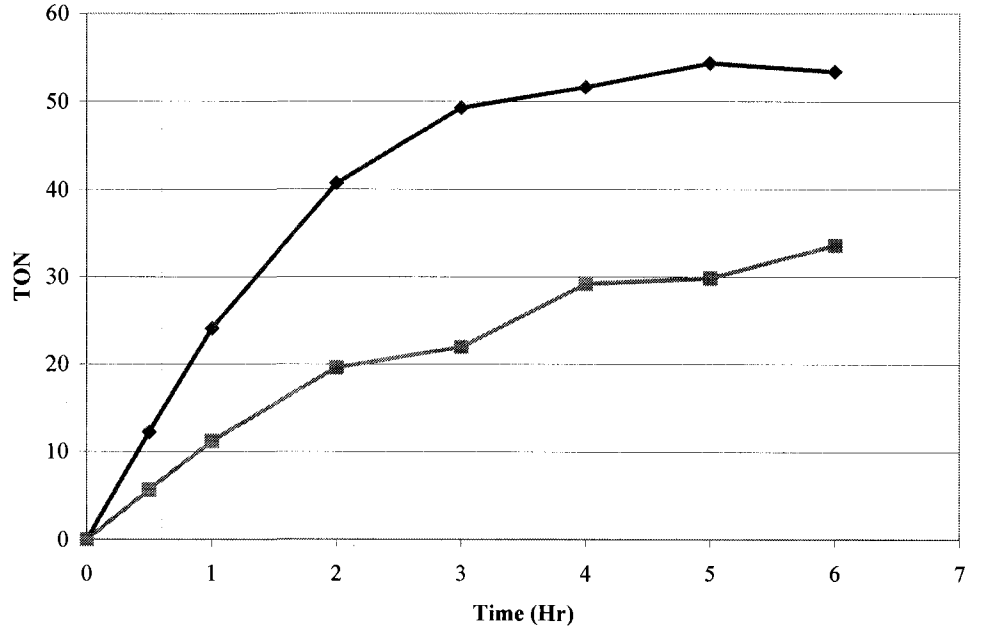


Figure 3.2.7: Reaction profile examining the nickel oxidation state effect. (♦)5%NiO-YSZ OH 600, (■)5%Ni-YSZ OH 600. The experiment used DMA/KOAc as solvent/base. The solutions contained Ibz (1.0mmol), Bu-cin (1.0mmol), DIPEA (2.0mmol), nickel catalyst (0.01mmol, S/C 100), Tetradecane (0.5mmol), DMF (270μL) at 140°C.

While the calcination temperature (600°C) is higher than the reduction temperature (400°C), additional sintering during the reduction is possible due to the higher atomic mobility of nickel, when compared with palladium.[91] This could affect the surface morphology and change the overall reactivity as both catalysts ($Ni^0$ and NiO) would differ in their oxidation state as well as their morphology (particle size, surface area). The experiment was repeated to ensure that the higher activity of NiO was only due to its oxidation state. In figure 3.2.8, the NiO tested had been previously reduced, then put in an oven at 130°C, overnight, to re-oxidize. As a result, both the $Ni^0$ and NiO catalysts had been calcinated to 600°C and reduced at 400°C in 5%$H_2$. The reoxidation of one of the catalysts was done at a low temperature where no morphological changes are expected to occur. This did not change the experimental results as NiO was again more reactive than $Ni^0$ (Fig. 3.2.8). We conclude that under our experimental conditions, nickel oxide (5%NiO-YSZ600) reacts faster than metallic nickel (5%Ni-YSZ600) in direct contrast with the Pd catalysts.

Lipshultz observed a decreased activity for their Ni(0)/C catalyst, for both the aromatic amination and the Kumada coupling, when it was reduced by heating under hydrogen compared to an *in situ* reduction by either BuLi or a Grignard based reduction. They propose that some hydrogen might still be present at the onset of the reaction blocking active metal sites. However, this would cause hydrodehalogenation as a side reaction that wasn't observed, both for them[25,91], and for us. It is hard to say if this phenomenon caused our $Ni^0$ catalyst to react slower than our NiO and if so, why the same thing did not occur for our Pd catalyst. Given that our goal was to produce an effective and easy to use methodology, we decided not to go with an air sensitive reduction pathway such as BuLi and kept the heat-$H_2$ reduction.

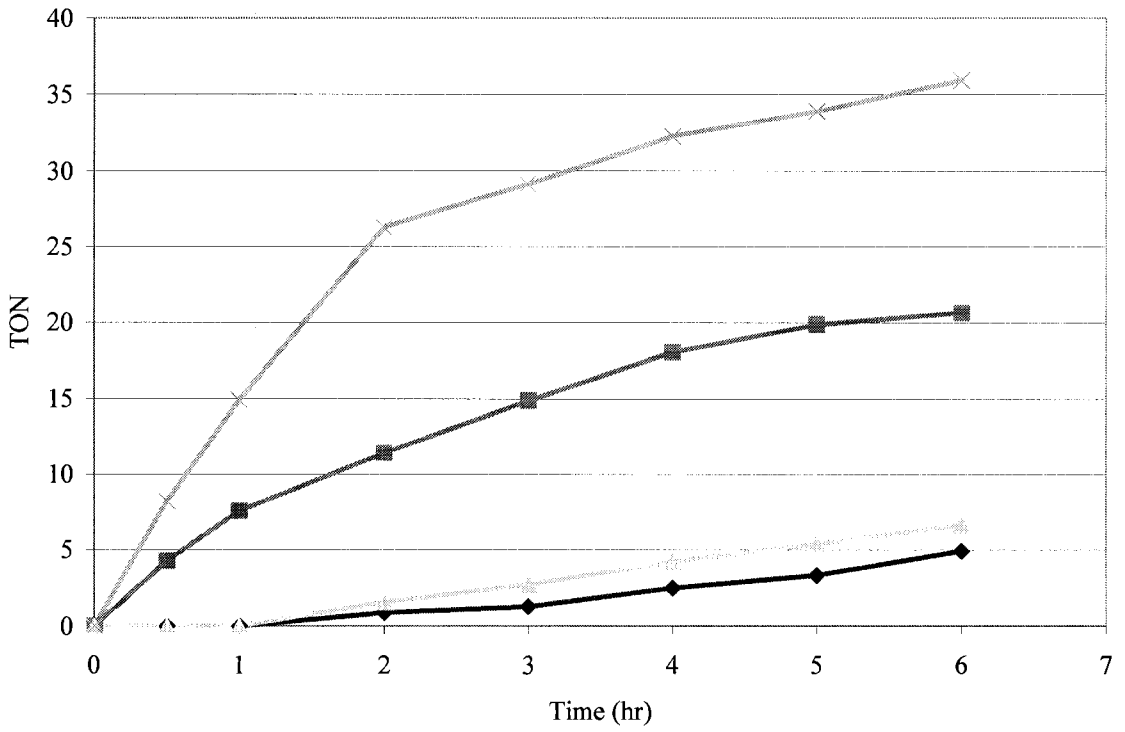


Figure 3.2.8: Reaction profile re-examining the nickel oxidation state effect under various oxidation state/base/solvent. (♦)Ni, DIPEA, DMF, (■)Ni, KOAc, DMA, (▲) NiO, DIPEA, DMF, (x) NiO, KOAc, DMA. The solutions contained Ibz (1.0mmol), Bu-cin (1.0mmol), base (2.0mmol), 5%Ni-YSZ OH 600 (0.01mmol, S/C 100), Tetradecane (0.5mmol), solvent (270μL) at 140°C.

Comparison of figure 3.2.8 with data presented in Figures 3.1.6 and 3.1.7 demands a discussion of the reproducibility in our experiments. The 5%NiO-YSZ OH 600 used in the three experiments was prepared using the same methodology. Its reactivity with DIPEA/DMF as base/solvent gave a TON of 90 if figure 3.1.6 and of 6 in figure 3.2.8. The same catalyst with KOAc/DMA as base/solvent gave a TON of 53 in figure 3.2.7 and of 36 in figure 3.2.8. Despite these discrepancies, the conclusions are consistent for all data sets, namely that NiO was more reactive. As such, reproducibility could be problematic for our nickel experiments, and for that reason, we will base our conclusions on comparisons within a data set rather than the respective numerical value.

### 3.2.6 Optimal conditions with Metallic Nickel

A few differences were noticed between the optimized conditions of nickel and palladium. We decided to verify if the variation in oxidation state (NiO for Ni and $Pd^0$ for Pd) could explain the difference in reactivity regarding the base and the solvent. Metallic nickel ($Ni^0$) was retested using every DIPEA/KOAc-DMF/DMA combinations (figure 3.2.9). The same results are obtained as DMA stand out as being the most favourable solvent while for the bases; KOAc causes the fastest initial reaction.

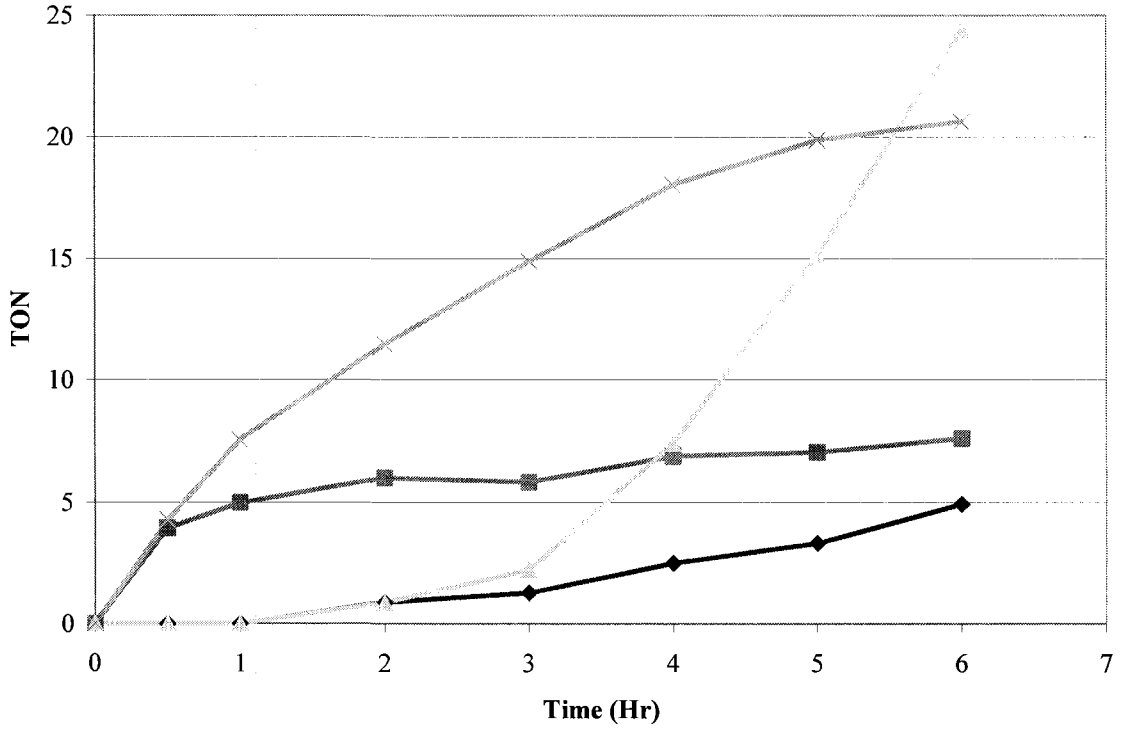


Figure 3.2.9: Reaction profile examining the base/solvent effect on the reactivity of $Ni^0$. (♦)DIPEA-DMF, (■)KOAc-DMF, (▲)DIPEA-DMA and (x)KOAc-DMA. The solutions contained Ibz (1.0mmol), Bu-cin (1.0mmol), base (2.0mmol), 5%Ni-YSZ 600 (0.01mmol, S/C 100), Tetradecane (0.5mmol), solvent (270µL) at 130°C.

However, we acknowledge that long-term reactions may benefit from the stabilisation that DIPEA, and other organic bases, can afford.[182] The DMA-DIPEA curve indicates a longer half-life that is best explained by the ability of coordinating bases to stabilise $Ni_{sol}$. In

accordance with deVries' high temperature anionic mechanism[10], a high concentration of metal in solution has been hypothesised to drive the equilibrium toward soluble cluster formation and even nickel black, and as a result, deactivated the catalyst.[179]

### 3.2.7 Summary of the optimal conditions

The final optimized conditions were; NiO, KOAc as the base, DMA as the solvent, 1.5M at 140°C.

## 3.3 Pd-YSZ Mechanistic Studies

This section goes through the different experiments used to elucidate the nature of our palladium catalyst as being either homogenous or heterogeneous.

A filtration test previously done in our laboratory[vii] found no traces of palladium in the solution mixture and it was concluded that there was no leaching of Pd species into solution, during the reaction. However, the validity of this test, which is the simplest and most used to determine heterogeneity in the HR, has been recently questioned since palladium leaching and re-precipitation has been shown to be rapid, thus leaving almost no visible palladium in solution.[90]

### 3.3.1 Effect of Reactant Incubation

The traditional HR mechanism begins by the oxidative addition of the aryl halide. Wanting to know if the same occurred with our catalyst, two solutions were prepared; one without iodobenzene and one without butyl-acrylate. Both solutions were heated for four hours and then the missing reactant was introduced. Having already established that our catalyst goes through a pre-activation (induction period, section 3.1), the solution incubated with the reactant responsible for the pre-activation would be the fastest of the two.

The main explanation of the pre-activation is thought to be leaching of palladium atoms in solution and it is believed to occur by oxidative addition on the kinks or steps of palladium nanoparticles.[147] This experiment will also enable us to analyse the feasibility of Shaw's $Pd^{2+}/Pd^{4+}$ homogeneous mechanism[38,114] as well as El-Sayed's heterogeneous mechanism[136-139]; both of which begin with the olefin's (boronic acid) binding as the first step.

[vii] Test done by Yamile Wasslen

The reaction incubated with iodobenzene resulted in a higher activity (Fig 3.3.1). This result indicates that the first step of our mechanism is related to iodobenzene. A similar diminution of the induction period by pre-heating reactants was also observed by Ying[183,184] and Kohler.[149]

While the induction period is not only associated with leaching and can also be explained by surface cleaning or an in situ reduction of surface atoms to allow catalysis, the present result is nonetheless in agreement with the leaching model and discounts Shaw's and El-Sayed's mechanisms.

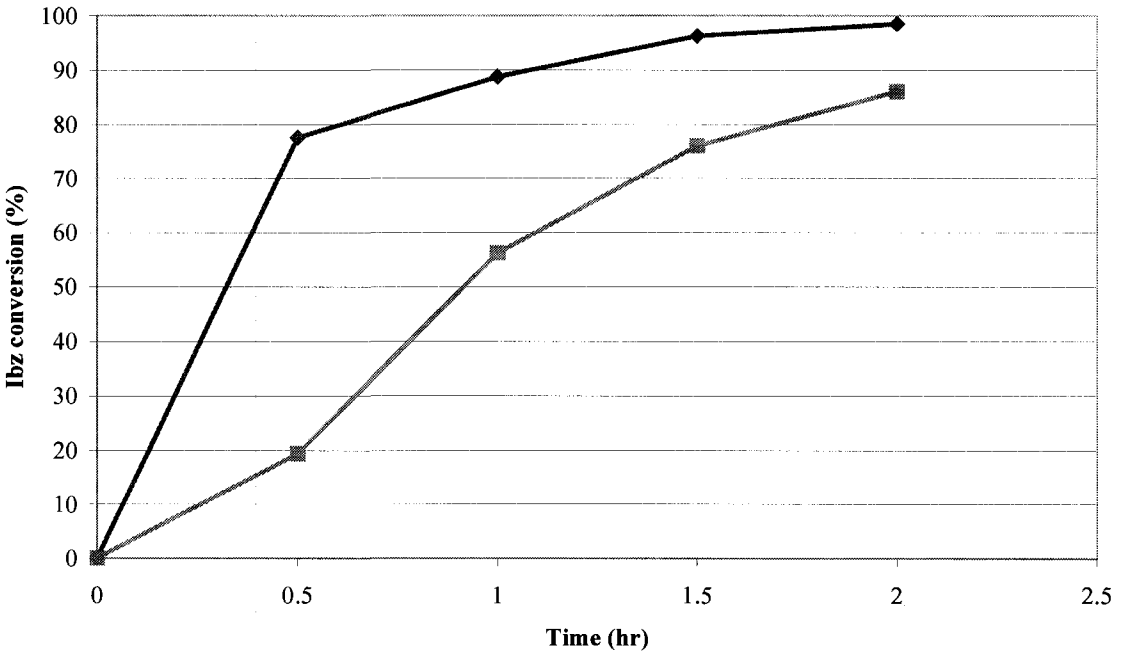


Figure 3.3.1 : Reaction profile comparing solutions pre-incubated with (♦) Ibz and (■) Bu-acr. The solutions contained: Ibz (4.0mmol), Bu-cin (4.8mmol), DIPEA (8.0mmol), 5%Pd-YSZ 950 (0.004mmol, S/C 1000), Decane (0.4mmol) and DMF (5.4mL) at 140°C.

### 3.3.2 Differences in the catalyst before and after use - kinetic and P-XRD analysis

A variation in the size of the nanoparticules can be explained by leaching and redeposition while the lack of changes may indicate surface catalysis. The literature shows examples of both; Dupont[143] clearly showed an increase in size throughout the reaction while Augustine found no variation.[63]

The intensity of an P-XRD peak is proportional to the quantity of crystalline material present and the area of a partially crystallised component corresponds only to the crystalline portion of that component.[185] Using YSZ as an internal standard, we decided to compare the ratio between the areas of palladium's highest peak ($2\theta \approx 40$) over the area of YSZ's highest peak ($2\theta \approx 30$) (figure 3.3.2).

The ratio was $2.2\pm0.2*10^{-2}$ Pd/YSZ for the catalyst before use (5%PdYSZ 950R) and $0.81\pm0.12*10^{-2}$ Pd/YSZ for catalyst after one use (5%PdYSZ 950 used). Only 37% ($0.81*10^{-2}/2.2*10^{-2} = 0.37$) of our metal was still present in crystalline form. This number is higher than the 14% reported for Pd/C but lower than the 86% measured for $Pd/TiO_2$.[149]

The loss of metallic Pd intensity has three main explanations. The first, since the palladium and palladium oxide P-XRD peaks position differ, if a portion of the palladium is oxidized during the reaction, its peak will not be at the same place as before and will, therefore, not be included in the area of crystallized palladium. No palladium oxide peaks were found in the P-XRD diffraction pattern but due to the low catalyst loading this hypothesis was not excluded. Second, if palladium leached, the literature proposes that it redeposits on the supports at the end of the reaction as palladium black.[158] Palladium black is uncrystalized and would not appear in the diffraction pattern. The third is that leaching occurred, and

palladium either stayed in solution (soluble palladium, colloids or nanoparticules) or re-deposited elsewhere than on the support (glassware).

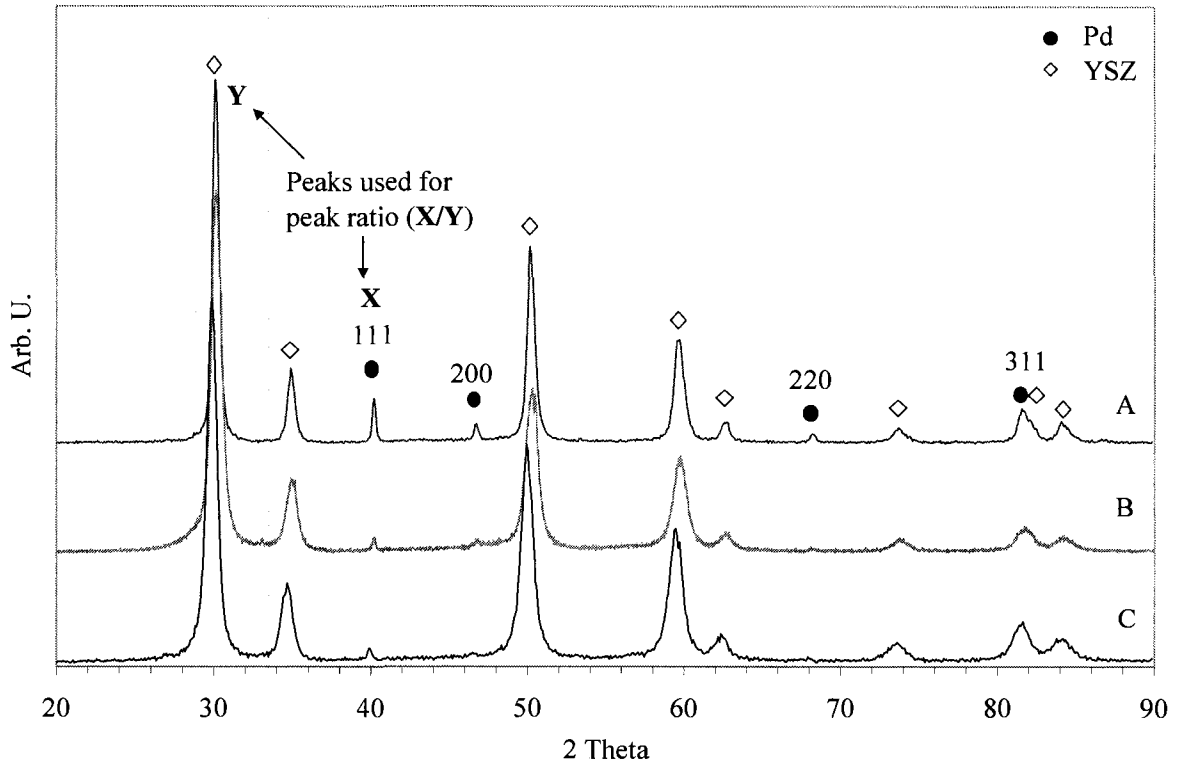


Figure 3.3.2: Powder X-ray diffractogram (P-XRD) of 5%Pd-YSZ 950: (***A***)Before catalysis, (***B***)after catalysis, (***C***)after catalysis and reduction. Reflection planes have been indicated for the Pd crystals.

We tested these hypotheses by reducing the used catalyst (5%PdYSZ 950 used) at 800C under $N_2$. At that temperature, any palladium oxide would reduce to palladium and any palladium black would recrystallize. The peak ratio Pd/YSZ for this catalyst (5%PdYSZ 950 used R) was of $0.90\pm0.25*10^{-2}$. The standard deviation of the measurements demonstrates no statistical differences between the used (5%PdYSZ 950 used) and the reduced used (5%PdYSZ 950 used R) sample (table 3.3.1) suggesting that the palladium catalyst leached into the solution and either recrystallized elsewhere than on the solid support or that it stayed in solution in the form of coordinated atoms or soluble clusters.

Table 3.3.1; Pd/YSZ peak ratio before and after reaction

| Sample | Peak ratio |
|---|---|
| Before reaction | $2.2\pm0.2*10^{-2}$ |
| After reaction | $0.81\pm0.12*10^{-2}$ |
| After reaction and calcination | $0.90\pm0.25*10^{-2}$ |

The use of P-XRD to assess the variation in crystalline palladium was also made by Arai who found that the redeposition occurred directly on the nanoparticules thus diminishing the number of particles but augmenting their size.[158]

The diffraction pattern of the ''unused'' (5%Pd-YSZ 950), the ''used'' (5%Pd-YSZ 950 used) and the ''used and reduced'' catalyst (5%Pd-YSZ 950 used R) is shown in figure 3.3.2. Neither new peaks nor any changes in the peaks positions are observed. From these measurements, we observe a reduction of the amount of palladium, on the YSZ support, after the reaction has occurred.

The diminution of palladium was corroborated by the reactivity of 5%PdYSZ 950 compared to 5%PdYSZ 950 used R as 5%PdYSZ 950 showed a higher reactivity (Figure 3.3.2).

To ensure that the support was not affected by the reaction conditions, we compared the crystallite sizes of the YSZ component. In both, the used and the reduced used samples, the P-XRD spectrum shows no major difference other than the palladium peak area. The YSZ crystallite size of the used catalyst and the reduced catalyst are $132\pm4$ Å and $114\pm6$ Å respectively. The crystallite size of the YSZ for the unused catalyst (5% Pd-YSZ cal 950 red 800) is between those values at $117\pm3$Å. It is reasonable to conclude that the support is not changed, nor affected by the HR reaction conditions.

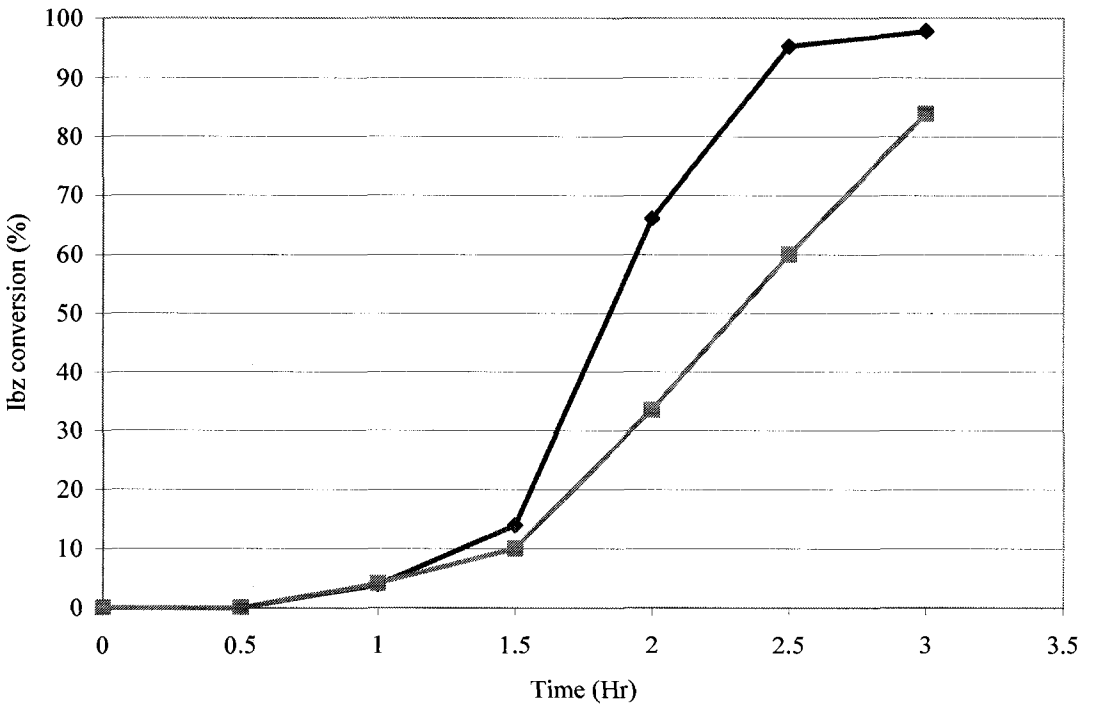


Figure 3.3.3: Reaction profile comparing the recyclability of our palladium catalyst. (♦)5%PdYSZ 950 (■)5%PdYSZ 950 used R. The solutions contained: Ibz (4.0mmol), Bu-cin (4.8mmol), DIPEA (8.0mmol), catalyst (0.004mmol, S/C 1000), Decane (0.4mmol) and DMF (5.4mL) at 140°C.

### 3.3.3 Triple Phase Test (TPT)

The heterogeneous HR is composed of two phases; the liquid solution (reactants, solvent etc.) and the solid catalyst. The TPT introduces a third phase and monitors the interactions. Two variations of the TPT were tried; a resin supported reactant as well as a thiol palladium scavenger.

The resin supported reactant test is based on the assumption that reactants on a macromolecule cannot interact with metallic nanoparticules[166]. Due to the immense steric hindrance of the resin, only a homogeneous catalyst should be able to adopt the right

orientation to promote a reaction (scheme 3.3.1). A positive result on this test is a strong indication of leaching.

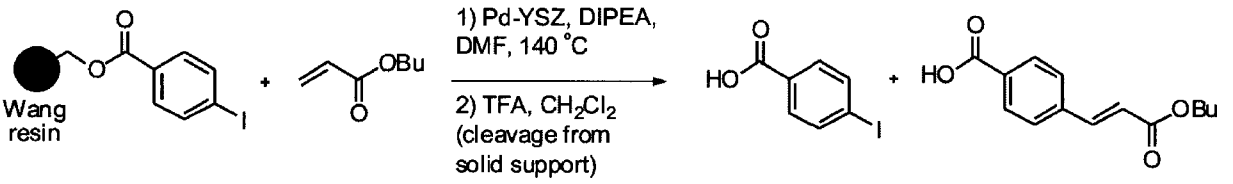


Scheme 3.3.1: Resin supported reactant TPT

The solid palladium scavenger used is in the form of a thiol resin (scheme 3.3.2). The thiol resin should bind every free, leached, palladium atom, therefore neutralising any homogeneous catalysis. Product formation would indicate heterogeneous catalysis.

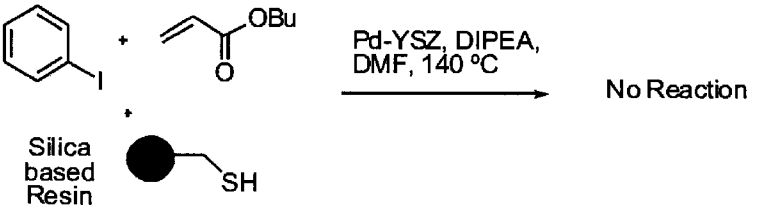


Scheme 3.3.2: Thiol resin palladium scavenger TPT

### 3.3.3.1 Resin Supported Reactant Test

At first, the resin and our experimental parameters were tested. The 4-iodobenzoic acid on the resin reacted with butyl-acrylate in presence of palladium acetate, a known homogeneous catalyst[12], proving that the resin can be used as a reactant with a homogenous catalyst (Figure 3.3.7, sample B).

We proceeded to examine the reactant loaded resin with our catalyst and we also observed product formation. The product pattern (4-((E)2-(butoxycarbonyl)vinyl)benzoic acid) as well as the reactant (4-iodobenzoic acid) were observed in the NMR spectra (Figure 3.3.4:C). Since no homogenous catalyst had been added to solution, some palladium had to leach in order to react with the substrate on the resin. Since products were observed (scheme 3.3.1),

this result confirms that our catalyst leaches into solution and that the leached species is responsible for, at least, a portion of the catalysis.

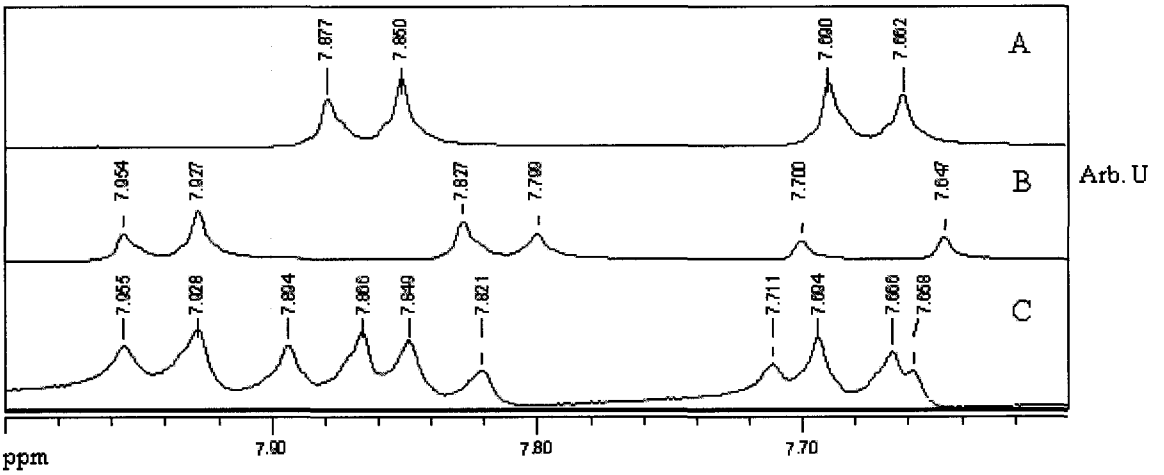


Figure 3.3.4: NMR pattern between 8.0-7.6 ppm of the TPT. A: Reactant (4-Iodobenzoic acid). B: Product (4-((E)2-(butoxycarbonyl)vinyl)benzoic acid). C: Reaction using Pd-YSZ

There are two events that can explain the leaching. The first is that the solvent or the base was able to extract palladium from the surface.[90] The ability of coordinating bases or solvents to facilitate leaching was observed by Arai.[158] The second possibility is that a small amount of 4-iodobenzoic acid was released from the resin and extracted the palladium. The leached palladium would be free to react with substrates on the resin.

Palladium leached and reacted in a homogeneous fashion but it does not tell us if the heterogeneous catalyst contributes, even in a small fraction, to the product formation in a regular reaction. To ascertain this, we turned to another type of triple phase test.

### 3.3.3.2 Thiol Resin Test

To see if the heterogeneous catalyst is active in the product formation, catalysts in solution were poisoned by the addition of a silica supported thiol scavenger resin. Thiols have a high

affinity for palladium and will strongly bind to it, rendering it inactive. In such a system, the only catalyst that would be able to react would be heterogeneous.

A conversion of less than 5% was observed after 16 hours while a side reaction, without the thiol resin, went to completion. This strongly shows that the heterogeneous catalyst does not play an active role in the reactivity of our catalyst and that any observed reactivity comes from leached palladium in solution. The small product formation can be explained by either the first cycle of every leached molecule of palladium which starts on the metal surface and cannot be poisoned; or by the palladium in solution at the end of the catalytic cycle, which is only inactivated if it binds to the thiol resin before reacting with another molecule of iodobenzene.

Our experiments indicate that iodobenzene directly extracts palladium from the metal surface and, afterward, react homogeneously and that the palladium extraction is facilitated by coordinating base and solvent. The contribution of true heterogeneous catalysis appears to be minimal.

## 3.4 Pd-YSZ: High S/C Ratio Heck Reactions

As discussed in section 3.1.1, a thousand turn-over was easily reached during the palladium optimization. This indicated that our palladium catalyst had a great potential for higher substrate to catalyst ratio (s/c) reactions. In order to test its reactivity, it was subjected to reactions containing s/c ratio of 100'000/1 and 1'000'000/1. The following sections contain the experimental results and analysis.

### 3.4.1 100'000 S/C Ratio

Our palladium catalysts reactivity was tested in a reaction containing a s/c ratio of 100'000/1. Half of the substrate had reacted after only five hours and it was near completion after ten hours. The reaction went to completion after 24 hour. The form of the curve was sigmoidal which is similar to previous experiments (figure 3.4.1).

### 3.4.2 1'000'000 S/C Ratio

The short time it took to complete 100'000 TON suggested that our palladium catalyst had not reached its TON limit. An experiment with a s/c of 1'000'000/1 was tried (Fig 3.4.2). The final TON was verified by NMR peak ratio to be 350'000.

Despite the high TON reached, this experiment did not seem to follow the same reactivity observed in Figure 3.4.1 for the 100'000/1 experiment as the overall rate in the 1'000'000/1 s/c ratio experiment was lower than for the 100'000/1 s/c reaction. The reaction was expected to follow De Vries's high temperature anionic model since our catalyst acts as reservoir of active, ligand-less palladium atoms.[179] DeVrie proposes that a higher s/c ratio slows the metal aggregation and accelerates the overall rate but we saw a diminution of the rate.

Pushing for the limits of the reaction, the experiment was repeated with our palladium catalyst calcinated to 600°C instead of 950°C and the concentration was augmented from 1.0M to 1.2M. The higher surface area catalyst and the higher concentration of reactants was expected to increase the TON, as described in the optimization sections.

A shorter induction period (less than 2hr) and a higher TON (770'000 TON) was observed. The diminution in the induction period is most likely due to the variation in the concentration. As was shown in figure 3.1.4, the palladium's induction period is greatly affected by the reactants concentration.

The turn over rate (TOR) was estimated by taking the most linear section of both curves (Fig 3.4.2 and 3.4.3) (between day 1-4 for Fig 3.4.2 and between day 1-8 for Fig 3.4.3). This method was judged best by Beletskaya[186] who argued that using the slope of the most linear part of a kinetic plot, by removing the induction period and the tail, gave a more representative TOR. TOR of 74'000 and 82'000 $day^{-1}$ respectively were calculated (Table 3.4.1). This is only an approximation but it indicates that the catalyst was only slightly more active in one reaction than the other.

Table 3.4.1: Turn-over rate calculated using the most linear portion of the kinetic curve for the 1'000'000 s/c ratio experiments.

| | Data source (days) | TOR (day-1) |
|---|---|---|
| 1st curve (figure 3.4.2) | 1-4 | 74'000 |
| 2nd curve (figure 3.4.3) | 1-8 | 82'000 |

The second trial was also active for a longer period. This is best explained by the use of a mesoporous catalyst for the second experiment which imprisoned the active particles inside its pores and thus prevented their diffusion into the solution mixture where the palladium aggregation would become easier.[143,158,179] However, the literature shows contradictory statements on the subject such as a recent experiment in a similar system in which the

reactivity was completely cancelled when they added an insoluble Pd poison[viii], indicating that leached palladium exited the pores and that reactivity occurs mostly outside the pore system.[90]

Based on the metal loss observed by p-XRD, the residual amount of Pd in solution is of <0.1ppm. This compares well with values obtained for palladium on activated carbon (0.05 ppm)[149] and is only faintly higher than mercaptopropyl-modified silica (0.003 ppm)[187] which is a Pd scavenger.

While homogeneous catalysts have been documented to reach TON of over 8.0 X 10,[6188] the highest results for heterogeneous catalysts we found in the literature were of 1'150'000 TON for a polymer-based ligand-coordinated palladium catalyst[75,77] and of 36'000 TON for palladium supported on activated carbon.[149,181] Since the later is more comparable to our Pd-YSZ, it indicates that our catalyst measures well with highest TON found in the literature for heterogeneous catalysts.

[viii] The TPT involving a palladium scavenger (section 3.3.4.2) was done with 5%Pd-YSZ 950 that contains no mesopores.

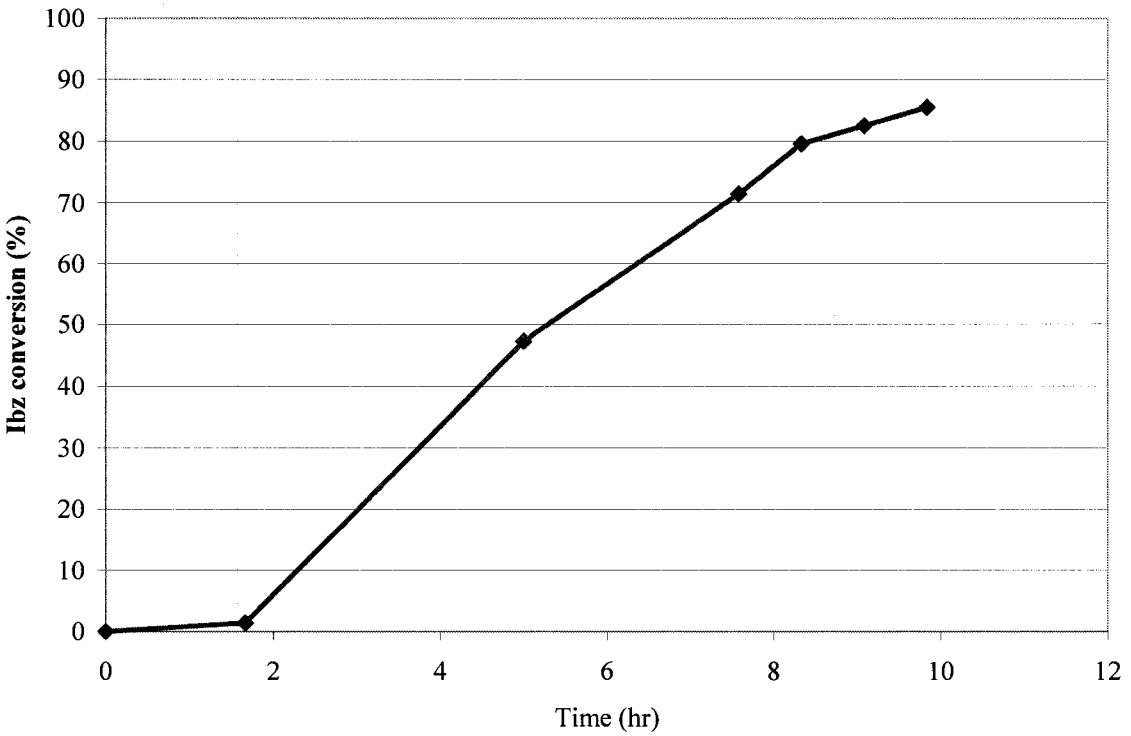


Figure 3.4.1: Reaction profile at a S/C ratio of 100'000/1. The solution contained: Ibz (0.20mol), Bu-cin (0.24mol), DIPEA (0.40mol), 5%Pd-YSZ 600 (0.002mol) and DMF (74.50mL) at 140°C.

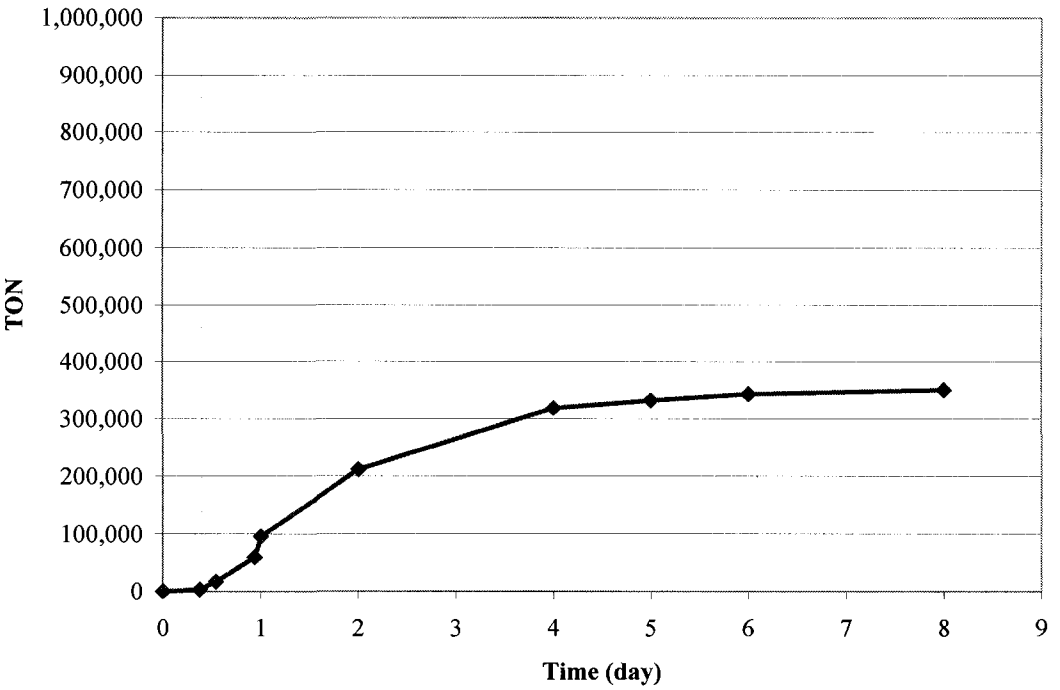


Figure 3.4.2: Reaction profile at a S/C ratio of 1'000'000/1. The solution contained: Ibz (1.0mol), Bu-cin (1.0mol), DIPEA (2.0mol), 5%Pd-YSZ 950 (0.001mol) and DMF (397mL) (1.0M) at 140°C.

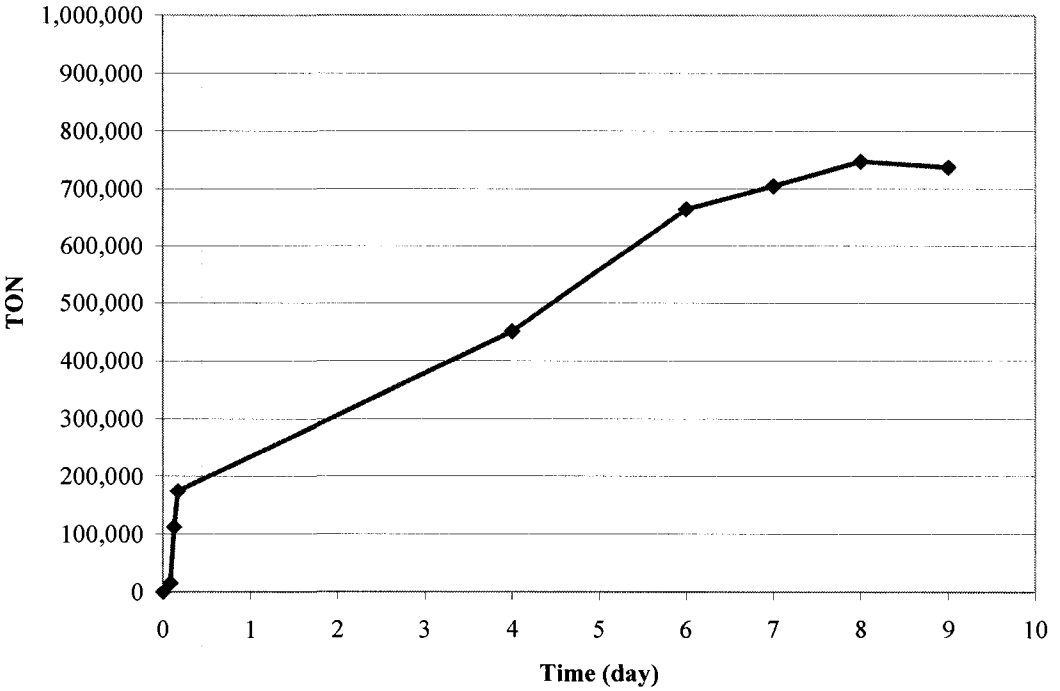


Figure 3.4.3: Second reaction profile at a S/C ratio of 1'000'000/1. The solution contained: Ibz (1.0mol), Bu-cin (1.0mol), DIPEA (2.0mol), 5%Pd-YSZ 950 (0.001mol), Decane (12mmol), and DMF (230mL) (1.2M) at 140°C.

## 3.5 Aryl Halide Scan

The reactivity toward oxidative addition is strongly affected by the strength of the C-X bond[11,92]. This makes the order or reactivity between aryl halides; Ar-I > Ar-Br > Ar-Cl. While the reactivity is higher with Ar-I, it would be advantageous for commercial purposes to be able to use the less expensive and readily available Ar-Cl or even Ar-Br.[48,156]

When using Pd-YSZ as the catalyst, no reaction was observed with either chloro- or bromobenzene under the optimal conditions of section 3.1.

For Ni-YSZ, chlorobenzene and chlorobenzene were tried as reactant, instead of iodobenzene, under reflux (DMA, 160°C). Only traces of products were observed with bromobenzene while no reactivity was observed with chlorobenzene.
Following this, due to recent reports of microwave assisted nickel HR[163,189], a reaction with microwaves as the energy source was tried. Despite the high temperature of that experiment (200°C), no product was observed.

We concluded that our catalysts, whether palladium or nickel, were not reactive toward aryl chlorides. As for aryl bromides, only nickel showed a very limited reactivity but only at high temperature. Lei Liu's[23] theoretical analysis of the nickel and palladium HR shows that the insertion into the C-X bond is easier for nickel than for palladium. This explains the reactivity of Ni toward Ar-Br but a reactivity toward chlorides was also expected considering that nickel oxide nanoparticules have been recently shown to activate C-Cl bonds.[190]

### 3.6 Pd-YSZ Structural Analysis

The calcination temperature determines the crystalline size and microstructure of the catalyst. The pores of our catalysts were created by the formation of the YSZ around CTAB micelles and subsequent removal of the organic component. This was confirmed on a P-XRD specially calibrated for low angles. It must be noted that high temperature creates molecular movement that crystallizes the YSZ and the higher the temperature, bigger is the crystallite size[191,192] and that an increase in Pd crystallite size can lead to a decreased reactivity.[69]

The P-XRD diffraction pattern of Pd-YSZ showed a decrease of the low angle peak for catalysts calcinated at 600°C and saw no low angle peak for the one calcinated at 950°C.

To verify whether the pores were collapsed or merely disordered after calcination at 950°C, we measured the surface area of the catalyst calcinated at 600°C (5%Pd-YSZ 600) and calcinated at 950°C (5%Pd-YSZ 950) and found respective surface areas of $157m^2/g$ and $9.03m^2/g$. Mesopores were measured in the catalyst calcinated at 600°C (figure 3.6.1) but none were observed for the catalyst calcinated to 950°C. It would seem that at 950°C, the atomic movement causes the pores to collapse. This was substantiated by a larger crystallite size for Pd and YSZ for the catalyst calcinated at 950°C ($544\pm168$Å and $277\pm23$Å respectively) than for the one calcinated at 600°C ($93\pm27$Å and $42\pm2$Å respectively). The increase in crystallite size and the decrease in surface area was reflected in activity where the palladium catalyst calcinated at 600°C had a faster initial reaction than the one calcinated at 950°C (figure 3.6.2).

The pose size of the 5%Pd-YSZ 600 samples was verified through isotherm desorption (section 2.1.4). Pore size distribution is shown in figure 3.6.1, which shows a majority of pore diameters around 16 angstroms. This is at the lower end of the meso regime but this

pore size is suitable to allow diffusion of reactants to the catalysts active sites. In these experiments, it seems that being at the lower limit of the meso range also has the effect of limiting the diffusion of leached palladium into the bulk solution, thereby extending the life of the catalyst as discussed in section 3.4.2 (figure3.6.2).

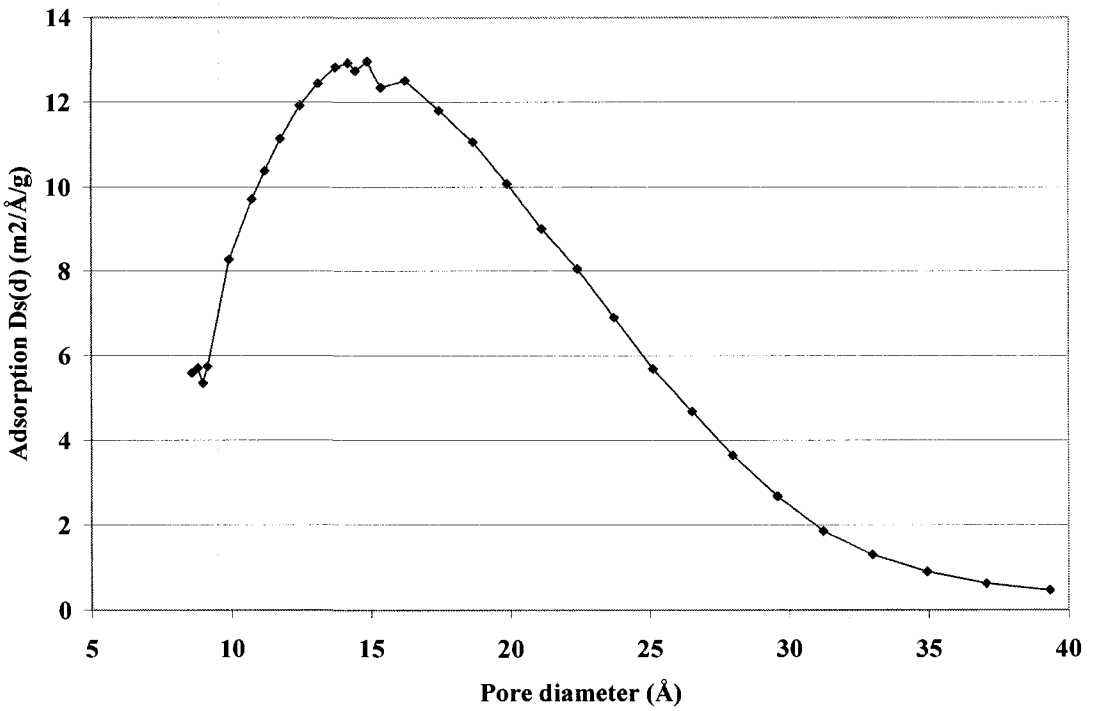


Figure 3.6.1: Pore size distribution for 5%Pd-YSZ 600

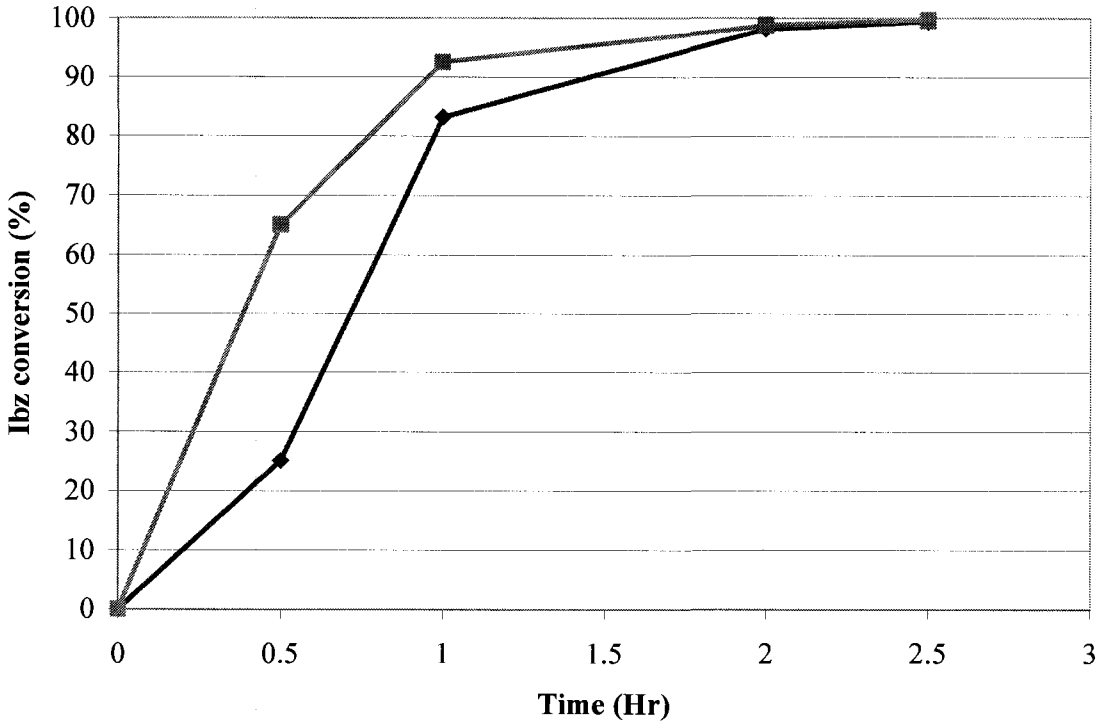


Figure 3.6.2: Reaction profile of Pd-YSZ comparing the effect on reactivity of the calcination temperature. (♦)950°C, (■)600°C. The solutions contained: Ibz (4.0mmol), Bu-cin (4.8mmol), DIPEA (8.0mmol), 5%Pd-YSZ 950 (0.004mmol, S/C 1000), Decane (0.04mmol) and DMF (5.4mL) at 140°C.

## 3.7 Ni-YSZ Structural and Reaction Profile Analysis

Certain catalysts are very active but have a limited range of substrates while other work wonders with many substrates but suffer from a low reactivity[11]. This lack of understanding prevents any reliable prediction as to the activity of newly synthesised Heck catalysts. It would be helpful to understand more of the fundamental principles that rule the HR.

While heterogeneous catalysts are now believed to go through the homogeneous anionic mechanism[10] by means of leaching and redeposition[158], the fact remains that various heterogeneous catalysts do not show the same reactivity suggesting that the structural characteristics of the catalyst affects the speed of the reaction.

Based on aryl-halide extraction through the oxidative addition of surface metal atom, it is generally believed that a high overall surface area will expose more metal to the reactant, therefore augmenting the reactivity. Also, a small metal crystallite size will create a higher active (i.e. metallic) surface area which means more surface metal atoms. In addition, the recapture of leached metal atoms was also proposed to be facilitated by certain substrates. However, the extent of these factors is arguable and merits further study.

In the current study, Ni-YSZ was analysed based on three factors; the synthetic method, the calcination temperature and the effect of metal loading. To facilitate the analysis, the collected data will be repeated in each section in the form of various tables and graphs which are organized to compare the applicable variable.

Every reaction profile presented in this section was made with the appropriate catalysts along with the following reactants: Ibz (1.0mmol), Bu-cin (1.0mmol), base (2.0mmol), NiO catalyst (0.01mmol, S/C 100), Tetradecane (0.5mmol) and DMA (270μL) at 130°C.

Table 3.6.1: Catalysts compared and analysed throughout section 3.7

| Synthetic method[ix] | Metal loading (mol%)[x] | Calcination temperature (°C) |
|---|---|---|
| SA | 1, 5, 10 | 400, 600, 950 |
| $ZrCl_4$ | 5 | 600, 950 |
| OH | 5, 10 | 600, 950 |
| $NH_3$ | 5, 10 | 600, 950 |

### 3.7.1 Synthetic Method Influence on the Reaction Profile

When calcinated at 600°C both catalysts synthesised via the self-assembly method (SA, $ZrCl_4$) reacted faster than the catalysts synthesised via the co-precipitation method (OH, $NH_3$) (Figure3.7.1)[xi]. While no perfect correlation is found in the data from table 3.7.2, some trends can still be extracted.

For example, a smaller particle size results in a higher metallic surface. As such, we expect the catalyst with the smallest particle size to be more reactive. A feature of the self-assembly method is the lower particle size as attested by both the P-XRD (YSZ) and chemisorption. Since the low catalyst loading makes nickel very hard to see in the P-XRD, we will sometimes use the YSZ particle size to estimate the trend in the nickel particle size. This assumption is validated by the fact that the YSZ particle size trend in the P-XRD is the same as the nickel particle trend in the chemisorption as both show; $ZrCl_4 < SA < OH < NH_3$.

Another trend is with the surface area. The self-assembly method produces a powder with a higher surface area than the co-precipitation method due to the meso-structure it creates. A higher surface area allows more substrate to penetrate into the pore structure of the catalysts which allows more metal sites to be active. A surface area of 78 $m^2/g$ for the self-assembly versus 30 $m^2/g$ and 21 $m^2/g$ for the co-precipitation by $NH_3$ and OH respectively, may

[ix] SA: self-assembly with $Zr(OEt)_4$ as reactant, $ZrCl_4$: self-assembly with $ZrCl_4$ as reactant, OH: co-precipitation using NaOH as base, $NH_3$: co-precipitation using $NH_3$ as base.
[x] Every metal loading was calcinated to each temperature indicated in the following collumn
[xi] As mentioned in the experimental section, the error is approximated at 10%.

explain the higher reactivity of both self-assembly catalysts. This order, based on the surface area is as follow; SA, $NH_3$, OH.

Table 3.7.2: Structural data organized by synthetic method

| Catalyst's synthetic method[xii] | Physisorbtion | | | Chemisorbtion | | | P-XRD Particule size | |
|---|---|---|---|---|---|---|---|---|
| | Surface area ($m^2/g$) | Pore distribution (A) | Pore peak (A) | Active surface area | Percent metal dispersion | Average crystallite size | YSZ (A) | Ni (A) |
| 5% Ni-YSZ 600°C | | | | | | | | |
| SA | 78.36 | 30-75 | 49 | 0.2287 | 1.373 | 737 | 96±3 | - |
| OH | 20.68 | 75-250 | 150 | 0.2329 | 1.299 | 778.6 | 177-15 | - |
| $NH_3$ | 29.9 | 70-200 | 130 | 0.03533 | 0.3646 | 2775 | 323-22 | - |
| $ZrCl_4$ | - | - | - | 0.2501 | 1.484 | 681.8 | 44-2 | - |
| 5% Ni-YSZ 950°C | | | | | | | | |
| SA | 4.95 | - | - | - | - | - | 418-13 | - |
| OH | - | - | - | - | - | - | 502-18 | 243-240 |
| $NH_3$ | 0.81 | - | - | - | - | - | 403-13 | 1101-791 |
| $ZrCl_4$ | 1.14 | - | - | 0.1192 | 0.7069 | 1431 | 515-30 | 51-38 |
| 10% Ni-YSZ 600°C | | | | | | | | |
| SA | 57.27 | 35-80 | 55.6 | 2.67 | 7.672 | 131.9 | 57-2 | 35-7 |
| OH | 31.71 | 70-200 | 123.2 | 0.4534 | 1.495 | 679.5 | 155-5 | 23-9 |
| $NH_3$ | 28.9 | 60-200 | 130 | 0.01713 | 0.04248 | 2382 | 306-33 | - |
| | | | | | | | | |
| 10% Ni-YSZ 950°C | | | | | | | | |
| SA | 0.32 | - | - | 0.3331 | 0.9548 | 1060 | 725-36 | 340-198 |
| OH | - | - | - | 0.4035 | 1.331 | 760.2 | 1158-220 | - |
| $NH_3$ | 3.73 | - | - | - | - | - | 555-56 | 142-55 |

However, while catalysts synthesised by the self-assembly method (SA and $ZrCl_4$) show more reactivity than those synthesised by the co-precipitation method (OH, $NH_3$), there are inconsistencies inside these group. For the particle size trend, SA showed a higher reactivity but had larger particle size than $ZrCl_4$. For the surface area trend, OH showed a higher reactivity but had a lower surface area than $NH_3$ (21 vs. 30 $m^2/g$).

[xii] SA: self-assembly with $Zr(OEt)_4$ as reactant, $ZrCl_4$: self-assembly with $ZrCl_4$ as reactant, OH: co-precipitation using NaOH as base, $NH_3$: co-precipitation using $NH_3$ as base.

Since both trends show exceptions, it is highly possible that both factors, the surface area and the particle size, affect the reaction speed. The observed reactivity could be based on the combined effect of these two factors.

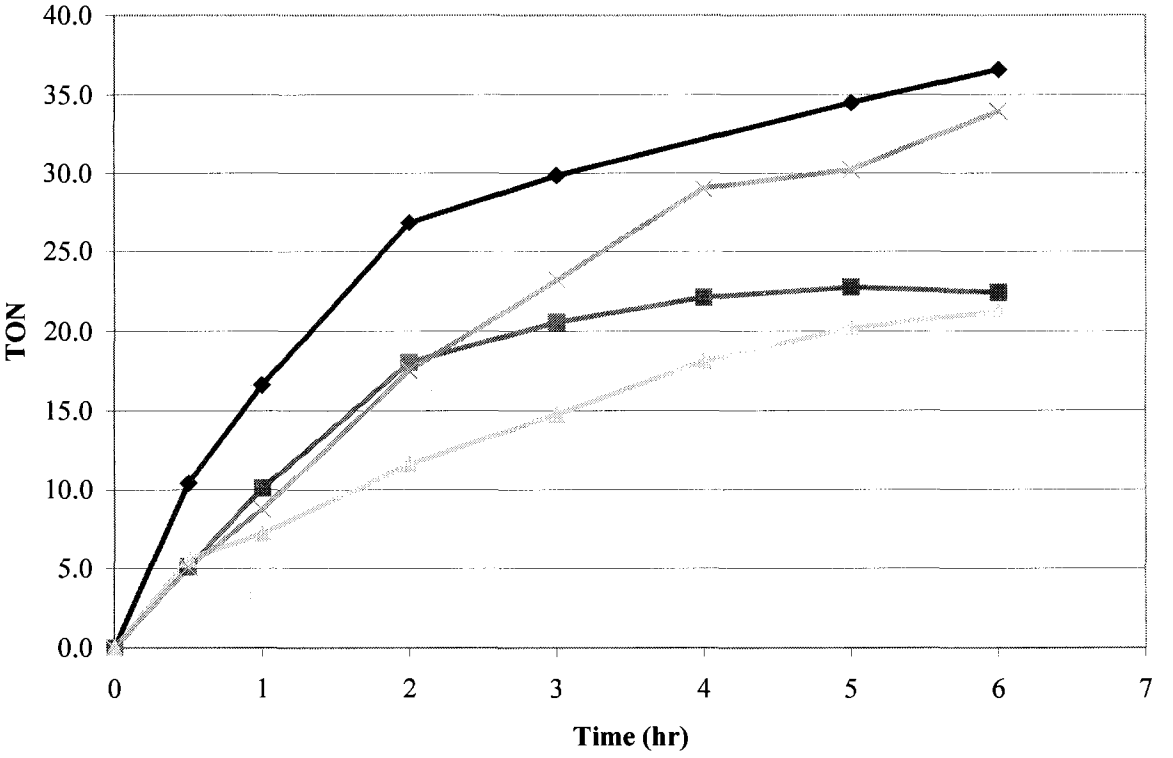


Figure 3.7.1: Reaction profile analysing the effect of the synthetic method on 5%NiO-YSZ 600. (♦)SA, (■)OH, (▲)$NH_3$, (x)$ZrCl_4$.

Figure 3.7.2 shows the same catalysts calcinated to 950°C. The surface area data indicates a correlation between the speed of reaction (SA, $ZrCl_4$, $NH_3$) and the surface area (4.95, 1.14, $0.81 m^2/g$)[xiii].

There is insufficient metallic particle size data to make a pertinent analysis. However, the P-XRD data for YSZ[xiv] we observe is between 400-500A. This may indicate that in the absence of any significant particle size difference, the surface area is the dominant factor for the catalyst reactivity.

[xiii] Due to the unknown surface area of OH, it was removed from the analysis
[xiv] Trends in the YSZ particle size are good indicators of the trend in the nickel particle size

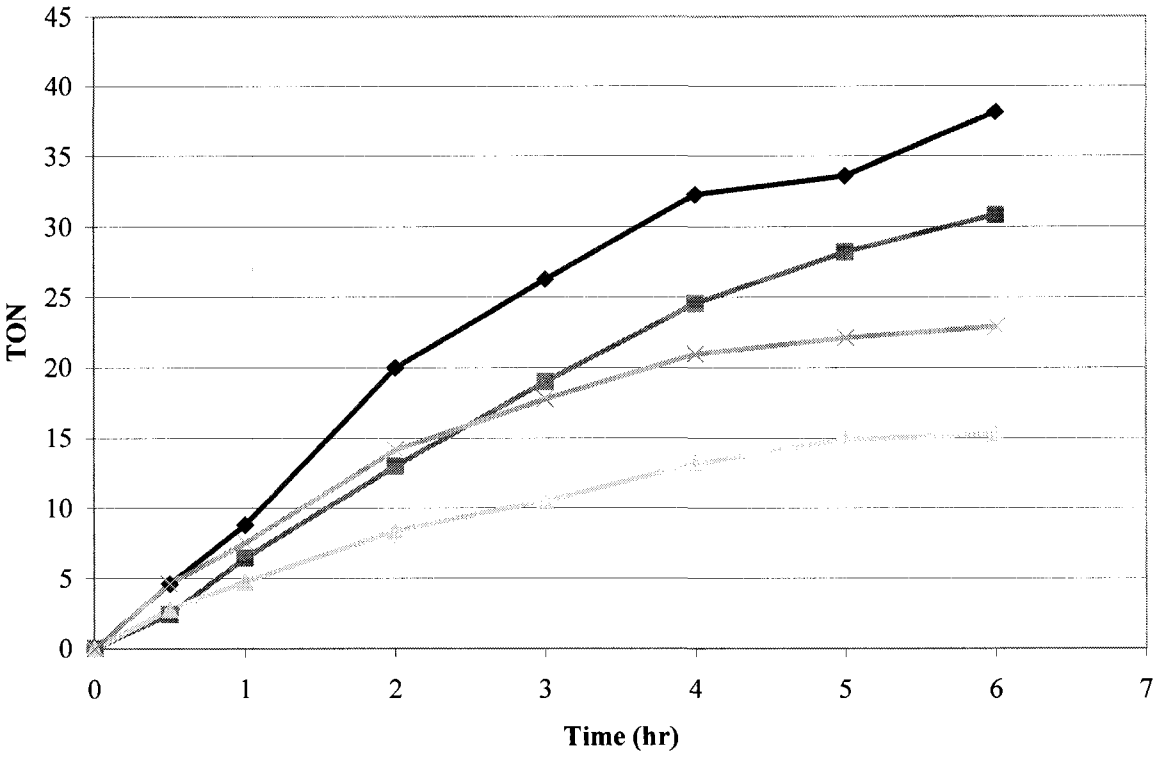


Figure 3.7.2: Reaction profile analysing the effect of the synthetic method on 5%NiO-YSZ 950. (♦)SA, (■)OH, (▲)$NH_3$, (x)$ZrCl_4$.

Figure 3.7.3 shows all catalysts with a loading of 10%Ni. The reactivity for all 10% catalyst calcinated at 600°C follows well with the surface area even if the differences between their reactivities are small. The SA catalyst is the fastest with a surface area of $57m^2/g$ and both co-precipitation catalyst follow with surface areas of $31.71m^2/g$ and $28.9m^2/g$. No trend could be found for the particle size.

For the 10% nickel catalysts calcinated to 950°C we were unable to find any trend for the surface area. However, the trend in the particle size is the opposite of what we expected since the catalyst with the highest reactivity is also the one with the largest particle size (SA).

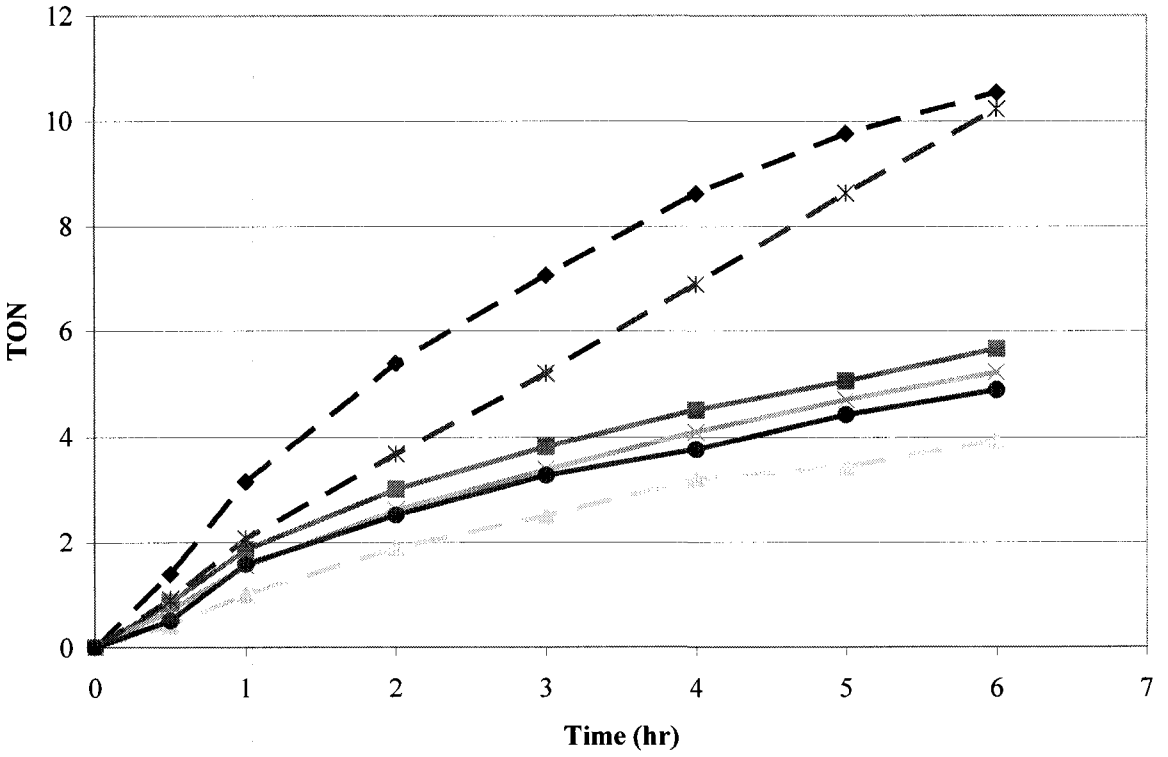


Figure 3.7.3: Reaction profile analysing the effect of the synthetic method on 10%NiO-YSZ. (♦)SA 950, (■)SA 600, (▲)$NH_3$ 950, (x)$NH_3$ 600, (*)OH 950, (•)OH 600.

### 3.7.2 Influence of the Calcination Temperature on Reactivity

Figures 3.7.4, 3.7.5 and 3.7.6 show the results for Ni-YSZ SA (1, 5 and 10%) calcinated at 400, 600 and 950°C respectively. As the calcination temperature augments, the long range order, created through the self-assembly method, is destroyed which greatly reduces the surface area. Higher calcination temperature also tends to increase the crystallite size as atomic mobility grows and causes aggregation. However, no trend could be drawn, either from the surface area or crystallite sizes.

Table 3.7.3: Structural data organized by calcination temperature

| Sample | Physisorbtion | | | Chemisorbtion | | | P-XRD Particule size | |
|---|---|---|---|---|---|---|---|---|
| | Surface area ($m^2/g$) | Pore distribution (A) | Pore peak (A) | Active surface area | Percent metal dispersion | Average crystallite size | YSZ (A) | Ni (A) |
| SA | | | | | | | | |
| 1% 400 | 94.14 | 14-38 | 22 | - | - | - | 90-16 | - |
| 1% 600 | 142.7 | 14-35 | 22 | 0.1672 | 4.079 | 248.0 | 40-1 | - |
| 1% 950 | - | - | - | - | - | - | 353-8 | - |
| 5% 400 | 85.7 | 14-40 | 25 | 0.4396 | 2.425 | 417.1 | 46-3 | 30-1 |
| 5% 600 | 78.36 | 30-75 | 49 | 0.2287 | 1.373 | 737 | 96-3 | - |
| 5% 950 | 4.95 | - | - | - | - | - | 418-13 | - |
| 10% 400 | 228.7 | 14-50 | 24.37 | 1.158 | 3.320 | 304.7 | 51-7 | 167-97 |
| 10% 600 | 57.27 | 35-80 | 55.62 | 2.67 | 7.672 | 131.9 | 57-2 | 35-7 |
| 10% 950 | 0.3165 | - | - | 0.3331 | 0.9548 | 1060 | 725-36 | 340-198 |
| $ZrCl_4$ | | | | | | | | |
| 5% 600 | - | - | - | 0.2501 | 1.484 | 681.8 | 44-2 | - |
| 5% 950 | 1.138 | - | - | 0.1192 | 0.7069 | 1431 | 515-30 | 51-38 |
| OH | | | | | | | | |
| 5% 600 | 20.68 | 75-250 | 150 | 0.2329 | 1.299 | 778.6 | 177-15 | - |
| 5% 950 | - | - | - | - | - | - | 502-18 | 243-240 |
| 10% 600 | 31.71 | 70-200 | 123.21 | 0.4534 | 1.495 | 679.5 | 155-5 | 23-9 |
| 10% 950 | - | - | - | 0.4035 | 1.331 | 760.2 | 1158-220 | - |
| $NH_3$ | | | | | | | | |
| 5% 600 | 29.9 | 70-200 | 130 | 0.03533 | 0.3646 | 2775 | 323-22 | - |
| 5% 950 | 0.8127 | - | - | - | - | - | 403-13 | 1101-791 |
| 10% 600 | 28.9 | 60-200 | 130 | 0.01713 | 0.04248 | 2382 | 306-33 | - |
| 10% 950 | 3.730 | - | - | - | - | - | 555-56 | 142-55 |

The structural data gathered generally follows the expected trends[xv] stated above (see table 3.7.3) but the reactivity shifts for each loading. At 1% loading, the fastest catalyst is the one calcinated at 400°C, at 5% it is the catalyst calcinated at 600°C and for the metal loading of 10%, it is the one calcinated at 950°C. We cannot ascertain the effect of the calcination temperature on the catalyst's reactivity based on the data we collected.

[xv] The only exception is the 1%Ni-YSZ SA 400 which shows a lower surface area and a larger crystallite size than it's counterpart calcinated to 600°C. As of now, we have found no explanation for the high activity of the 1%Ni-YSZ SA 400.

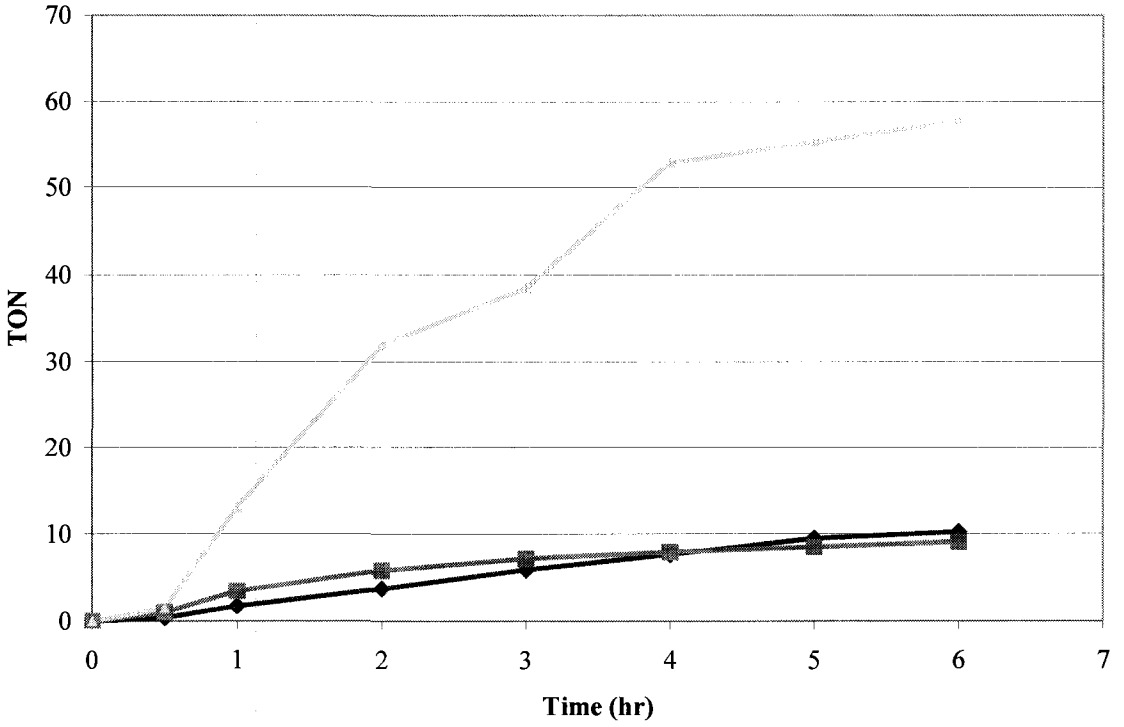


Figure 3.7.4: Reaction profile analysing the effect of the calcination temperature for 1%NiO-YSZ SA. (♦)950, (■)600, (▲)400.

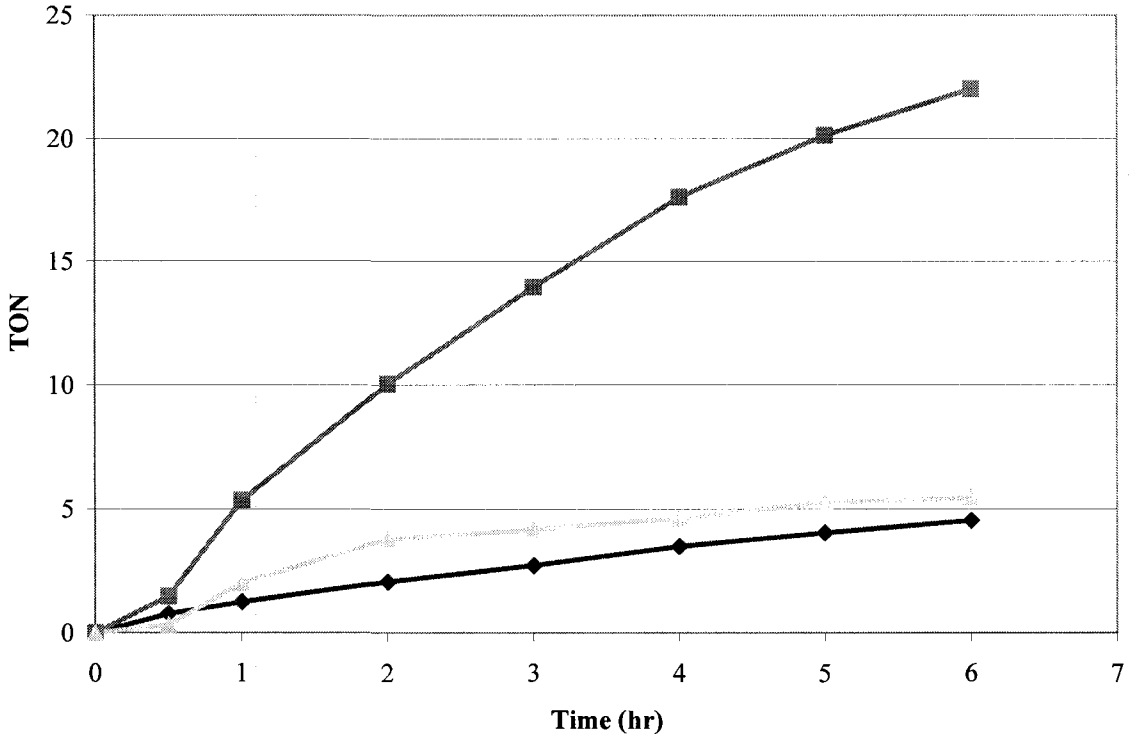


Figure 3.7.5: Reaction profile analysing the effect of the calcination temperature for 5%NiO-YSZ SA. (♦)950, (■)600, (▲)400.

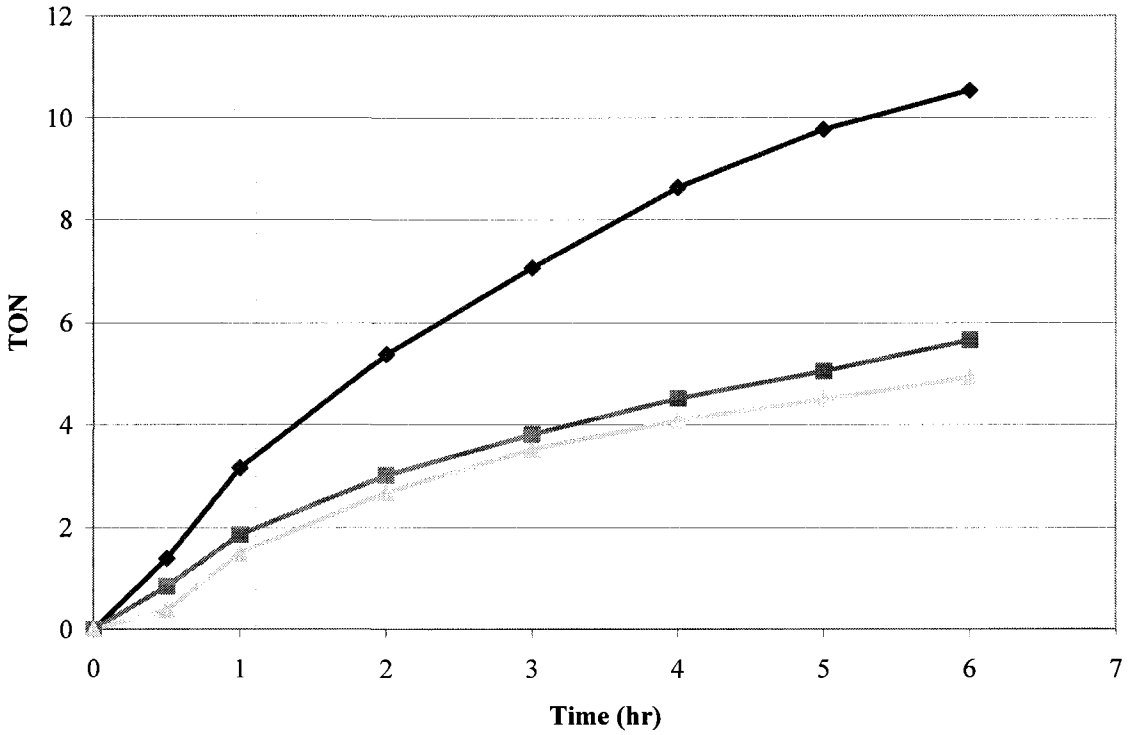


Figure 3.7.6: Reaction profile analysing the effect of the calcination temperature for 10%NiO-YSZ SA. (♦)950, (■)600, (▲)400.

Figure 3.7.7 shows the reactivity for 5%Ni-YSZ OH, $NH_3$ and $ZrCl_4$ calcinated at 600°C and 950°C. The order of reactivity for the $ZrCl_4$ and $NH_3$ catalysts are: 600°C > 950°C. The OH catalysts reactivity is: 950°C > 600°C. $NH_3$ shows a trend is the surface area (29.9$m^2$/g and 0.81$m^2$/g for 600°C and 950°C)

The behaviour of the OH catalyst is non-conclusive since the one calcinated at 600°C starts to react faster but is active for less time and is surpassed after four hours by the one at 950°C. We were unable to establish why this occurred.

All calcination temperature comparison pertaining to the 10% Ni-YSZ catalysts, OH and $NH_3$ are made using figure 3.7.3. $NH_3$ follows the expected reactivity, 600 > 950, which is matched by the larger surface area as well as smaller particle size (P-XRD only) of the 600°C catalyst.

The OH catalyst again shows unexpected behaviour as the catalyst calcinated to 950°C reveals a faster reaction. The 10% Ni-YSZ OH 950 catalyst has an expected lower surface area[xvi] than its 600°C counterpart and it also has a higher crystallite size (P-XRD). The 10% SA catalyst shows the same trend of 950 > 600.

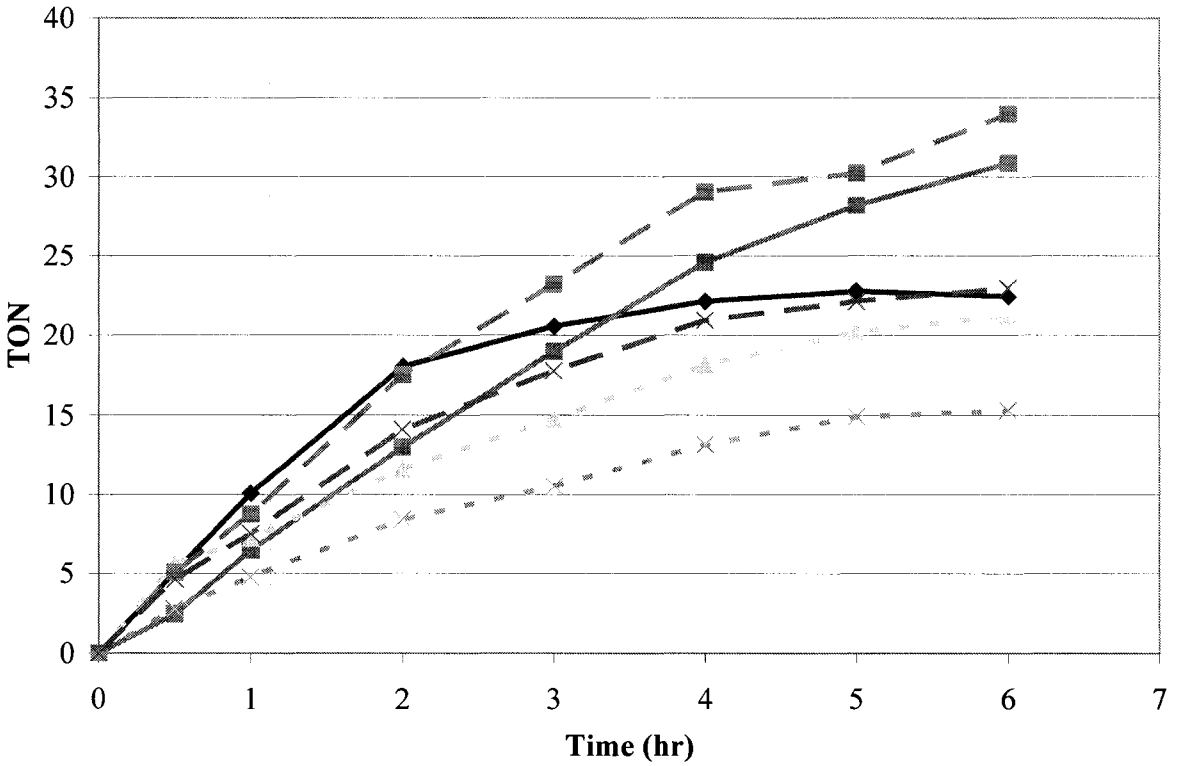


Figure 3.7.7: Reaction profile analysing the effect of the calcination temperature of 5%NiO-YSZ. (♦)OH 600, (■)OH 950, (▲)$NH_3$ 600, (x")$NH_3$ 950, (■-)$ZrCl_4$ 600, (x-)$ZrCl_4$ 950.

[xvi] The surface area of the 10%Ni-YSZ OH 950 catalyst is expected to be lower than the 10% Ni-YSZ 600 since all catalyst calcinated to 950°C always showed a surface area below $10m^2/g$. The 10% Ni-YSZ OH 600 has a surface area of $21m^2/g$.

### 3.7.3 Effect of the metal loading on Reactivity

This section will analyse the correlation between the catalyst loading and the reactivity. The reaction profiles show that for the SA catalysts, at 400°C, the 1% loading is fastest, at 600°C it is the 5% while at 950°C it is the 10% (figure 3.7.8, 3.7.9 and 3.7.10). We were unable to associate this trend with any structural data.

Table 3.7.4: Structural data organized by metal loading

| Sample | Physisorbtion | | | Chemisorbtion | | | P-XRD Particule size | |
|---|---|---|---|---|---|---|---|---|
| | Surface area ($m^2/g$) | Pore distribution (A) | Pore peak (A) | Active surface area | Percent metal dispersion | Average crystallite size | YSZ (A) | Ni (A) |
| SA | | | | | | | | |
| 1% 400 | 94.14 | 14-38 | 22 | - | - | - | 90-16 | 467-149 |
| 5% 400 | 85.7 | 14-40 | 25 | 0.4396 | 2.425 | 417.1 | 46-3 | 30-1 |
| 10% 400 | 228.7 | 14-50 | 24 | 1.158 | 3.320 | 304.7 | 51-7 | 167-97 |
| 1% 600 | 142.7 | 14-35 | 22 | 0.1672 | 4.079 | 248.0 | 40-1 | - |
| 5% 600 | 78.36 | 30-75 | 49 | 0.2287 | 1.373 | 737 | 96±3 | - |
| 10% 600 | 57.27 | 35-80 | 55.62 | 2.67 | 7.672 | 131.9 | 57-2 | 35-7 |
| 1% 950 | - | - | - | - | - | - | 353-8 | - |
| 5% 950 | 4.95 | - | - | - | - | - | 418-13 | - |
| 10% 950 | 0.3165 | - | - | 0.3331 | 0.9548 | 1060 | 725-36 | 340-198 |
| OH | | | | | | | | |
| 5% 600 | 20.68 | 75-250 | 150 | 0.2329 | 1.299 | 778.6 | 177-15 | - |
| 10% 600 | 31.71 | 70-200 | 123.21 | 0.4534 | 1.495 | 679.5 | 155-5 | 23-9 |
| 5% 950 | - | - | - | - | - | - | 502-18 | 243-240 |
| 10% 950 | - | - | - | 0.4035 | 1.331 | 760.2 | 1158-220 | - |
| $NH_3$ | | | | | | | | |
| 5% 600 | 29.9 | 70-200 | 130 | 0.03533 | 0.3646 | 2775 | 323-22 | - |
| 10% 600 | 28.9 | 60-200 | 130 | 0.01713 | 0.04248 | 2382 | 306-33 | - |
| 5% 950 | 0.8127 | - | - | - | - | - | 403-13 | 1101-791 |
| 10% 950 | 3.730 | - | - | - | - | - | 555-56 | 142-55 |

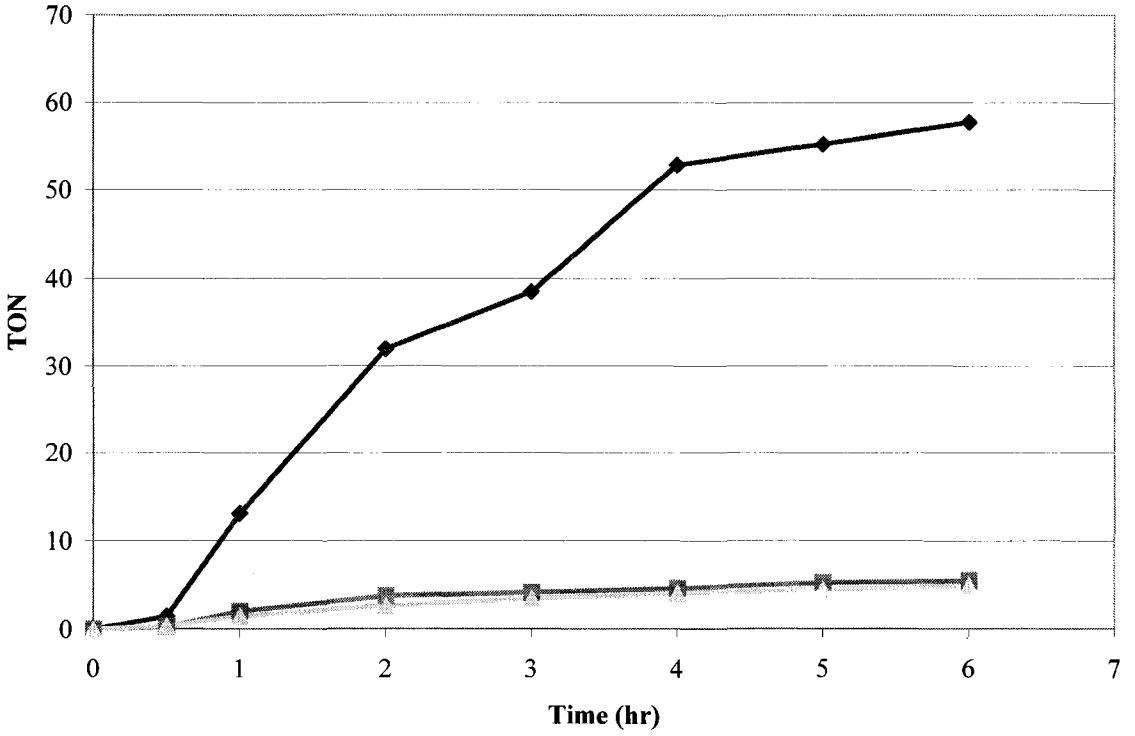


Figure 3.7.8: Reaction profile analysing the effect of the metal loading for NiO-YSZ SA 400 (♦)1%, (■)5%, (▲)10%.

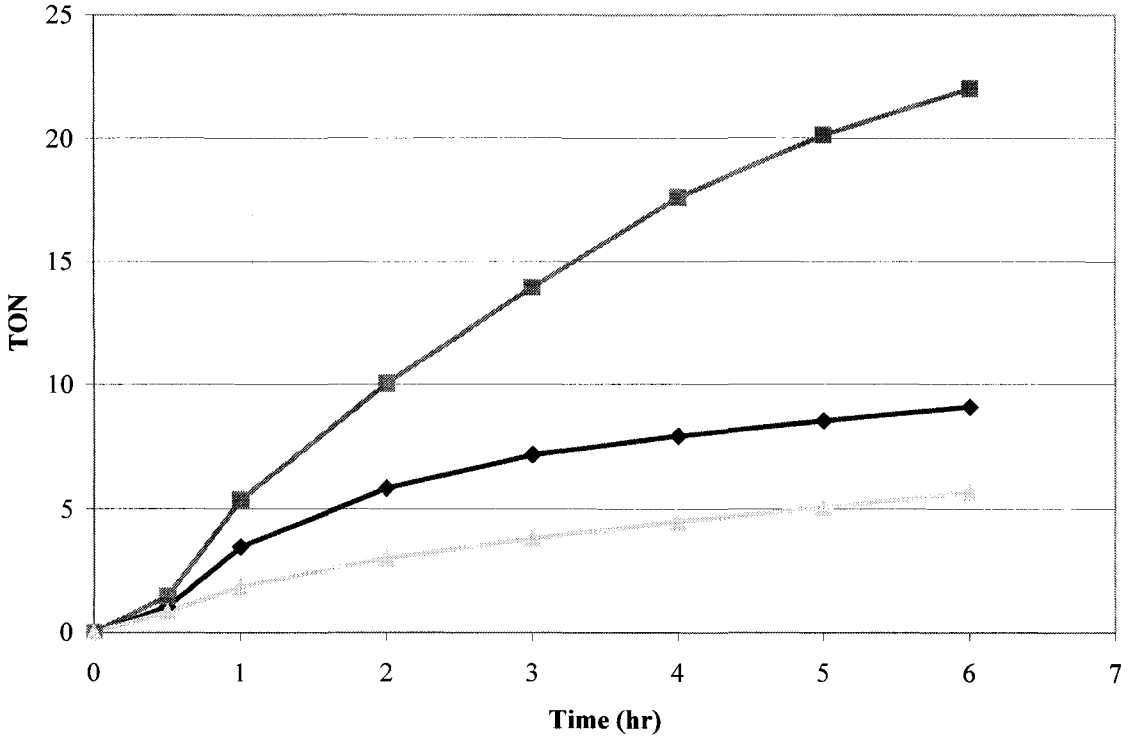


Figure 3.7.9: Reaction profile analysing the effect of the metal loading for NiO-YSZ SA 600 (♦)1%, (■)5%, (▲)10%.

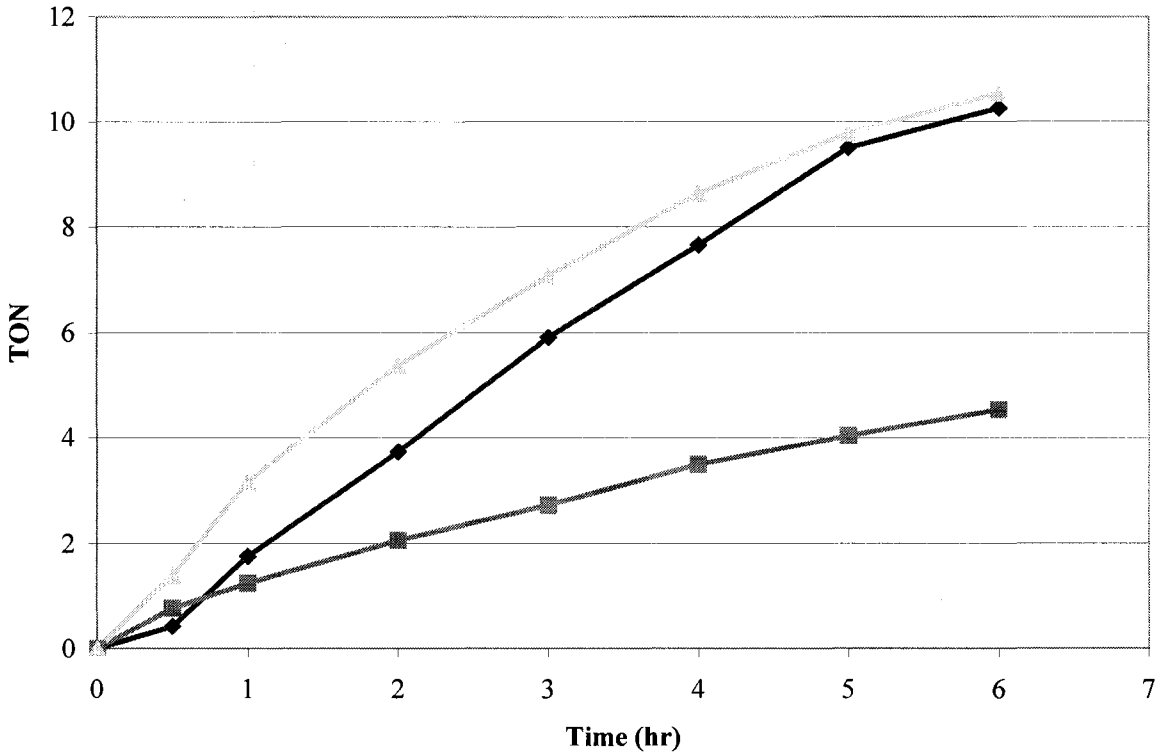


Figure 3.7.10: Reaction profile analysing the effect of the metal loading for NiO-YSZ SA 950 (♦)1%, (■)5%, (▲)10%.

For the OH catalyst, a lower catalyst loading resulted in a faster reaction both in the catalyst calcinated to 600 and 950°C. While the structural data cannot explain the occurrence in the 600°C catalyst (the surface area is higher for the 10% and both particle sizes are similar), the P-XRD data of the 950°C data clearly shows the 5% loading to have a lower particle size than the 10%.

The $NH_3$ catalyst also reacts in the same fashion as the OH catalyst since the 5% loading reacted faster than the 10% at both 600 and 950°C. However, in both cases, the structural data does not establish a clear trend since there is a great similarity in both the surface area and the particle size.

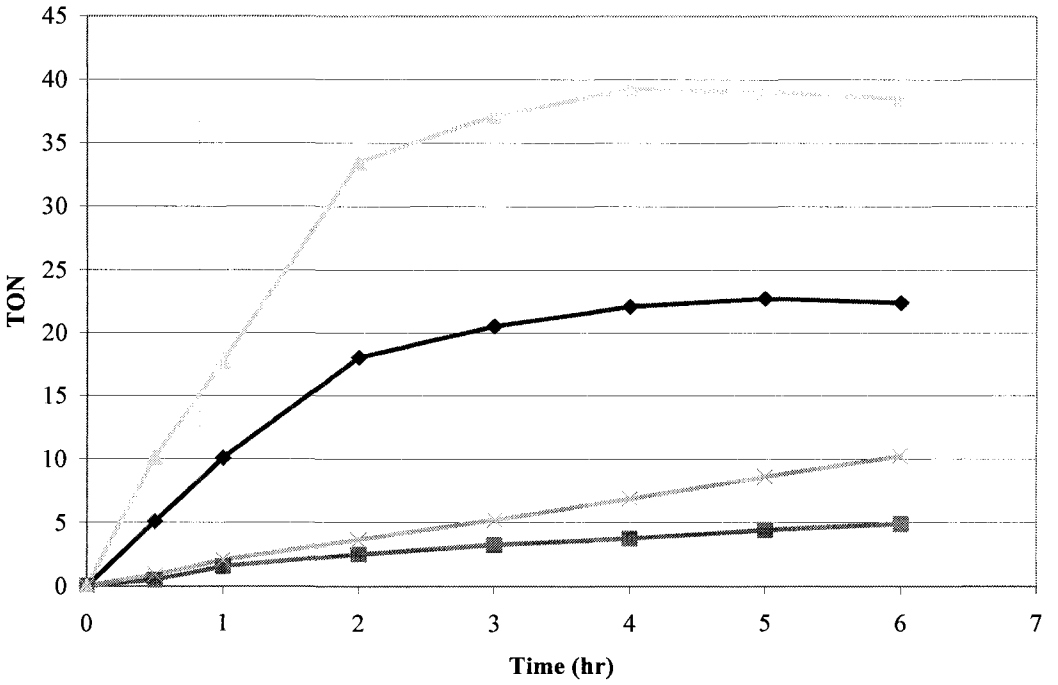


Figure 3.7.11: Reaction profile analysing the effect of the metal loading on NiO-YSZ OH. (♦)5% 600, (■)10% 600, (▲)5% 950, (x)10% 950.

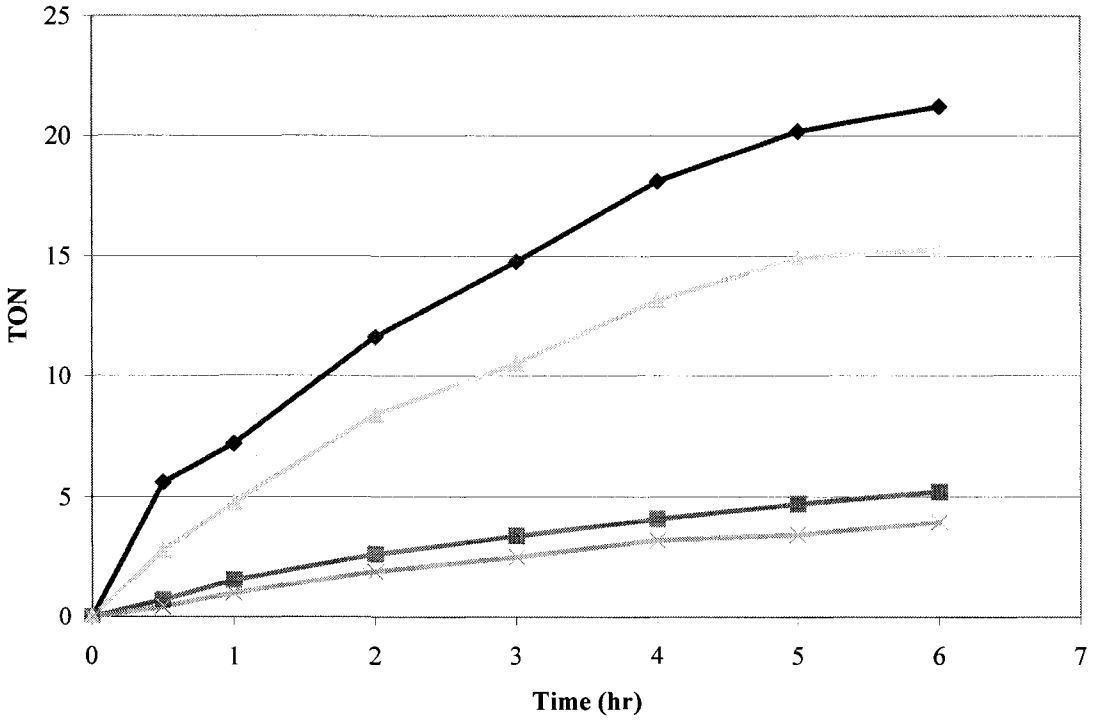


Figure 3.7.12: Reaction profile analysing the effect of the metal loading on NiO-YSZ $NH_3$. (♦)5% 600, (■)10% 600, (▲)5% 950, (x)10% 950.

Lipshultz found that storage of Ni/C under an inert atmosphere was required to retain its activity but was unable to explain why[91]. Our Pd-YSZ catalyst was kept under an inert atmosphere since we used $Pd^0$ but since, for nickel, its oxide (NiO) was used, it was felt that an oxygen free atmosphere was not necessary. Since not all catalyst were synthesised at the same time, they were exposed to air for various length of time and we may have suffered the same effect observed by Lipshultz.

The reaction profiles studied suggests that while a larger surface area and a smaller particle size were mostly correlated with a higher reactivity, the kinetic data seems to suggest that other factors, not analysed in our current experiment, have an important effect in the reactivity.

# Chapter 4-CONCLUSION

## 4.1 Introduction

The Heck-Mizoroki reaction is a C-C coupling reaction between an aryl halide and an olefin. While palladium is the metal that is most used, nickel, largely due to its low cost, has shown promise to replace palladium. The HR mechanism is believed to be guided by the types of ligands present and their concentration with low-temperature metal-ligand catalyzed reaction going through the neutral or cationic cycle and high-temperature or heterogeneously catalyzed reaction going through the anionic cycle. Although heterogeneous catalysts were initially believe to react through surface catalysis, it is becoming accepted that metal leaching occurs and that catalysis occurs in solution, homogeneously.

## 4.2 Reaction optimization

In order to find the optimal experimental conditions for Pd-YSZ and Ni-YSZ, various bases, solvents, temperatures, concentrations of reactant and metal oxidations states were tested. The result differed as Pd-YSZ was more reactive with DIPEA as the base and DMF as the solvent while Ni-YSZ was more reactive with KOAc as the base and DMA as the solvent. In regard to the oxidation state, $Pd^0$ showed more reactivity than PdO but NiO showed more reactivity than $Ni^0$. Using a simple methodology, we were able to easily reach 1000TON.

## 4.3 Mechanistic studies

In heterogeneous HR mechanism, leaching is believed to be due to the reaction of the aryl halide on metal kink sites. Pre-incubations with a missing reactant showed an absence of induction period when iodobenzene was present.

Using p-XRD to quantify the amount of palladium before and after reaction, we discovered that only 37% remained was no longer on the support after a HR. This is a strong indication of leaching and indicates that redeposition may have occurred elsewhere than on the solid support or that palladium stayed in solution as soluble atoms or clusters.

Two variations of the triple phase test were performed. The resin supported reactant was positive confirming leaching. The thiol resin scavenger was done to analyse the feasibility of true heterogeneous catalysis. By neutralizing leached homogeneous palladium species, it showed that surface catalysis minimal.

The structural trends indicate that self assembly synthesis produces mesoporous catalysts with higher surface areas which are more suitable for reaction. Increases in calcination temperatures decrease the surface area and increase particle size of the crystallites in the material with direct consequences in reactivity.

### 4.4 High S/C ratios

Using the optimal conditions of described in section 3.1, reactions with s/c ratios of 100'000 and 1'000'000 were tried. While the 100'000 s/c experiment went to completion, both trials at 1'000'000 s/c did not, reaching 350'000TON and 770'000TON. Using the most linear portion of both curves, TOR were calculated and showed that the second trial was not necessarily more active, but was active longer and this was explained by the use of a mesoporous catalyst.

### 4.5 Aryl halide scan

An important mechanistic difference between nickel and palladium is the lower oxidative addition barrier for nickel. This theoretically allows nickel to more easily react with aryl

bromides and chlorides. While palladium was unreactive toward bromobenzene and chlorobenzene, nickel showed very limited reactivity toward bromobenzene but only at high temperature (160°C).

## 4.6 Pd-YSZ structural analysis

Pd-YSZ was only synthetised by the self-assembly method and calcinated to 600°C and 950°C. The lower calcination temperature of 600°C resulted in lower crystallite sizes (Pd and YSZ) and higher surface area than the catalyst calcinated to 950°C. The sample calcinated to 600°C showed higher reactivity and we postulate that it is due to its lower crystallite sizes that allowed more metal to be exposed and that its higher surface area allowed more substrate to penetrate into the catalyst, thus also exposing more catalytically active sites. Based on the mechanistic analysis of section 3.3, since palladium leaches into solution, an increase of surface sites will facilitate leaching.

## 4.7 Nickel structure-activity relationship analysis

Nickel catalysts (Ni-YSZ) of 1%, 5% and 10% metal loading were synthetised using four methods;self-assembly using $Zr(EtO)_4$, self-assembly using $ZrCl_4$, co-precipitation with NaOH and co-precipitation $NH_3$. These catalysts were calcinated to 400°C, 600°C and 950°C. Correlating the reactivity with the overall surface area, nickel surface area and crystallite sizes, the analysis revealed that while a high surface area and a low crystallite size usually result in a higher reactivity, we were unable to definitely explain the reactivity of each catalyst.

## Chapter 5-REFERENCES


(1) Heck, R F *J. Am. Chem. Soc.* **1968**, *90*, 5518.
(2) Heck, R F *J. Am. Chem. Soc.* **1968**, *90*, 5526.
(3) Heck, R F *J. Am. Chem. Soc.* **1968**, *90*, 5531.
(4) Mizoroki, T; Mori, K; Ozaki, A *Bull. Chem. Soc. Jap.* **1971**, *44*, 581.
(5) Mori, K; Mizoroki, T; Ozaki, A *Bull. Chem. Soc. Jap.* **1973**, *46*, 1505.
(6) Heck, R F *Acc. Chem. Res.* **1979**, *12*, 146.
(7) Heck, R F; Nolley, J P *J. Org. Chem.* **1972**, *37*, 2320.
(8) Dieck, H A; Heck, R F *J. Am. Chem. Soc.* **1974**, *96*, 1133.
(9) Dieck, H A; Heck, R F *J. Am. Chem. Soc.* **1974**, *96*, 1136.
(10) de Vries, Johannes G *Dalton Trans.* **2006**, 421.
(11) Beletskaya, Irina P ; Cheprakov, Andei V. *Chem. Rev.* **2000**, *100*, 3009.
(12) Littke, Adam F. ; Fu, Gregory C. *Angew. Chem. Int. Ed.* **2002**, *41*, 4176.
(13) Littke, Adam F; Fu, Gregory C *Angew. Chem. Int. Ed.* **2002**, *41*, 4176.
(14) Miyaura, N; Yamada, K; Suzuki, A *Tetrahedron Lett.* **1979**, 3437.
(15) Miyaura, N; Suzuki, A *Chem. Rev.* **1995**, *95*, 2457.
(16) Kumada, Makoto; Tamao, Kohei; Koji, Sumitani *J. Am. Chem. Soc.* **1972**, *94*, 4374.
(17) Corriu, R J; Masse, P *Chem. Commun.* **1972**, 144.
(18) Negishi, E; King, A O; Okukado, N *Chem. Commun.* **1977**, 683.
(19) Kosugi, M; K. Sasazawa; Shimizu, Y. *et al. Chem. Lett.* **1977**, 301.
(20) Stille, J K *Angew. Chem. Int. Ed.* **1986**, *25*, 508.
(21) Sonogashira, K; Tohda, Y *Tetrahedron Lett.* **1975**, 4467.
(22) Hiyama, T; Hatanaka, Y *J. Org. Chem.* **1988**, *53*, 918.
(23) Bo-Lin Lin; Lei Liu; Yao Fu *et al. Organometallics* **2004**, *23*, 2114.
(24) Iyer, Suresh; Ramesh, Chinnasamy; Ramani, A *Tetrahedron Lett.* **1997**, *38*, 8533.
(25) Lipshutz, Bruce H.; Stefan Tasler *J. Org. Chem.* **2003**, *68*, 1190.
(26) Songyan Ma; Hongjun Wang; Kaimin Gao *et al. J. Mol. Catal. A Chem.* **2006**, *248*, 17.
(27) Frieman, Bryan; Taft, Benjamin R; Lee, Ching-Tien *et al. Synthesis* **2005**, *17*, 2989.
(28) Wei Wang; Rongliang Wang; Fan Wu *et al. React. Kinet. Catal. Lett.* **2004**, *85*, 277.
(29) Sustmann, Reiner; Hopp, Peter; Holl, Peter *Tetrahedron Lett.* **1989**, *30*, 689.
(30) Iyer, Suresh *J. Organomet. Chem.* **1995**, *490*, C27.
(31) Iyer, Suresh; Ramesh, C.; Sarkar, A. *et al. Tetrahedron Lett.* **1997**, *38*, 8113.
(32) Fujioka, T; Nakamura, T; Yorimitsu H *et al. Org. Lett.* **2002**, *4*, 2257.
(33) Ikeda, Yousuke; Nakamura, Tomoaki; Yorimitsu, Hideki *et al. J. Am. Chem. Soc.* **2002**, *124*, 6514.
(34) Iyer, Suresh; Thakur, Vinay V. *J. Mol. Catal. A Chem.* **2000**, *157*, 275.
(35) Li, George Y; Zheng, Gang; Noonan, Andrew F *J. Org. Chem.* **2001**, *66*, 8977.
(36) Reetz, Manfred T; Lohmer, Gunther; Schwickardi, Renate *Angew. Chem. Int. Ed.* **1998**, *37*, 481.
(37) Tucker, Charles E; De Vries, Johannes G *Top. Catal.* **2002**, *19*, 111.
(38) Shaw, Bernard L; Perera, Sarath D *Chem. Commun.* **1998**, 1863.
(39) Scrivanti, A *J. Mol. Catal. A Chem.* **2005**, *235*, 12.
(40) Hartwig, John F; Janis, Louie *Angew. Chem. Int. Ed.* **1996**, *35*, 2359.
(41) Shibasaki, Masakatsu; Miyazaki, Futoshi; Yamaguchi, Kentaro *Tetrahedron Lett.* **1999**, *40*, 7379.

(42) Nowotny, Mathias; Hanefeld, Ulf; Koningsveld, Henk van *et al. Chem. Commun.* **2000**, 1877.
(43) Jones, Christopher W. *Adv. Synth. Catal.* **2005**, *347*, 161.
(44) Bergbreiter, David E; Osburn, Philip L ; Frels, Jonathon D *Adv. Synth. Catal.* **2004**, *347*, 172.
(45) McGuinness, David S. ; Cavell, Kingsley J.; Skelton, Brian W. *et al. Organometallics* **1999**, *18*, 1596.
(46) Yao, Qingwei; Mark Zabawa; Joyce Woo *et al. J. Am. Chem. Soc.* **2007**, *129*, 3088.
(47) Ambulgekar, Girish V; Bhanage, Bhalchandra M; Samant, Shriniwas D *Tetrahedron Lett.* **2005**, *46*, 2483.
(48) LeBlond, Carl R; Arthur T. Andrews; John R. Sowa, Jr. *et al. Org. Lett.* **2001**, *3*, 1555.
(49) Marck, Guy; Villiger, Alois; Buchecker, Richard *Tetrahedron Lett.* **1994**, *35*, 3277.
(50) Corma, Avelino; Garcia, Hermenegildo; Leyva, Antonio *J. Mol. Catal. A Chem.* **2005**, *230*, 97.
(51) Walter, Jurgen; Jörg Heiermann; Gerald Dyker *et al. J. Catal.* **2000**, *189*, 449.
(52) Shmidt, A. F. ; V.V. Smirnow; O.V. Starikova *et al. Kinet. Catal.* **2001**, *42*, 199.
(53) Tribolet, P. ; Kiwi-Minsker, L. *Catalysis Today* **2005**, *105*, 337.
(54) Gruber, Marcus ; Sandra Chouzier; Klaus Koehler *et al. Appl. Catal. A Gen.* **2004**, *265*, 161.
(55) Conlon, David A *Adv. Synth. Catal.* **2003**, *345*, 931.
(56) Mukhopadhyay, Sudip *Adv. Synth. Catal.* **2002**, *344*, 348.
(57) Ji, Yaying; jain, Surbhi; Davis, Robert J *J. Phys. Chem. B* **2005**, *109*, 17232.
(58) Solodenko, Wladimir; Hongliang Wen; Stefanie Leue *et al. J. Org. Chem.* **2004**, 3601.
(59) Papp, Attila; Krisztina Miklós; Péter Forgo *et al. J. Mol. Catal. A Chem.* **2005**, *229*, 107.
(60) Martinez, Sandra; Marcial Moreno-Mañas; Adelina Vallribera *et al. New J. Chem.* **2006**, *30*, 1093.
(61) Martinez, Sandra ; Adelina Vallribera; Cosmin L. Cotet *et al. New J. Chem.* **2005**, *29*, 1342.
(62) Li, Jintong; Mau, Albert W H; Strauss, Christopher R *Chem. Commun.* **1997**, 1275.
(63) Augustine, Robert L; O'Leary, Shaun T *J. Mol. Catal. A Chem.* **1995**, *95*, 277.
(64) Augustine, Robert L; O'Leary, Shaun T *J. Mol. Catal.* **1992**, *72*, 229.
(65) Wali, Anil; Pillai, S Muthukumaru; Kaushik, V K *et al. Appl. Catal. A Gen.* **1996**, *135*, 83.
(66) Cwik, Agnieszka; Hell, Zoltan; Figueras, Francois *Adv. Synth. Catal.* **2006**, *348*, 523.
(67) Kantam, M Lakshmi; Sarabindu, Roy; Moumita, Roy *et al. Synlett* **2006**, *17*, 2747.
(68) Kaneda, Kiyotomi; Higuchi, Masato; Imanaka, Toshinobu *J. Mol. Catal.* **1990**, *63*, L33.
(69) Kohler, Klaus *Top. Catal.* **2000**, *13*, 319.
(70) Choudary, Boyapati M ; Sateesh Madhi; Naidu S. Chowdari *et al. J. Am. Chem. Soc.* **2002**, *124*, 14127.
(71) Molnar, Arpad; Papp, Attila *Synlett* **2006**, *18*, 3130.
(72) Mori, Kohsuke ; Kazuya Yamaguchi; Takayoshi Hara *et al. J. Am. Chem. Soc.* **2002**, *124*, 11572.
(73) Mandal, Saikat; Debdut Roy; V., Raghunath *et al. Chem. Mat.* **2004**, *16*, 3714.

(74) Okumura, Kazu; Nota, Kumiko; Yoshida, Keiko *J. Catal.* **2005**, *231*, 245.
(75) Yamada, Yoichi M A; Takeda, Koji; Takahashi, Hideyo *et al. Tetrahedron* **2004**, *60*, 4097.
(76) Yamada, Yoichi M A; Takeda, Koji; Takahashi, Hideyo *et al. Org. Lett.* **2002**, *4*, 3371.
(77) Yamada, Yoichi M A; Takeda, Koji; Takahashi, Hideyo *et al. Tetrahedron Lett.* **2003**, *44*, 2379.
(78) Bedford, Robin B; Catherine S. J. Cazin; Michael B. Hursthouse *et al. J. Organomet. Chem.* **2001**, *633*, 173.
(79) Baleizao, Carlos; Corma, Avelino; García, Hermenegildo *et al. Chem. Commun.* **2003**, 606.
(80) Baleizao, Carlos *J. Mol. Catal. A Chem.* **2004**, *69*, 439.
(81) Li, Liang; Shi, Jian-lin; Yan, Ji-na *Chem. Commun.* **2004**, *17*, 1990.
(82) Liang Li; Ling *Appl. Catal. A Gen.* **2005**, *283*, 85.
(83) Pathak, Srikant; Greci, Marcia T.; Kwong, Raymond C *et al. Chem. Mat.* **2000**, *12*, 1985.
(84) Gniewek, Andrzej; Trzeciak, Anna M; Ziolkowski, Jozef J *et al. J. Catal.* **2005**, *229*, 332.
(85) Antonietti, M; Klingelhofer, S; Heitz, W *et al. J. Am. Chem. Soc.* **1997**, *119*, 10116.
(86) Reetz, Manfred T; lohmer, Gunther *Chem. Commun.* **1996**, 1921.
(87) Bars, Joël Le ; Ullrich Specht; John S. Bradley *et al. Langmuir* **1999**, *15*, 7621.
(88) Beller, Matthias; Fisher, Hartmut; Kuhlein, Klaus *et al. J. Organomet. Chem.* **1996**, *520*, 257.
(89) Reetz, Manfred T; Breinbauer, Rolf; Wanninger, Klaus *Tetrahedron Lett.* **1996**, *37*, 4499.
(90) Jones, Christopher W; Phan, Nam T.S. ; Van Der Sluys, Matthew *Adv. Synth. Catal.* **2006**, *348*, 609.
(91) Lipshutz, Bruce H. ; Stefan Tasler; Will Chrisman *et al. J. Org. Chem.* **2003**, *68*, 1177.
(92) Knowles, Jonathan P.; Whiting, Andre *Org. Biomol. Chem.* **2007**, *5*, 31.
(93) Tsou, T.T.; Kochi, J.K. *J. Am. Chem. Soc.* **1979**, *101*, 6319.
(94) Fauvarque, J.-F.; Pfluger, F.; Troupel, J. *J. Organomet. Chem.* **1981**, *208*, 419.
(95) Wolfe, J P; Buchwald, S L *Angew. Chem. Int. Ed.* **1999**, *38*, 2413.
(96) Casado, A.L.; Espinet, P *Organometallics* **1998**, *17*, 954.
(97) Beller, Matthias; Riermeier, T H *Eur. J. Inorg. Chem.* **1998**, 29.
(98) Urata, H; Tanaka, M; Fuchikami *Chem. Lett.* **1987**, 751.
(99) Cabri, W; Candiani, I; Bedeschi, A *et al. J. Org. Catal.* **1992**, *57*, 3558.
(100) Amatore, Christian; Jutand, Anny *J. Organomet. Chem.* **1999**, *576*, 254.
(101) Albert, Katrin; Gisdakis, Philip; Rosch, Notker *Organometallics* **1998**, *17*, 1608.
(102) Cabri, W *J. Org. Chem.* **1992**, *57*, 1481.
(103) Thorn, David L; Hoffmann, Roald *J. Am. Chem. Soc.* **1978**, *100*, 2079.
(104) kawataka, F; Shimizu, I; Yamamoto, A *Bull. Chem. Soc. Jap.* **1995**, *68*, 654.
(105) Fristrup, Peter ; Quement, Sebastian Le; Tanner, David *et al. Organometallics* **2004**, *23*, 6160.
(106) Buezo, Nuria Diaz; Alonso, Inés; Carretero, Juan C *J. Am. Chem. Soc.* **1998**, *120*, 7129.
(107) Gilbertson, Scott; Fu, zice *Org. Lett.* **2001**, *3*, 161.

(108) Jeffery, T *Chem. Commun.* **1984**, 1287.
(109) Schmidt, A F; Smirnow, V V *Kinet. Catal.* **2001**, *42*, 800.
(110) Chrismann, U; Vilar, R *Angew. Chem. Int. Ed.* **2005**, *44*, 366.
(111) de Vries, Johannes G *Eur. J. Inorg. Chem.* **1999**, 1073.
(112) Herrmann, Wolfgang A; Christoph Brossmer; Karl Öfele *et al. Angew. Chem. Int. Ed.* **1995**, *34*, 1844.
(113) Hermann, W. A. *Angew. Chem. Int. Ed.* **1997**, *3*, 1357.
(114) Shaw, Bernard L *New J. Chem.* **1998**, *22*, 77.
(115) Bocelli, G; Catellani, M; Ghelli, S *J. Organomet. Chem.* **1993**, *458*, C12.
(116) Campora, J *Organometallics* **2005**, *24*, 3624.
(117) Biffis, Andrea; Zecca, Marco; Basato, Marino *J. Mol. Catal. A Chem.* **2001**, *173*, 249.
(118) McGuinness, David S. ; Cavell, Kingsley J.; Skelton, Brian W. *et al. Organometallics* **1999**, *18*, 1596.
(119) Amatore, Christian; Jutand, Anny *J. Am. Chem. Soc.* **1993**, *115*, 9531.
(120) Amatore, Christian; Jutand, Anny *Organometallics* **1992**, *11*, 3009.
(121) Amatore, Christian; Jutand, Anny *Organometallics* **1995**, *14*, 5605.
(122) Amatore, Christian; Jutand, Anny *J. Organomet. Chem.* **1989**, *363*, C41.
(123) Amatore, Christian; Jutand, Anny *J. Am. Chem. Soc.* **1991**, *116*, 8375.
(124) Amatore, Christian; Jutand, Anny *Chem.-Eur. J.* **1996**, *2*, 957.
(125) Amatore, Christian; Jutand, Anny *Organometallics* **1995**, *14*, 1818.
(126) Amatore, Christian; Jutand, Anny *Acc. Chem. Res.* **2000**, *33*, 314.
(127) Broring, M; Brandt, C D *Chem. Commun.* **2003**, 2156.
(128) Hansson, Sverker ; Norrby, Per Ola; Soegren, Magnus P. T. *et al. Organometallics* **1993**, *12*, 4940.
(129) Sundermann, A; Uzan, O; Martin, J M L *Chem.-Eur. J.* **2001**, *7*, 1703.
(130) Goossen, J L; Koley, D; Hermann, H *et al. Chem. Commun.* **2004**, 2141.
(131) Goossen, Lukas J. ; Debasis Koley; Holger L. Hermann *et al. Organometallics* **2005**, *24*, 2398.
(132) Evans, John; O'Neill, Lynn; Kambhampati, Vijaya L *et al. Dalton Trans.* **2002**, 2002.
(133) de Vries, Johannes G *Can. J. Chem.* **2001**, *79*, 1086.
(134) de Vries, Andre H. M.; Parlevliet, Floris J; de Vondervoort, Lizette Schmieder-van *et al. Adv. Synth. Catal.* **2002**, *344*, 996.
(135) de Vries, Andre H. M. ; Jan M. C. A. Mulders; John H. M. Mommers *et al. Org. Lett.* **2003**, *5*, 3285.
(136) El-Sayed, Mostafa A; Narayanan, Radha *J. Am. Chem. Soc.* **2003**, *125*, 8340.
(137) El-Sayed, Mostafa A; Li, Y *J. Phys. Chem. B* **2001**, *105*, 8938.
(138) El-Sayed, Mostafa A; Narayanan, Radha *J. Phys. Chem. B* **2005**, *109*, 4357.
(139) El-Sayed, Mostafa A; Narayanan, Radha *Langmuir* **2005**, *21*, 2027.
(140) Augustine, Robert L; Tanielyan, S K *J. Mol. Catal.* **1993**, *80*, 277.
(141) Augustine, Robert L; Thompson, M M; Doran, M A *Chem. Commun.* **1987**, 1173.
(142) Reetz, Manfred t; Westermann, Elke *Angew. Chem. Int. Ed.* **2000**, *37*, 165.
(143) Dupont, Jairton ; Cassol, Claudia C; Umpierre, Alexandre P *et al. J. Am. Chem. Soc.* **2005**, *127*, 3296.
(144) Koehler, Klaus; Sandra S. Prockl; Kleist, wolfgang *et al. Angew. Chem. Int. Ed.* **2004**, *43*, 1881.
(145) Reetz, Manfred T; de Vries, Johannes G *Chem. Commun.* **2004**, 1559.
(146) Koehler, Klaus; Djakovitch, Laurent *J. Mol. Catal. A Chem.* **1999**, *142*, 275.

(147) Jenkins, Peter. M. ; Tsang, Shik Chi *Chem. Res. Chinese U.* **2002**, *18*, 175.
(148) Shmidt, A F; Mametova, L V *Kinet. Catal.* **1996**, *37*, 406.
(149) Kohler, Klaus; Heidenreich, Roland G. ; Jurgen G.E. Krauter *et al. J. Mol. Catal. A Chem.* **2002**, *182*, 499.
(150) Koehler, Klaus; Djakovitch, Laurent *J. Am. Chem. Soc.* **2001**, *123*, 5990.
(151) Koehler, Klaus; Wagner, Micheal; Djakovitch, Laurent *Catalysis Today* **2001**, *66*, 105.
(152) Kohler, Klaus; Roland G. Heidenreich; Jürgen G. E. Krauter *et al. Chem.-Eur. J.* **2002**, *8*, 622.
(153) Fujita, S ; T Yoshida; Bhanage, B.M. *et al. J. Mol. Catal. A Chem.* **2002**, *180*, 277.
(154) Fengyu Zhao; Kenji Murakami; Masayuki Shirai *et al. Chem.-Eur. J.* **2000**, *6*, 843.
(155) Arai, Masahiko; Bhanage, Bhalachandra M; Zhao, Fengyu *et al. Catal. Lett.* **1998**, *54*, 195.
(156) Arai, Masahiko; Zhao, Fengyu *React. Kinet. Catal. Lett.* **2004**, *81*, 281.
(157) Arai, Masahiko; Zhao, Fengyu; Shirai, Masayuki *J. Mol. Catal.* **2000**, *154*, 39.
(158) Arai, Masahiko; Zhar, Fengyu; Shirai, Masayuki *et al. J. Mol. Catal. A Chem.* **2002**, *180*, 211.
(159) Arai, Masahiko *J. Catal.* **2000**, *194*, 479.
(160) Lipshutz, Bruce H.; Blomgren, Peter A. *J. Am. Chem. Soc.* **1999**, *121*, 5819.
(161) Lipshutz, Bruce H; Bryan Frieman; Birkedal, Henrik *Org. Lett.* **2004**, *6*, 2305.
(162) Lipshutz, Bruce H; Frieman, Bryan *Tetrahedron* **2004**, *60*, 1309.
(163) Lipshutz, Bruce H.; Frieman, Bryan; Lee, Ching-Tien *et al. Chem.-Asian. J.* **2006**, *1*, 417.
(164) Lipshutz, Bruce H; Takashi Tomioka; Peter A. Blomgren *et al. Inorg. Chim. Acta.* **1999**, *296*, 164.
(165) Che, M; Bennett, C O *Adv. Synth. Catal.* **1989**, *36*, 55.
(166) Davies, Ian W.; Matty, Louis; Hughes, David L *et al. J. Am. Chem. Soc.* **2001**, *123*, 10139.
(167) Grigicak, Catherine M; Green, Richard G; Giorgi, Javier B. *J. Mat. Chem.* **2006**, *16*, 885.
(168) Mamak, Marc; Neil Coombs; Ozin, Geoffey *J. Am. Chem. Soc.* **2000**, *122*, 8932.
(169) Skoog, Douglas A.; F.J.H.; Nieman, Timothy A. *Principles of Instrumental Analysis*; 5th ed.; Hancourt Brace and Company: Orlando, 1982.
(170) Atkins, P *Physical Chemistry*; 5th ed.; WH Freeman and Company: New-York, 1994.
(171) Grieken, R.E. Van; Markowicz, A. A. *Handbook of X-Ray Spectrometry*; Marcel Dekker Inc: New-York, 2002.
(172) Rouquerol, F.; J. Rouquerol; Sing, K. *Asdorption by Powders & Porous Solids*; Academic press: Marseille, 1999.
(173) Brauner, S; Emmet, P H; Teller, E *J. Am. Chem. Soc.* **1938**, *60*, 1938.
(174) Lambert, Joseph B. *Organic Structural Spectroscopy*; Prentice-Hall: Upper Saddle River, 2001.
(175) Poulin, Carl; Matthew A. Brown; Yamile A. Wasslen *et al. Can. J. Chem.* **2006**, *84*, 1520.
(176) Shriver, Duward F; Cooper, P A; Langford, H *Inorganic Chemistry 2nd Edition*; WH Freeman and Company: New-York, 1994.
(177) Houdayer, Axel; Schneider, Raphael; Billaud, Denis *et al. Synthetic Met.* **2005**, *151*, 165.

(178) Wasslen, Yamile A., *Reusable Palladium Catalyzed Heterogeneous Coupling Reactions*, University of Ottawa, 2004.
(179) deVries, Johannes G *Dalton transaction* **2006**, 421.
(180) M. Dams; L. Drijkoningen; B. Pauwels *et al. J. Catal.* **2002**, *209*, 225.
(181) Heidenreich, Roland G. ; Klaus Kohler; Jurgen G.E. Krauter *et al. Synlett* **2002**, *7*, 1118.
(182) Lebedev, S A; Lopatina, V S; Petrov, E S *et al. J. Organomet. Chem.* **1988**, *344*, 253.
(183) Mehnert, Christian P; Ying, Jackie Y *Chem. Commun.* **1997**, 2215.
(184) Mehnert, Christian P; Weaver, David W; Ying, Jackie Y *J. Am. Chem. Soc.* **1998**, *120*, 12289.
(185) Bish, D; Chipera, S.J. *Advances in X-ray Analysis* **1988**, *31*, 295.
(186) Beletskaya, I P; Alexander N. Kashin; Natalia B. Karlstedt *et al. J. Organomet. Chem.* **2001**, *622*, 89.
(187) Crudden, Cathleen M.; Mutyala Sateesh; Lewis, Roxanne *J. Am. Chem. Soc.* **2005**, *127*, 10045.
(188) Miyazaki, F; Yamaguchi, K; Shibasaki, M *Tetrahedron Lett.* **1999**, *40*, 7379.
(189) Bruce H. Lipshutz; Frieman, Bryan *Tetrahedron* **2004**, *60*, 1309.
(190) Kang Hyun Park; Il Gu Jung; Young Keun Chung *et al. Adv. Synth. Catal.* **2006**, *349*, 411.
(191) He, H; V., J.; Gorte, R.J. *J. Electochem. Soc.* **2003**, *150*, 1470.
(192) Badesha, S Santokh; G.T.F; Tamawskyj, Ihor *J. Mat. Res.* **1996**, *1*, 234.